Characteristics and origin of hydrothermal pebble dykes and associated host rock alteration on the Thames coast, Coromandel Volcanic Zone

A thesis

submitted in partial fulfilment of

the requirements for the degree

of

Master of Science (Research*)*

in Earth Science

at

The University of Waikato

by

Holly Simone Sarah Harvey-Wishart

2019

Abstract

During the Miocene to early Pliocene (c. 18 Ma to 2 Ma), subduction-related volcanism migrated down the Coromandel Peninsula forming the Coromandel Volcanic Zone. This period resulted in the development of extensive hydrothermal systems which interacted with the associated volcanic sequences, the Coromandel Group andesites and dacites. As well as introducing extensive alteration and epithermal Au-Ag deposits, the active environment resulted in the emplacement of co-hydrothermal pebble dyke units. Examples of these features have been identified on the Coromandel west coast, exposed as bodies of fractured rock material, hosting well-rounded clasts due to milling during transport forming “pebbles”. This material has been incorporated from a variety of lithologies from different stratigraphic depths, providing a ground surface expression of the subsurface. As the formation of these dykes is not well-defined, whether they are a result of volcanic or hydrothermal activity, this study aims to investigate their origin and the influence they may have had on the character of proximal hydrothermal alteration.

A combination of field descriptions, optical petrology, SEM, XRD, XRF and ICP-MS geochemistry was all involved in investigating the study site along the Thames coastline, where two clusters of dykes are exposed within a ~ 600 m span of beach. The local hydrothermal character was determined from the mineralogy, reflective of the fluids and physical conditions involved in the mineralization of altered products. The extent of the site hosts multiple alteration zones, recognised as propylitic and phyllic alteration associated with periods of mineralisation, and supergene argillic overprinting. The gangue mineralogy also mirrors the character of the broader system, reflecting near-neutral fluids associated with the low-sulfidation epithermal environment at temperatures of ~ 240 – 260 °C.

To understand the role of the pebble dykes within this setting and the origin of their deposits, identifying the mechanisms involved in their formation is crucial. Characteristics of dyke morphologies, clast lithologies and morphologies, and

alteration character suggest fluidisation played a large role, particularly so in the transport of fragmented rock material from depth. The extent of their ascent is best reflected by the occurrences of greywacke argillite and sandstone components found in each of the exposures. These lithologies are sourced from the Manaia Hill group of the Waipapa Terrane, a deep basement unit recognised as the basement rock of New Zealand. Therefore, the presence of greywacke and argillite clasts suggest possible significant depths of material transport and the interaction with high volumes of hydrothermal solutions. However, due to the alteration style and morphologies of the clasts, it is also possible they were instead fragmented at similar depths to the shallower local volcanic stratigraphy.

If pebble dykes were to act as permeable pathways for ore-bearing solutions within a hydrothermal system, it is possible they could play a significant role in the concentration of metals in economically viable quantities. Therefore, under the right circumstances; emplacement during or pre-mineralisation, orientated preferential to fluid flow direction and hosted within otherwise impermeable host rock, they could yet act as a vector towards potential mineralisation.

Acknowledgements

I would like to thank many people who have helped me to successfully finish this project. Firstly, I would like to thank my supervisor Adrian Pittari for providing much guidance, and for always being very supportive with each step of the way. Also, Shaun Barker for providing me with the initial interest and direction of the project. Thanks to the technical staff of the earth sciences department, especially Kirsty Vincent, Renat Radosinky and Helen Turner for their help with thin slide preparation and SEM, XRF, LA-ICP-MS and XRD analysis. I would also like to thank AusIMM and the Geological Society of New Zealand for scholarships granted during my studies and Waikato University for providing me the opportunity to accomplish a MSc.

Lastly, I want to acknowledge the love and support that was always there from my mother, father, partner Tobias and extended family. Without you, this would have been nearly impossible.

Table of Contents

List of Figures

Chapter 2: Regional Geology and Volcanism

Chapter 3: Field-scale Characteristics and Distribution of Host Rock and Pebble Dykes

Chapter 4: Host Rock and Pebble Dyke Petrography

Chapter 5: X-Ray Diffraction

Chapter 6: Geochemistry

Chapter 7: Discussion

List of Tables

Chapter 2: Regional Geology and Volcanism

Chapter 3: Field-scale Characteristics and Distribution of Host Rock and Pebble Dykes

Chapter 4: Host Rock and Pebble Dyke Petrography

Chapter 5: X-Ray Diffraction

Chapter 6: Geochemistry

1.Introduction

1.1 Background

Hydrothermal activity related to the active volcanism within the now ancient Coromandel Volcanic Zone (CVZ) caused extensive host rock alteration and precious metal mineralisation. The Hauraki Goldfield within this volcanic arc hosts epithermal Au-Ag deposits associated with mineralisation during the Miocene. Within this productive district, bodies of breccia recognised as pebble dykes can be found within the shallow epithermal setting. These features are tabular bodies of breccia which contain fragments of well-rounded pebble-sized clasts. Exposures found along the beachline to the north of the Thames township provide a means to investigate their formation and possible relationship to the broader hydrothermal system. A major clue to the subsurface mechanisms involved is the occurrence of greywacke clasts hosted within the pebble dykes. Greywacke is the regional basement rock; therefore, the vertical extent of formation may have been significant to account for its presence within the shallow epithermal setting associated with the site.

The formation of these dykes is not well understood, for example, whether they are a result of volcanic or hydrothermal activity, this study aims to investigate their origin. The influence on the area due to alteration and the structural and geochemical relationship of the dykes to the now inactive CVZ has also been explored. For this purpose, structural, mineralogical and geochemical detail of local lithologies, alteration, hydrothermal features and the geometries and composition of the dykes and their components have all be considered. Pebble dykes are commonly found within ore-bearing hydrothermal environments, as in the case of the Coromandel Peninsula, therefore, understanding their formation and structural significance in such environments may contribute to explorative geology.

1.2 Aim

This thesis involves a study of the mineralogy and geochemistry of the rocks within the Hauraki Goldfield epithermal vein system, with focus on the Thames coast setting and an investigation into the presence of pebble dykes and their relationship to the site. The aim is to determine the distribution of the local alteration zones, nature of ancient hydrothermal activity and relationship of how pebble dykes fit within the hydrothermal system. This allows for an understanding of the possible processes involved in their formation at depth, and what role they may have played in proximal alteration of host rock and their possible relationship to mineralisation.

Objectives

The objectives of the study are:

- To map and characterise the host rock and pebble dykes found within the field site,
- To document the petrography of host rock and pebble dykes, with focus on the variation and character of hydrothermal alteration textures and mineralogy,
- To determine alteration assemblages and associated alteration styles,
- To determine geochemical characteristics of host rock and pebble dykes relating to hydrothermal alteration processes which have acted upon them, and
- explore the relationship between alteration and the presence of pebble dykes.

1.3 Methodology

This study involves the thorough understanding of the composition and nature of the country rocks within the Thames Coast study site and pebble dyke units hosted within them. Field work included recording and taking photos of all the visible features and outcrops, with key focus on alteration intensity and style, mineralogy, hydrothermal features and their orientations, rock texture and weathering intensity. Hand samples were collected across to represent the different lithologies and alteration styles.

Polished thin sections were prepared and examined by transmitted and reflected light microscopy. These sections were also further observed via scanning electron microprobe (SEM), using both backscatter and EDS settings to gain further detail of compositions and textures of samples representative of the varied alteration characteristics present.

The residual rock samples were prepared for geochemical and mineralogical analysis with bulk rock crushing. Powdered samples were then used for X-ray diffraction (XRD) analysis, where both bulk rock and clay separates were analysed. It was also used to create pressed powder and fusion beads for both X-ray fluorescence (XRF) spectrometry and inductively coupled mass spectrometry (LA-ICP-MS) analysis for major, minor and trace element geochemistry. Further methodology is described in more detail within corresponding analysis chapters.

1.4 Thesis Structure

This thesis is structured around the objectives which have been listed. Chapter 2 provides a literature review of the regional geology, volcanism and hydrothermal activity of the Hauraki Goldfield. It also discusses what pebble dykes are and possible mechanisms involved in their formation, providing examples of them elsewhere globally. Chapter 3 details and characterizes the observations of the host rocks and hydrothermal features in the field, with a strip map of the field site for their spatial relationships. Chapter 4 and 5 focus on the petrology of the

samples collected from the field, describing primary and secondary alteration features, alteration intensity and mineral assemblages from the variably altered host rocks and pebble dykes. The geochemistry related to the varied alteration within the site is then summarised in Chapter 6, where the source of the hydrothermal fluids which would have acted on the site is also considered. Chapter 7 is the final discussion of the alteration styles present within the site and the hydrothermal conditions which acted to form them, the role the pebble dykes may have had in influencing the styles and intensity of alteration, possible mechanisms for the pebble dykes formation and how they may relate to explorative geology when found in ore bearing districts.

2. Regional Geology and Volcanism

2.1 Coromandel Volcanic Zone

Subduction at the boundary of the Australian and Pacific plates, at about 20 Ma, drove a series of major geological changes for New Zealand. One important change in the North Island manifested as the formation of a continental volcanic arc, associated with a period of intense volcanic activity in the Northland Volcanic Arc, then later along the Coromandel Peninsula (Fig. 1). Subduction-related activity within the Coromandel Volcanic Zone (CVZ) began during the late Miocene, to early Pliocene (c. 18 Ma) and ended c. 2 Ma (Christie et al., 2007). Eruptions first began on the northern tip of the peninsula then migrated to the east and south as the plate boundary spread through the North Island (Ballance, 1976).

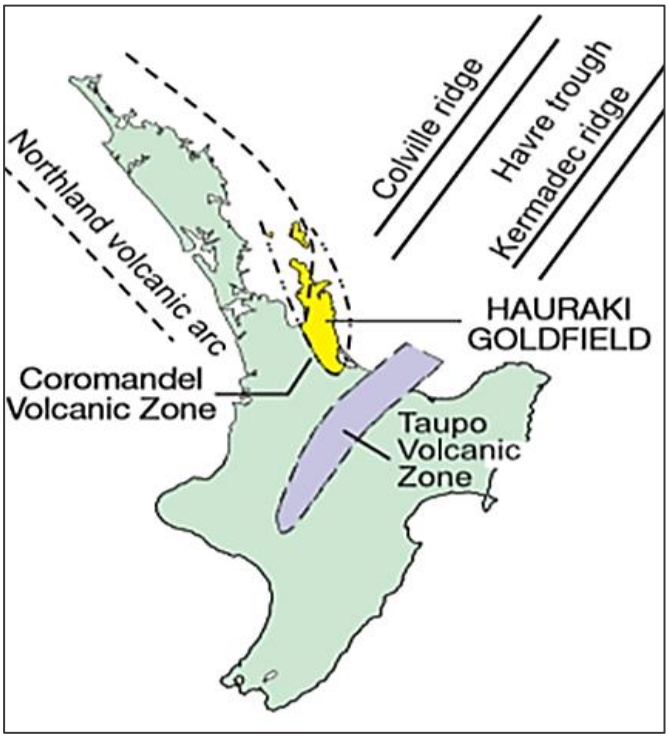

Figure 1: The Coromandel Volcanic Zone located within the Hauraki Goldfield along the Coromandel Peninsula (John, 2011).

Despite the predominantly continuous activity, with regional breaks of volcanic activity of no more than 1 – 2 Ma, the style of volcanism was seen to evolve over time along the arc (Adams et al., 1994). Beginning in the north, near Cape Colville, the CVZ produced predominantly calc-alkaline or high alumina basaltic andesite, andesite and dacite between 18 and 12 Ma (Suggate et al., 1978). From c. 12 Ma, continued andesitic volcanism was joined with rhyolite and basaltic activity (Spörli et al., 2007). These compositional changes are thought to be a result of various factors including tectonism, changes to the composition and thicknesses of the crust and variations in composition of the mantle source and subduction slab (Booden, 2011). The eruptions along the Coromandel Peninsula halted at 2 Ma in the Tauranga area, where the focus of volcanism then migrated to the Rotorua-Taupo region where it continues today along the Taupo Volcanic Zone (TVZ) (Booden et al., 2011).

The activity of the CVZ provided the backbone of the Coromandel Peninsula in the form of eroded volcanic deposits and cones (Homer & Moore, 1992). It also developed the region economically, as associated hydrothermal activity caused widespread alteration of the country rocks and developed precious metal mineralisation. This was realised in the mid to late nineteenth century when extensive exploitation of gold-bearing quartz reefs began. The region hosts the deposits of the Hauraki Goldfield, named so relating to its prosperous nature. Therefore, the ancient activity of the CVZ is a centre of great geological interest, both in terms of the evolution of volcanism and its potential for explorative geology.

2.2 Regional Geology of the Hauraki Goldfield

The Hauraki Goldfield is a 200 km by 45 km belt within the CVZ (Fig. 2). Over 200 km^3 of material was deposited as a result of the activity within the CVZ (Booden et al., 2012), resulting in sequences largely of lavas as well as mass flow deposits, autoclastic breccias, lahar deposits, tuffs and dykes (Skinner, 1986). The Coromandel Group, dominated by andesites and dacites, is the most dominant

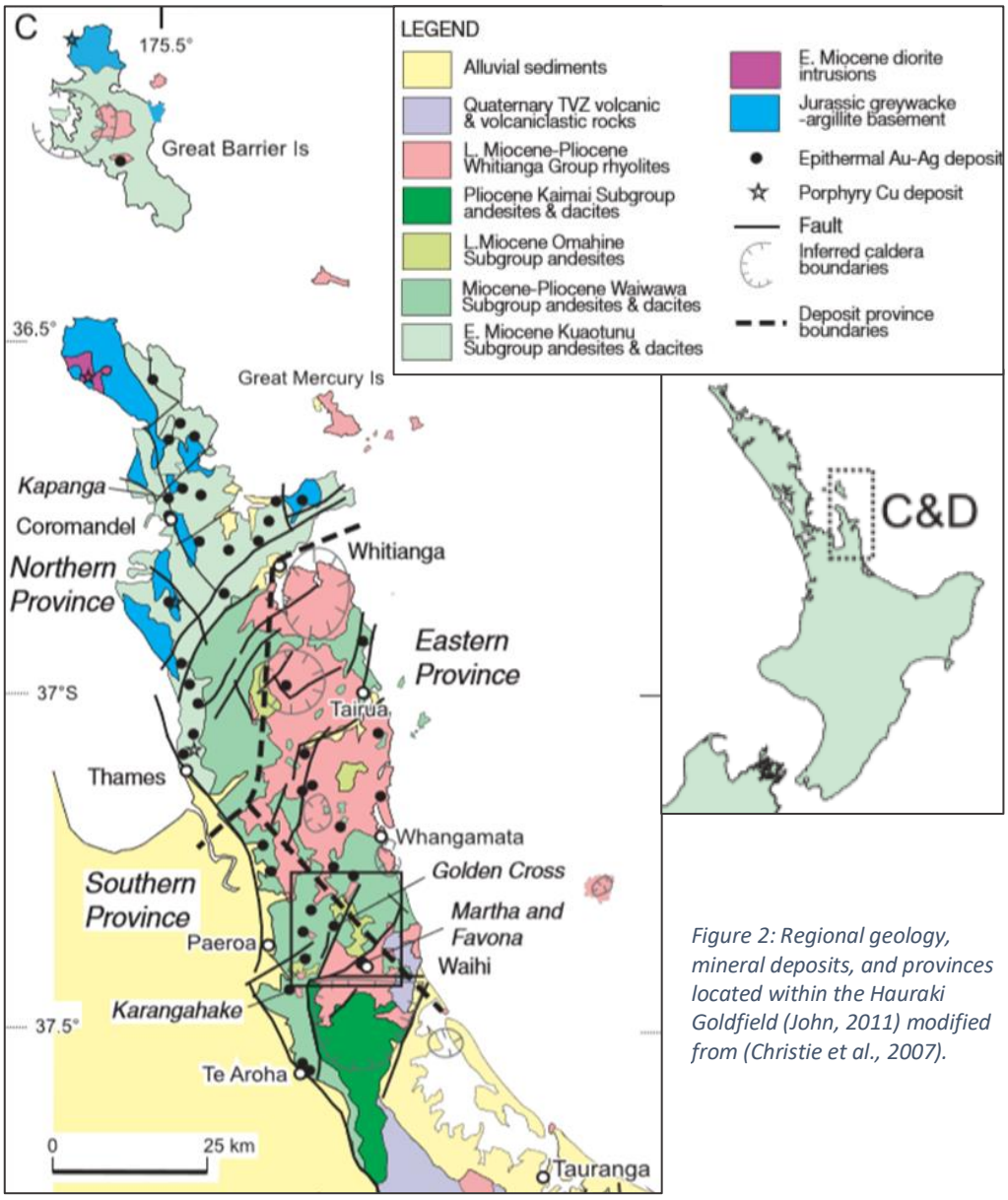

Figure 2: Regional geology, mineral deposits, and provinces located within the Hauraki Goldfield (John, 2011) modified from (Christie et al., 2007).

sequence, representing 61% of the exposed rock. The younger sequences of the Whitianga Group dacite, rhyolite and rhyodacite represent 30%, while the Kerikeri Group basalts makes up less than 1 %. The final 9 % consists of exposed basement greywacke sandstone and argillite (Christie et al., 2007).

The greywacke occurs in the area unconformably beneath younger volcanic sequences. This well indurated metasedimentary basement is from the Manaia Hill group of the Waipapa Terrane. Greywacke is sands of texturally and mineralogically immature deep water turbidites formed between 140 – 150 Ma due to convergent plate tectonism leading to accretion onto Gondwana's margin

(Spörli, 1987; Fraser, 1907; Homer & Moore, 1992; Blatt, 1992). It can be characterised by volcanic lithic greywackes and sandstone (sub-greywackes) ranging in grade from conglomerates down to argillite (Skinner, 1967).

Provinces

The Hauraki Goldfield is broken into three provinces, the northern, eastern, and southern, which vary in age and style of mineralization, preserving the evolution of volcanism on the peninsula (Adams et al., 1994). Due to periods of quiescence and erosion, the Coromandel Group is further divided into subgroups. Within the Hauraki Goldfield, the Kuaotunu Subgroup is to the north (18 to 11 Ma) and Waiwawa Subgroup (10 to 5.6 Ma) is hosted to the south and east of the region (Christie et al., 2007; Mauk et al., 2011) (Fig. 2). Mineralogically, these two subgroups can be differentiated; as the Kuaotunu Subgroup consists of alternating pyroxene and hornblende-pyroxene andesite to dacite sequences whereas the Waiwawa Subgroup is predominantly pyroxene andesite (Christie et al., 2007). The remaining younger Omahine (8.6 to 6.6 Ma) and Kaimai (5.6 to 3.8 Ma) subgroups have a comparatively minor exposed distribution in the area.

Faulting

Reactivation of block faulting within the basement greywacke, associated with its formation during the development of Gondwana, has led to the creation of some of the large-scale faults across the peninsula (Christie et al., 2007). These NNW and NNE-striking faults and fractures are major structural features of the Hauraki Goldfield, significantly affecting the stratigraphy of the region (Mauk et al., 2011) (Skinner, 1986). The NNW striking faults have caused downward displacement of rocks to the east and west, whereas most of the NNE striking faults have displaced them in the same manner to the south. The result of this displacement has caused an increase in the exposure of greywacke to the north of the peninsula, but to the south, it is buried below the volcanics 900 m below sea-level (Adams et al., 1994; Christie et al., 2007; Irwin, 2004). Consequently, the

volcanic sequences are thicker to the south, and have also adopted an associated eastern tilt, so that farther south they are overlain by the TVZ volcanic sequences (Gadsby & Spörli, 1989; John, 2011). This burial may also contribute to the SSE trend of younging seen across the peninsula associated with the migration of the volcanic arc (Booden et al., 2012).

2.3 Hydrothermal Alteration and Mineralisation

Hydrothermal systems can develop in a variety of geological settings, requiring the presence of permeable or fractured host rocks and a heat source, such as the faulting and volcanism seen during the activity of the CVZ. A system establishes as fluids percolate down through fissures and connected pore spaces within the reservoir rock. This fluid is heated at depth, most commonly by a proximal magmatic chamber, which lowers its density causing the fluids to then rise buoyantly. This process repeats, creating a convective cycle of reactive fluids. The solutions may be derived from a variety of sources, but primarily from meteoric waters, deeply penetrating groundwater, metamorphic waters or from depth via a magmatic source. The system drives the redistribution of mass through the movement of this circulating fluid, disrupting the chemical equilibria of the surrounding rock and driving reactions. These fluid-rock reactions are known as hydrothermal alteration.

Alteration results in the conversion of a primary mineral assemblage to a new assemblage that is more stable under the new conditions created by the active hydrothermal system (Barnes, 1997). Under hydrothermal conditions, there are typical alteration products which replace the original minerals, predominantly controlled by the original mineral's chemical composition (Table 1). These altered conditions are primarily a result of changes to temperature, pressure and fluid, with permeability and duration of activity determining the extent and intensity of the system (Browne, 1978). Minerals which are in equilibrium with these changes are favoured by the system, those which are not are instead driven to dissolution within the host rock. Each factor is independent, however,

the response to a few variables can have a huge influence on the location, style and size of zones of hydrothermal alteration (Lagat, 2007).

Table 1: Common replacement minerals of primary rock minerals during hydrothermal alteration (Browne, 1982).

Original mineral	Replacement products
volcanic glass	zeolites (e.g. mordenite, laumontite), cristobalite, quartz, calcite, clays (e.g. montmorillonite)
magnetite/ilmenite/titano-magnetite	pyrite, leucoxene, sphene, pyrrhotite, hematite
pyroxene/amphibole/olivine/ biotite	chlorite, illite, quartz, pyrite, calcite, anhydrite
calcic plagioclase	calcite, albite, adularia, wairakite, quartz, anhydrite, chlorite, illite, kaolin, montmorillonite, epidote
anorthoclase/sanidine/ orthoclase	adularia

Epithermal Mineralization

Epithermal is a term used to describe Au ± Ag ± Cu deposits found in hydrothermal settings at low temperatures of <150 - ~300°C and at depths of 1 – 2 km below the surface. The typical physical and chemical attributes of epithermal systems are summarised in Table 2. Most deposits form within these elevated crustal settings as a result of the sudden transition from lithostatic to hydrostatic pressure, altering both physical and chemical conditions (White & Hedenquist, 1990). Epithermal deposits have been classified and differentiated based on ore mineralogy and textures proposed by Lindgren (1913), from mesothermal and hypothermal settings as each of their very similar deposits can develop at widely different temperatures (Skinner & Barton, 1973). Because of the shallow environment they are situated in, they may also be poorly preserved. When located within high relief settings and convergent boundaries they are particularly prone to high uplift and erosion rates. This results in most major deposits which are classified as epithermal being of Cenozoic age (Simmons et al., 2005).

Table 2: Characteristics which classify an epithermal system (after Lindgren, 1933) modified by (Silberman, 1985)

Depth of formation	Surface to 1000 m
Temperature of formation	50 to 300 °C
Form of deposits	Thin to large veins, stockworks, disseminations, replacements
Ore textures	Open-space filling, crustification, colloform banding, comb structure, brecciation
Ore elements	Au, Ag, (As, Sb), Hg, [Te, Tl, U], (Pb, Zn, Cu) *
Alteration	Silicification, argillization, sericite, adularia, propylitization
Common Features	Fine-grained chalcedonic quartz, quartz pseudomorphs, after calcite, brecciation
* [] indicates elements seldom present in more than sub-economic concentrations; () indicate elements often present in economic concentrations but are less valuable than associated precious metals.	

Epithermal deposits can develop within a variety of geological settings, of varied igneous, tectonic, and structural characteristics, although are most common within volcanic areas (White & Hedenquist, 1990). Host settings are most commonly medial to proximal to an igneous heat source, and deposits hosted in volcanics typically occur within lavas or pyroclastic rocks (Sillitoe & Bonham, 1984). The structural setting is significant for ore deposits due to the related permeability enhancement resulting from fractures in the near surface, as a brittle environment plays a major role in the location of veins within an epithermal system (Irwin, 2004). Despite major regional scale faults likely guiding emplacement of magmatic heat sources and influencing the subsequent activity, mineralisation is more often localised on subsidiary or splay faults (White & Hedenquist, 1995). At a more localised scale, minor structures such as bedding planes may also affect permeability and act as a mineralisation centre. There is also an association with felsic calderas and andesitic vent complexes with areas of mineralisation (White & Hedenquist, 1995).

Epithermal deposits are most associated with intermediate to acid volcanic settings (White & Hedenquist, 1990). They are often hosted in intermediate host rocks which may reflect more favourable lithologic properties relative to felsic compositions. For example, epithermal veins in rhyolites are typically narrower but more clustered than those seen in andesites (Brathwaite et al., 2001b; Booden, 2011). Therefore, the broader fractures of andesites promote the development of larger accumulations of mineralisation. 97% of the total gold production from the Hauraki Goldfield is hosted in the 18 to 2.5 Ma Coromandel Group andesites and dacites which host the thickest and most persistent veins (Christie et al., 2007). These major veins dip steeply, ranging from 300 to 1,300 m in length, with a width of 1 to 5 m (Simpson & Mauk, 2011). Rhyolitic rocks are a lesser host, characterised by zones of thinner veins (Brathwaite et al., 2001a) and the basement greywacke is only mineralised in the uppermost strata (Gadsby & Spörli, 1989). Despite the limited host rocks, these epithermal deposits display a range of structural variability due to the varied processes involved in their formation (Irwin, 2004).

High and Low-Sulfidation Settings

Epithermal ore deposits can be further classified as forming in either high or low sulfidation systems. Hedenquist & Houghton (1987) proposed the terms 'low sulfidation' and 'high sulfidation', referencing the redox state of the sulphur content of the hydrothermal solution. White & Hedenquist (1990) also refers to these classifications as adularia-sericite and acid-sulphate types. The pH of the interacting solutions is the driving influence in which of the two styles form. Sulphur in the near-neutral system is typically in its lowest redox state, therefore this style is termed low-sulfidation. Whereas for more acidic solutions, sulphur is at a high oxidation state of +4, present as SO_2 (White & Hedenquist, 1990).

The distinction is an important one to make as in high-sulfidation deposits, the ore is commonly associated with zones of acid alteration assemblages, surrounded by assemblages associated with more neutral conditions. The

reverse is true for low-sulfidation deposits which are associated with the least acid assemblages (White & Hedenquist, 1995) (Fig. 3). The two styles can therefore be primarily distinguished from one another based on gangue and ore mineralogy (Corbett, 2002).

For a low-sulfidation system to form, ore-forming fluids need to be neutral. In a typical system, the metal-bearing fluids are sourced from condensed sulfur dioxide and hydrogen chloride gases from underlying magma, resulting in an acidic pH. This fluid mixes with overlying meteoric fluids which then dominate the solution and wall-rock interactions then act to further neutralise it, becoming more pH neutral closer to the surface (Shanks & Thurston, 2012). The hydrothermal fluids created typically have a low salinity of less than 1 to 2 wt. % NaCl equivalent and may also be rich in CO_2 and H_2S (Hedenquist et al., 2000). Near neutral fluids at shallow depths are reduced but in equilibrium with rock at greater depth. Therefore, the resulting alteration assemblages form to reflect this gradation of composition. This results in extensive propylitic alteration in the surrounding regions of low water-rock ratios, such as outside conduit zones. White mica forms in high water-rock ratios and clay species dominate with decreasing temperature (White & Hedenquist, 1990) (Fig. 3). Fluids at boiling point ascend while depositing ore and gangue minerals within zones of

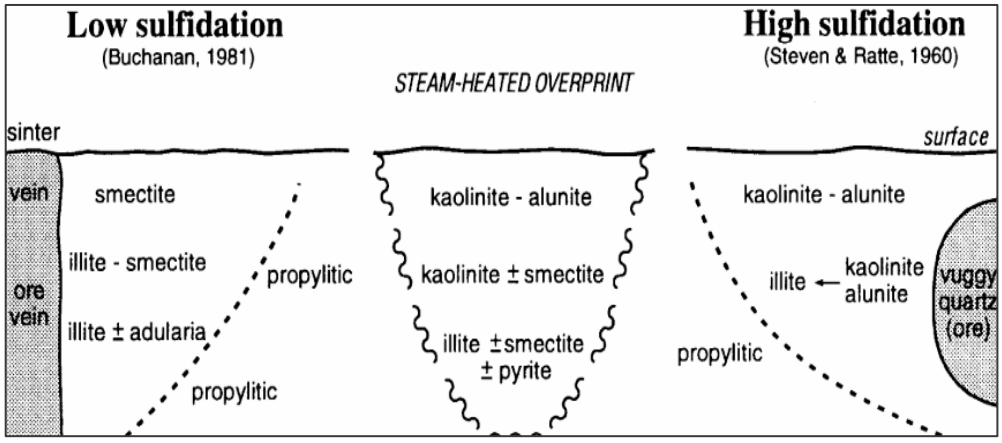

Figure 3: The hydrothermal assemblages and distribution associated with low and high sulfidation deposits, each zoning vertically and horizontally. Low sulfidation assemblages are markedly different to high sulfidation environments, due to the neutral rather than acidic fluids interacting with host rock. This is reflected by the mineral assemblages associated with their corresponding mineralisation zones. Zones of propylitic alteration occur in low water-rock ratios, where the mineralogy is more controlled by the parent lithology. Steam heated overprinting can occur in either environment. Silica sinters may also develop if there is a focused discharge of the fluids at the surface (White & Hedenquist, 1995).

permeability in the host rock (White & Hedenquist, 1995). Boiled off gases, which cause an increase in acidity, may also develop argillic and advanced argillic alteration. This may occur peripheral to or on top of pre-existing alteration from deep fluids as a steam-heated zone (White & Hedenquist, 1990).

Contrasting to this, for a high sulfidation environment to form, the dominant component of the fluid is often derived from an oxidised magmatic source. This fluid rises to elevated levels in the system with low water-rock interaction at depth, therefore preventing the same manner of neutralising as in low-sulfidation settings (White & Hedenquist, 1995). At shallow depths, groundwater may absorb HCl and SO_2 rich vapour, altering it to a hot (200 - 300 °C), highly acidic (pH 0-2) and oxidized fluid. This fluid reacts extensively with, and leaches, host rock, creating characteristic acid gangue mineralogy.

2.4 Hauraki Goldfield Hydrothermal System and Deposits

The Hauraki Goldfield hosts epithermal deposits of Au-Ag veins and some instances of Cu which are Miocene in age (Irwin, 2004). Two discrete periods of epithermal mineralization have been recognised to have acted within the Hauraki Goldfield, the earliest occurring at 14 – 10 Ma in the north, the second occurring near Thames between 11 to 10 Ma (Christie et al., 2007). Therefore, the associated veins are seen to young to the south, mirroring the trend of the movement of the volcanic arc. This system was driven by mineralising intrusives providing a heat source, host andesite and porphyries acting as the reservoir rock and the circulation of solutions controlled by fracture and vein conduits (Merchant, 1978). Most of the andesites and dacites in the Thames area are hydrothermally altered as a result of this activity, with increased intensity proximal to epithermal quartz veins and porphyry copper mineralization (Sheppard et al., 2009). Alteration of these rocks was pervasive and has been described as predominantly propylitic or argillic in nature and having undergone extensive pyritization (Fraser, 1907; Brathwaite et al., 2001).

The deposits of Hauraki Goldfield are characterised as low-sulfidation due to adularia ± illite or adularia sericite zones of alteration enclosing gold-bearing quartz veins of ore grade electrum and acanthite (Christie et al. 2007). This mineralogy indicative of the near neutral epithermal setting. These styles of alteration are typically locally distributed and display varied intensities in relation to the 50 adularia-sericite Au-Ag deposits (Christie et al., 2007) (Fig.2). Due to the economic significant these deposits represent; where between 1862 and 2009 mining yielded a total of approximately 335,000 kg gold and 1.5 million kg silver (Mauk et al., 2011), understanding the alteration in the region associated with the interaction of ore bearing fluids, benefits reconstruction of the now ancient hydrothermal system and enables alteration zones to be used as vectors towards precious metal mineralisation.

2.5 Pebble Dykes

Hydrothermal breccia formations, including features such as diatremes, breccia pipes, and breccia dykes, are created through fracturing and transport by thermal fluids and have been identified at and linked to productive mining districts worldwide. Typically, they represent a host for, or indicator of valuable hydrothermally deposited ore bodies (Sillitoe, 1985). This is due to the occurrence of breccias often providing the necessary permeability for ore-bearing thermal fluids to use as a conduit (Byrne & Tosdal, 2014).

Within the productive Hauraki Goldfield, bodies of breccia recognised as pebble dykes have be found within the shallow epithermal setting, both along the Thames coast and within Waihi. Pebble dykes are a variety of hydrothermal breccia, described as a tabular body of breccia which contains fragments of well-rounded material, or “pebbles”, clay to gravel in size and often of varied lithology (Fig.4). They likely represent hydrothermally related processes of brecciation at depth then possible extensive vertical transport of material before emplacement. Examples of pebble dykes, therefore, provide a means for recognising subsurface processes and conditions during the active system.

Despite this, the Hauraki Goldfield pebble dykes, particularly examples along the Thames coast, have not been described in significant detail despite the possible association with ore in the area. More study around them is required to define the nature of the geological processes involved in their formation and to recognise criteria in evaluating them as guides to ore in the hydrothermal system of the Hauraki Goldfield and those alike.

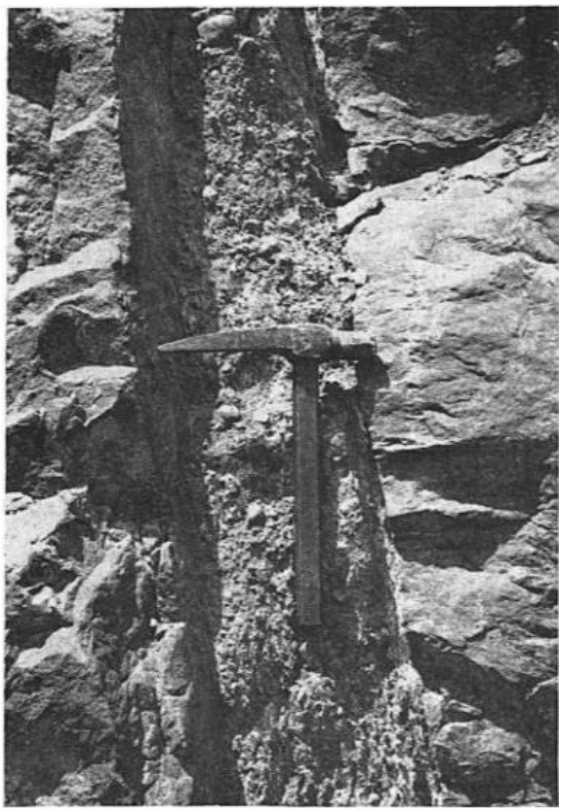

Figure 4: Pebble dyke from Mount Morgan open pit with milled granitic pebbles of up to 5 cm in diameter with a sharp contact to silicified host rock (Cornelius, 1967)

There has been difficulty in defining the processes involved in pebble dyke formation, often due to attempts to explain it by a single process and due to confusion between the origin of the fractured clasts and the origin of the mechanism allowing for their transportation (Bryant, 1968). However many (Sillitoe, 1985; L. Bryner, 1961; Richard, 1969) have suggested multiple processes are likely involved. Therefore, the primary mechanism for the brecciation may entirely differ from the primary means of transportation. Theories on mechanisms which could be attributed to the creation of breccias have been compiled by both Bryant (1968) and Jébrak (1997) which include subsurface hydrothermal eruption, tectonic brittle fracture, intruding magma pressure causing fracturing, chemical weathering, subsidence and collapse of host rock and fluidisation.

Vertical Transport Via Fluidisation

The leading suggestion for the primary process allowing for vertical transport of rock material is fluidisation (Bryant, 1968; Bryner, 1961; Oliver et al., 2006). Fluidization in the hydrothermal system is the passing of buoyant gases or fluids through the mass of solid brecciated rock. This changes the character of the immobile fractured material to a viscous flow, allowing fluid-like movement and suspension in a "fluidised state" (McCallum, 1985). With high enough fluid velocities, displacement of matrix and clasts occurs. An increase in the velocity of flow widens the fluid pathway, likely fracturing and incorporating more material, which results in suspended particles having less and less contact until individual particles flow freely allowing vertical mobility (McCallum, 1985). The initiation of this fluid driven transport would be the result of either an increase in fluid density or a change in the flow pathways, from low permeability small shear zones to open extension fractures (Bryant, 1968). Along the transport pathways, the clasts would be physically and chemically weathered. Weathering would manifest as the rounding of clasts, a higher intensity indicating a longer duration of effect. This is reflected in the characteristic well-rounded clasts found within pebble dykes, often suggesting significant distances of transport to create their form. The size ranges would instead represent the energy input or pressrues involved during brecciation and transport via fluidisation (Jébrak, 1997).

Tuffisites

Reynolds (1954) compared the process of fluidisation to the process of "tuffisitization", a mechanism resulting in the creation of tuffisites. A tuffisite is a term introduced by Cloos (1942) but broadened to encompass dykes, sills, and swellings of intrusive tuff by Reynolds (1954). It is used to describe breccia bodies which penetrate country rock at or near margins of volcanic pipes or other channels of eruption. They are deposits of intrusive, fine-grained pyroclastic material, a mix typically of fragments of both country rock and parent magma (Francis, 1989). Therefore, they are comparable units to pebble dykes.

The conception of tuffisite deposits is better defined, however, as they are known to occur due to volcanic activity, common in volatile explosive volcanic environments. This induces fragmentation, transport and deposition in conjunction with hydrothermal flow whilst creating or making use of pre-existing fracture networks (Kolzenburg et al., 2012). Variables in the hydrothermal-magmatic environment controlling the frequency of these brittle events and where they occur can include magma flow rate, viscosity and pressure exposed to vent, and the temperatures at depth (Tuffen et al., 2002).

Their fragmental nature has shown to increase permeability, doubling when the tuffisite vein is orientated in favour of fluid flow direction (Kolzenburg et al., 2012). This permeability allows the escape of magmatic volatiles, which consequently enables a higher fluid flow rate. If this process of formation mirrors that of the pebble dyke, then similar conditions and mechanisms leading to their formation can be expected. Therefore, a pebble dyke deposit would also represent a similar structure of amplified permeability channelling fluid flow. This may be the case due to both deposits linked to magmatic-hydrothermal environments, so the role of tuffisites in such systems may provide insight into determining how pebble dykes interact with ore-bearing fluid.

Examples of Pebble Dyke Systems

Examples of pebble dykes which can be compared to the Hauraki Goldfield instances have been found around the world. Similar locations associated with mining districts include Bisbee (Arizona), El Salvador (Chile), Tintic (Utah) and Mount Morgan (Australia). Pebble dykes within these sites are often localised by well-defined faults and fractures (Sillitoe, 1985), occupying and therefore adopting the strike and dip of the pre-existing structures. At Tintic they are also commonly proximal to igneous dykes, where they appear in higher abundance as tabular forms which resemble veins (Farmin, 1934). Their thicknesses can range between 1 cm to 10 m, consistently displaying an abrupt contact with host rock (Fig.4) and are observed to both pinch and broaden horizontally and vertically

(Sillitoe, 1985). At El Salvador, the pebble dykes decrease in abundance with depth, until they terminate at about 600 m depth (Gustafson & Hunt, 1975). A similar depth is seen in the Tintic system (Morris & Lovering, 1979). They may occur as single dykes as at Mt. Emmons, or as major bodies splitting into minor, narrower branches, creating swarms (Sillitoe, 1985). At El Salvador, these smaller instances of dykes are more prone to displaying an irregular thickness and attitude (Gustafson & Hunt, 1975).

Within each district, the pebble dykes they host all display components of angular to rounded clasts, with varied lithologies, commonly supported by a sand to silt-sized matrix (Sillitoe, 1985). The ratios can vary considerably however, where within the Mt. Morgan dyke series, the matrix is seen to range between 50 – 70 % (Cornelius, 1967). The continuity of the bodies, their geometries and textural features all demonstrate characteristics of turbulent flow (Cornelius, 1967); for example, El Salvador dykes matrix material displays flow banding and consists largely of fragmented rock (Gustafson & Hunt, 1975) (Fig. 5).

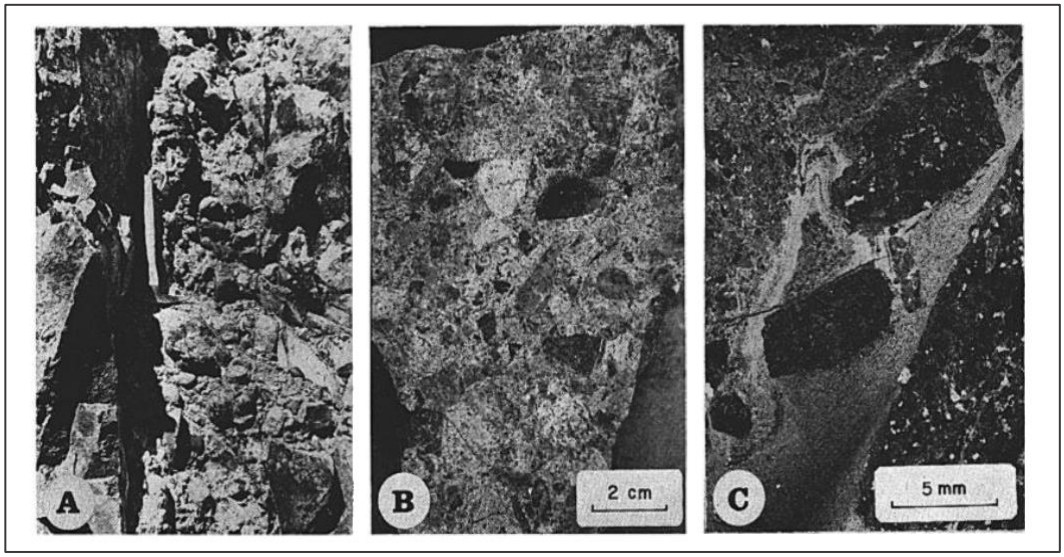

Figure 5: Images from Gustafson & Hunt (1975) of pebble dykes within the El Salvador porphyry copper deposit, Chile.A. Exposure of rounded pebbles in a sandy clastic matrix. B. Freshly cut surface from the deepest level of a pebble dyke, reflecting sub-angular to round, unaltered pebbles. C. Photomicrograph of matrix flow banding.

Based upon the clast rock types and the local stratigraphy, the maximum vertical transport of material in pebble dykes is 500 m at Mt. Emmons (Thomas & Galey,

1982), more than 1000 m at Bisbee (Bryant, 1968) and a minimum of 1,800 m at Tintic (Farmin, 1934). The clasts within the dykes are noted as becoming more rounded upwards at both Tintic (Farmin, 1934) and El Salvador (Gustafson & Hunt, 1975). Particularly well-rounded fragments, some with hypogene exfoliation, are seen in Tintic (Farmin, 1934) and Bisbee (Bryant, 1968) and a rough correlation of distance transported and clast form was recognised at El Salvador. This is suggested by the angular clasts hosted within the same lithology in the immediately enclosing rock (Gustafson & Hunt, 1975). At Tintic, pebbles become smaller the higher above their parent formation they have been deposited, and quartzite pebbles are recognised as being more abundant, likely due to being able to withstand chemical and physical weathering (Farmin, 1934). These observations of well-rounded clasts, and their association with evidence of significant vertical transport via turbulent flow, support fluidisation as the means of transport (Bryner, 1961).

Within most settings, the pebble dyke bodies are often weakly altered or unaltered and are seen to host sulphides but mainly in the rock fragments they contain. In contrast, dykes at shallow depths in El Salvador were emplaced while intense sericitic and advanced argillic alteration was still active at elevated levels of the system. However, at depth, ore-related alteration had ceased as the dykes are relatively fresh except for weak calcite and chlorite alteration in the matrix (Gustafson & Hunt, 1975). Their alteration, or lack of, is likely related to the commonly close relationship they have with late to post-mineralisation intrusions. This suggests that most examples were emplaced late in the mineralisation sequences of these districts (Sillitoe, 1985), therefore, forming too late in the system for significant alteration. Tintic is an exception however as although its pebble dykes only make ore locally, Lovering et al. (1949) and Morris & Lovering (1979) interpret them as having emplaced prior to mineralisation. Therefore, although pebble dykes in these systems do not appear to display a direct connection with mineralisation phases, they may possibly have an association with the mineralising system.

3. Field-scale Characteristics and Distribution of Host Rock and Pebble Dykes

This chapter provides an overview of the study site including the character and spatial relationships of host rock as well as their associated hydrothermal and structural features. Occurrences of different rock types, their primary and secondary textures and their variance across the length of the site is characterised. The pebble dykes are a major feature of interest at the site, so their morphologies, relationships to one another and the lithologies and character of their "pebble" components are also a major focus.

3.1 Physiography and Outcrop Exposure

The study site is a ~600 m long, north-south stretch of beach, adjacent to the Thames coast road, to the north of the Thames township (Fig. 6). This section features multiple exposures of pebble dykes, which are thought to be associated with hydrothermal activity that accompanied the now ancient volcanism of the Coromandel Volcanic Zone (CVZ). The setting for this site is a beach wave-cut platform bounded by steep coastal hills, within an area that is famous for historic mining. Multiple exposures of host rock and pebble dykes are visible on the beach face and as a bank outcrop on an adjacent road cutting.

The site is located within the northern province of the Hauraki Goldfield, which is dominated by host andesitic breccias and lavas of the Coromandel Group volcanics (Kuaotunu subgroup) (18 – 9 Ma). A less significant host lithology within the study site is the Manaia Hill Group metasedimentary basement greywacke of the Waipapa Terrane, which underlies Coromandel volcanic succession. Greywacke elsewhere on the peninsula is generally buried by the volcanic succession, except around the northern Coromandel Peninsula and Great Barrier (Chp. 2: Fig. 2) where it is exposed. This limited ~25 m exposure within the study site is therefore roughly 15 km south of the nearest northern

exposure (Edbrooke, 2001), so represents an isolated greywacke occurrence on the peninsula.

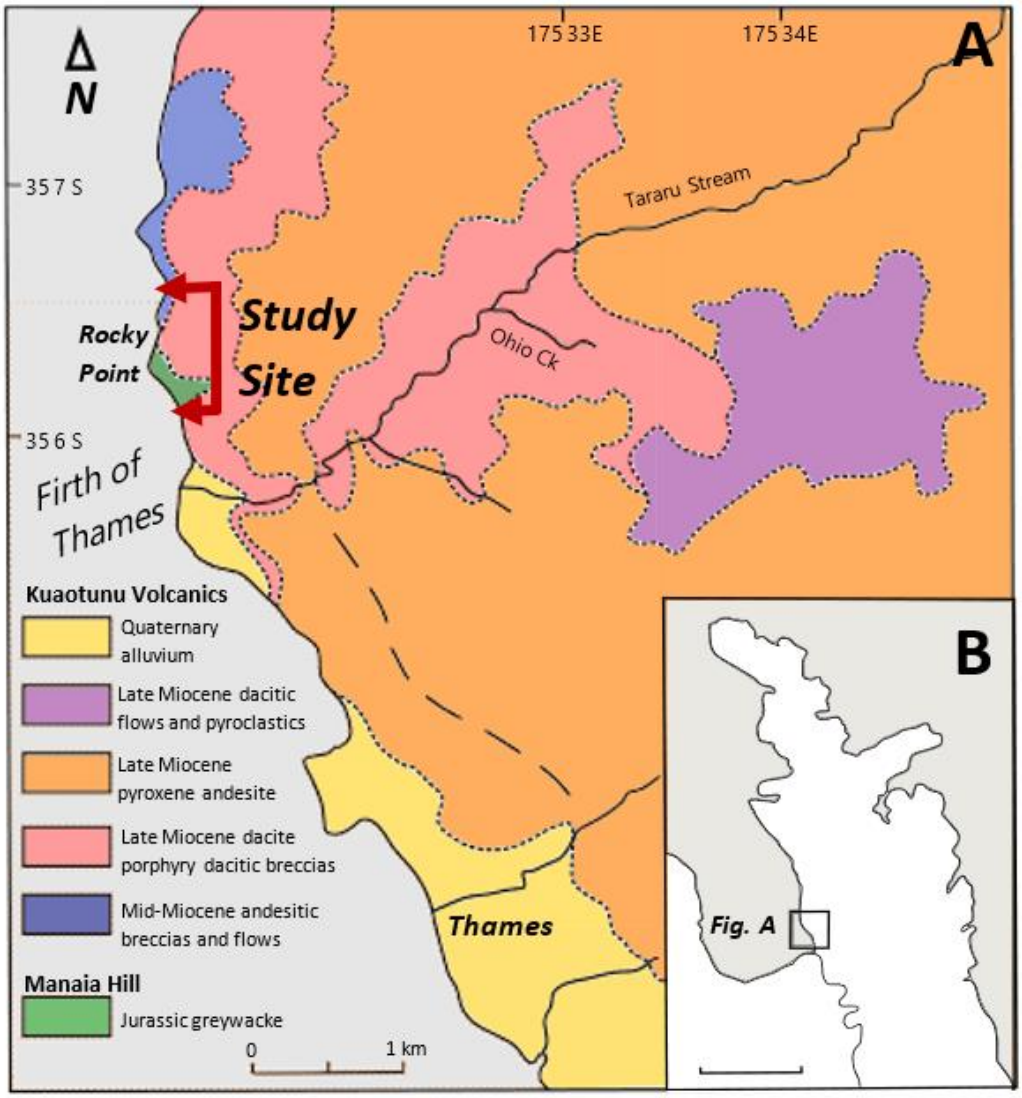

Figure 6: A. Location of the study site and regional geology near the Thames township dominated by Kuaotunu subgroup volcanics but with a small site of Manaia Hill greywacke. B. Location of map A on the Coromandel Peninsula. Modified from Brathwaite et al. (2001a).

3.2 Coastal Strip Geological Map

The purpose of field mapping was to classify and describe the host rock types present, the hydrothermal characteristics and pebble dykes spatial relationships within the site. A geological strip map was constructed and is shown in Figure 7, which focuses on the host rock lithology and alteration characteristics along the

site. The host rocks present include northern, southern and central exposures of cohesive andesite, volcanic breccia and greywacke which are described in detail in section 3.3. The varied alteration characteristics that have modified the rock lithologies are also described in detail later in chapters 4 and 5 and discussed in the final discussion chapter 7.

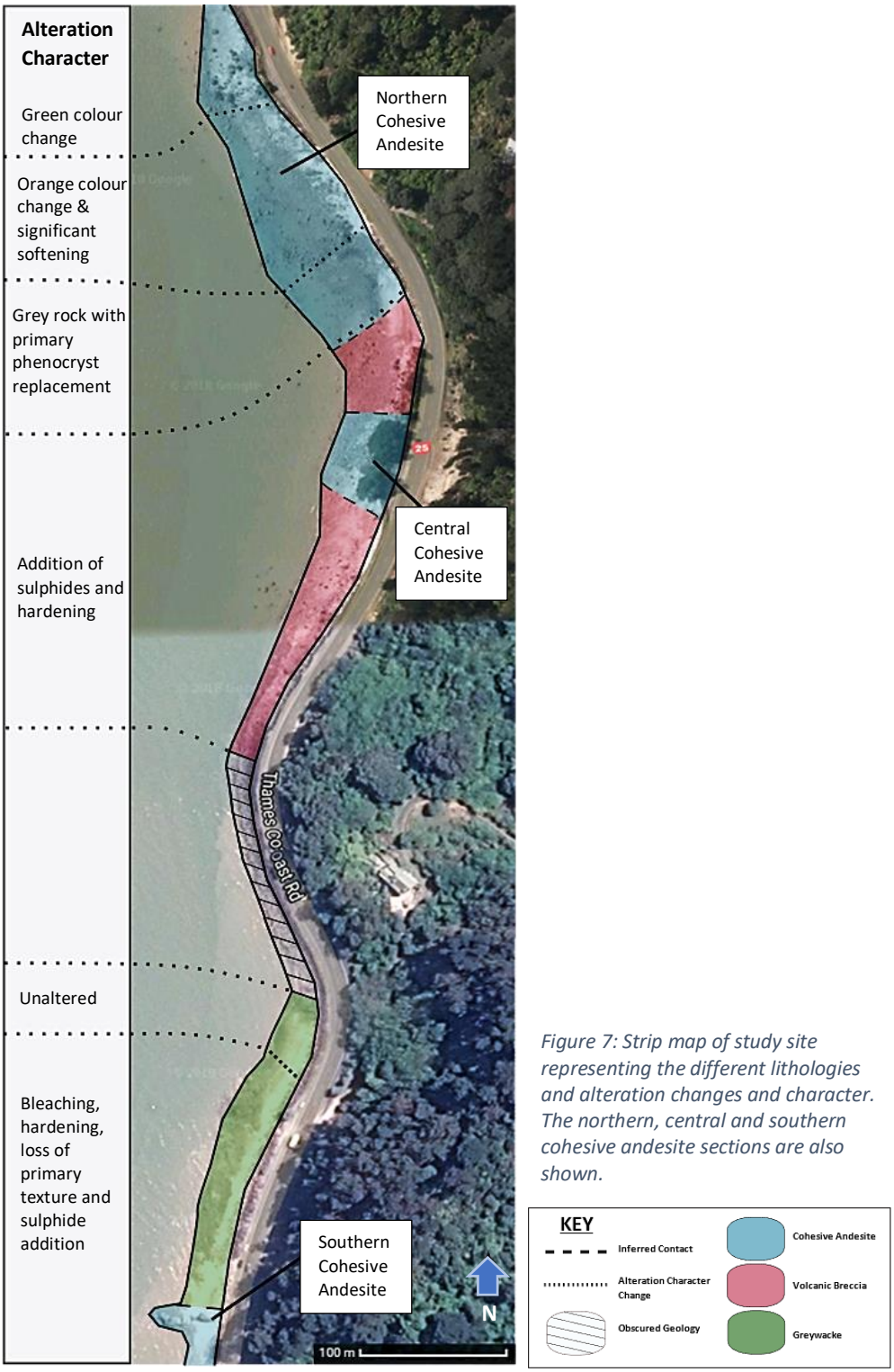

Figure 7: Strip map of study site representing the different lithologies and alteration changes and character. The northern, central and southern cohesive andesite sections are also shown.

Samples were taken along the stretch of the strip map at appropriate sites, from each pebble dyke and representative host rock lithologies as well as where is was evident alteration character had changed. The samples and their associated rock units are summarised in Table 3, as well as laboratory analyses undertaken on these samples (see following chapters).

Table 3: Summary table of samples retrieved from the field, the units they were taken from (see Fig.7 units) and lab analyses that were used on each explored in later chapters.

Rock Unit	Sample	Thin Section	SEM	XRD	XRF	ICP-MS
	Northern:					
	UN-AND	●	●	●	●	●
	OR-AND	●		●	●	●
	GR-AND	●	●	●	●	●
Cohesive	**Central**:					
Andesite	HST-AND	●		●	●	●
	HST-TRAN*	●		●	●	●
	Southern:					
	RP1	●	●	●	●	●
	RP2	●		●	●	●
Volcanic	BRC-1	●	●	●	●	●
Breccia	BRC-2	●		●	●	●
	G1	●		●	●	●
	G2	●	●	●	●	●
Greywacke	G3	●		●	●	●
	6-HST-G*	●		●	●	●
	PBL-1	●		●	●	●
	PBL-2	●		●	●	●
	PBL-3	●				
Pebble Dykes	PBL-4	●				
	PBL-5	●				
	PBL-6	●	●			
	PBL-7	●				

** Host rock samples proximal to a pebble dyke body.*

Throughout the process of mapping and sampling, hydrothermal alteration complicated the identification of host rock types recognised in the field. Therefore, classifications are supported by petrology in chapter 4. As the study site is located on a beach, sand and debris build-up periodically obscured areas

of the geology, further complicating mapping. As a result, a sizeable buried section is indicated in Figure 7 which has been left unclassified. Also due to burial and difficulties in sampling the pebble dykes in the southern site, only enough rock for petrology but not geochemical or optical analysis was collected for the associated bodies.

3.3 Unit Descriptions

Cohesive Andesites

One of the main host rock types within the field area are lavas from the Coromandel Group volcanics. They occur as cohesive and well-exposed andesites, described as cohesive due to their massive, homogenous texture compared to the fragmental texture of the breccia units elsewhere on the beach. The presence of this host rock is not continuous, with three separate exposures separated by other lithologies along the beach strip. Due to this geographic separation and as each of the cohesive andesite exposures display different alteration characteristics, they have been subdivided into the Northern, Central and Southern andesites (seen in Fig.7). The Central andesite is described first as it hosts the largest cluster of pebble dykes. The Northern and Southern andesites are then described, each representing the upper and lower boundaries of the field site.

Central Cohesive Andesite

Appearance: This unit is located just north of the centre of the site, visible both along the beach face and as a bank face outcrop created through wave action. It is one the best exposed of the cohesive andesites however it is also one of the smaller outcrops, spanning just ~ 50 m. It's surface colouring has an orange/brown discolouring resulting from weathering, whereas the fresher surface is a dark almost purplish-grey. The outcrop displays the massive, featureless character recognised in the other cohesive andesites elsewhere,

linking them stratigraphically. The relict porphyritic texture has been modified, resulting in the loss of much of the original grain boundaries creating instead a fine-grained homogenous character. However, despite the alteration, occasional individual feldspars grains are visible and due to the association with the Northern and Southern exposures and later petrographic observations, the andesitic classification is made with confidence.

Alteration: Although the section does not appear as visibly altered as some of the other cohesive andesite outcrops, it hosts the highest density of pebble dykes within the field, making it one the most important host rock sites. Two samples were collected from this outcrop (HST-AND and HST-TRAN) to compare the host rock mineralogy and chemistry both proximal and distal to the pebble dykes (Fig. 8A).

Much of the original igneous texture is masked with a "cloudy" appearance due predominantly to silicification, which has also hardened the rock making it very hard and brittle. The addition of quartz is also evident in the form of infrequent clusters of quartz, the largest appearing close to a dyke body (Fig. 8B). Addition of sulphides is also apparent, with visible (up to 1 – 2 mm) euhedral grains occurring in clusters or as fine mm scale veinlets appearing sparsely in the rock with no orientation preference. The sulphides are clearly visible and are not

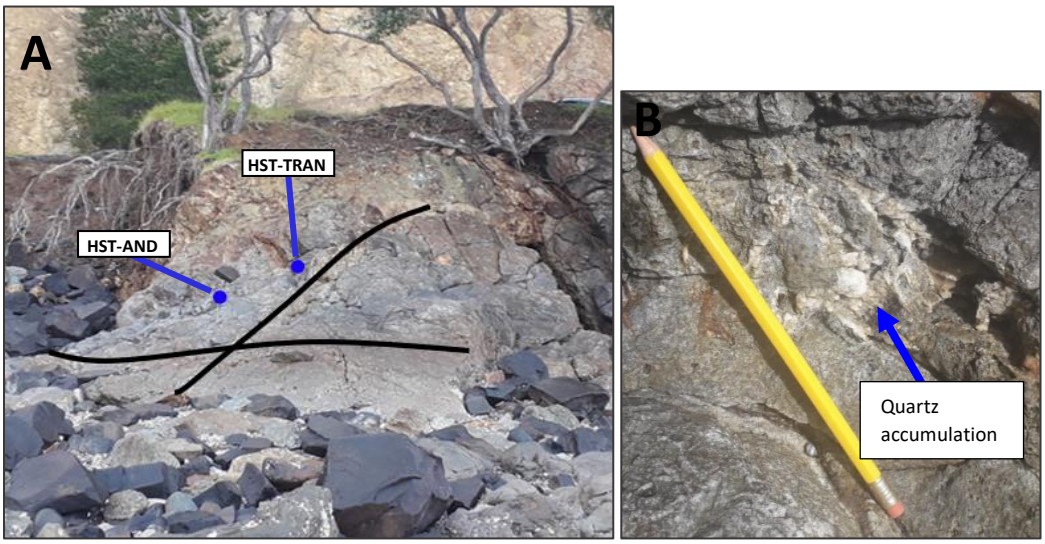

Figure 8: A. Outcrop of Central altered andesite unit. Two locations were sampled, indicated by the blue points, with varied proximity to a pebble dyke hosted in the unit. Visible pebble dykes are indicated by black lines, sample HST-TRAN retrieved adjacent one of these bodies. B. Accumulation of quartz located proximal to the site of HST-AND sample.

masked by the cloudy texture affecting the original igneous texture. This may, therefore, indicate sulphide addition at a later stage of the hydrothermal system.

Northern Cohesive andesite

To the north of the Central andesite (but separated by a breccia outcrop) is a series of cohesive andesites with varied alteration character (Fig. 7). Successively to the north, they are referred to as “Grey”, “Orange” and “Green” for the following outcrop descriptions to separate the different alteration facies of the same continuous Northern andesite unit. Unlike the Central cohesive andesite, these outcrops only appear as exposures along the beach face and as a result are more poorly exposed due to burial by sand.

- ***Grey***

Appearance: The first of the Northern andesites is present as multiple, small (< 1 m) exposures on the beach, appearing as a dark grey/green rock (Fig.9). It displays a better-defined porphyritic texture compared to the Central cohesive andesite and lacks the same cloudy texture. The parent phenocrysts texture is also coarser-grained, with the larger forms in the shape of euhedral amphiboles and pyroxene phenocrysts.

Alteration: The outcrop does not display the same brittle nature as the Central andesite exposure and is also lacking the visible sulphide grains. Hydrothermal

Figure 9: Small beach exposure of the “Grey” andesite from the Northern cohesive andesite.

structures are also absent (e.g. veinlets, pebble dykes or other associated features). This exposure is however not very extensive; therefore, such hydrothermal features may be buried. The main indication of alteration of this grey andesite is the appearance of the amphibole and pyroxene forms, which are a white colour and are soft, giving them a “dusty” quality, reflecting their replacement by pale secondary minerals. This aspect is expanded on further in chapter 4, where petrological observations reflect this is a result of alteration preserving igneous textures rather than destroying them.

- ***Orange***

Appearance: This outcrop lies adjacent to the north of the grey andesite but is better exposed as larger sections due to less sand burial. The colour of this variant of the Northern cohesive andesite changes to a rusty orange colour which persists in freshly broken rock rather than just surface weathering (Fig.10). A colour change of this manner may be indicative of oxidation occurring due to hydrothermal alteration (Schwartz, 1959). The primary volcanic texture preserved in the orange outcrop is also much less apparent, having been more strongly replaced by alteration.

Figure 10: Outcrop from the Northern cohesive andesite which has been altered to a uniform orange colour, contrasting to the neighbouring grey exposure to the south.

Alteration: The much softer nature and porous character of the orange rock, where some sections easily crumble, implies more intense alteration. This is also reflected in the obvious colour change. Many of the phenocrysts within the rock have also been altered to a reddish-brown colour, which is mirrored in the colour of infrequent pseudo-clasts which are not present within any of the other Northern andesite sections (Fig.11A).

Figure 11: Alteration textures and structures in the orange zone of the Northern cohesive andesite. A. The largest of the clast-like features which have been altered to an orangey-red colour within an otherwise cohesive andesite. B. Possible hydrothermal related brecciation within the altered andesite. C. Thin veinlets filled with quartz.

Despite the lack of disseminated sulphide grains, sulphides are present in the form of millimetre-wide meandering veinlets, however, they are less abundant than similarly sized quartz veinlets (Fig.11C). The porphyritic texture, although still present, is less well-preserved than seen in the Grey outcrop. The alteration character of the Grey outcrop is however similar, with obvious secondary mineral replacement and softening of original phenocrysts, however to a more

intense degree and causing more obvious destruction of their shape. The grain size of the rock also appears to have diminished and the phenocrysts where visible have taken on a more homogenous mineral size and form.

A localised brecciation was found (Fig.11B) in a partially buried outcrop that does not appear to be related to any pebble dyke. It consists solely of fragmented host rock material with poor sorting and unoriented clasts.

- ***Green***

Appearance: The alteration within this exposure of Northern cohesive andesite has developed a distinctively green colour, with some brown surface weathering in areas (Fig.12A). It extends past the end of the northern boundary of the study site but is present within the site across half the distance of the Orange section. The contact between the altered Green and Orange units is exposed and is gradational in character over roughly 20 cm (Fig.12B).

Alteration: The green colour is again the most obvious sign of alteration and is likely due to the presence of chlorite. Apart from the colour, the Green andesite shares much of the same characteristics as the Orange section, however, with a lesser alteration intensity. The rock is soft, has infrequent sulphide veinlets and displays a modified grain form and size but with less intensity. The main difference is that its matrix is more indurated and dense compared to the uniform porosity of the Orange andesite. The Green unit may represent a

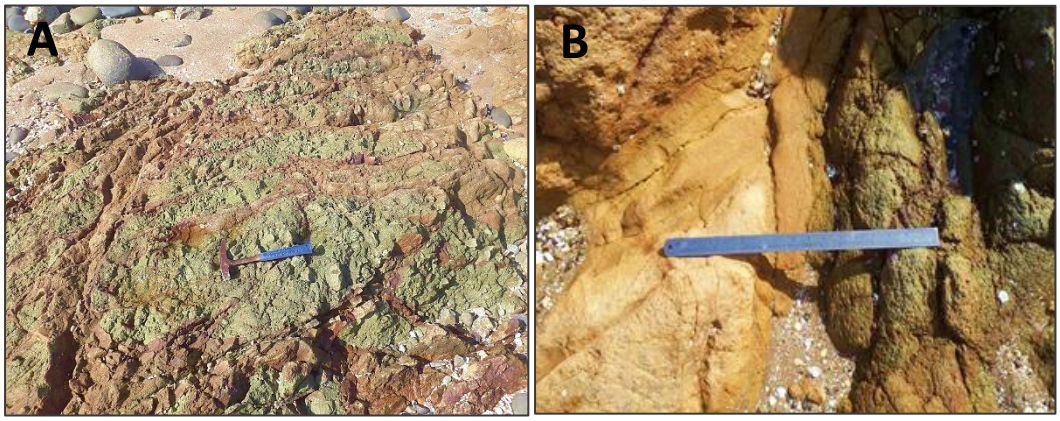

Figure 12: A. The northern-most outcrop of the Northern coherent andesite altered to a green colour with brown surface weathering. B. Gradational contact between the altered Orange and altered Green exposures of andesite.

transitional degree of alteration between the grey andesite with its preserved texture, and the more intensely altered orange section.

Southern Cohesive Andesite

Appearance: The Southern cohesive andesite is a bleached yellow/grey rock which extends past the southern boundary of the study site hosting a 50 m stretch. It is non-uniform along its length as the grain size becomes marginally coarser and displays a more intense surface weathering to a rusty orange-red colour father to the south. Due to these noted changes two samples were taken (RP1 and RP2) to reflect any variance in mineralogy, particularly as a pebble dyke exposure is located between the two sample sites (Fig.13).

The boundary of the southern section of andesite and the neighbouring greywacke is difficult to define due to their similar manner of alteration. However, the initiation of this outcrop appears to be suggested by the morphology of the beach, where a tall outcrop (locally known as Rocky Point

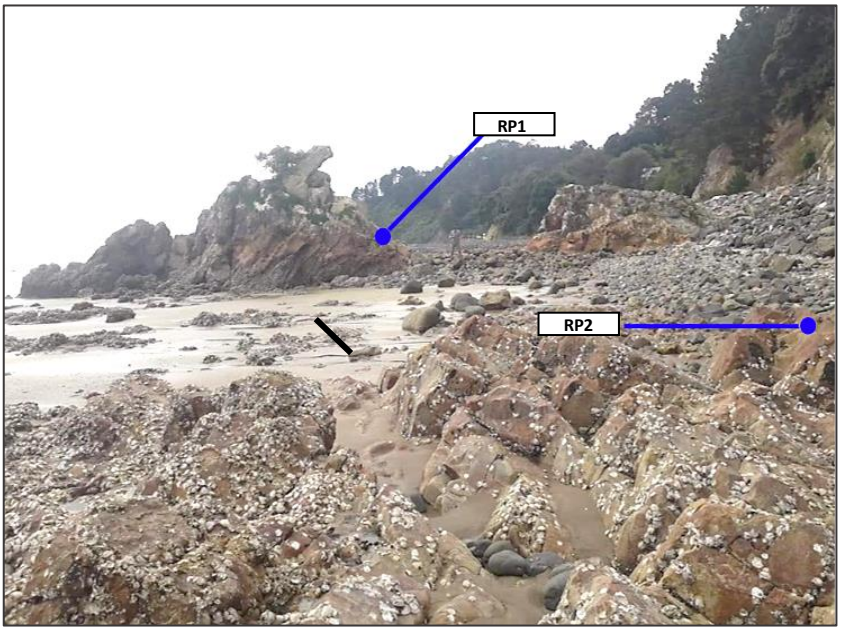

Figure 13: Outcrop of the Southern cohesive andesite near the southern boundary of the field site with the location of RP1 and RP2 sample sites. The approximate position of the identified pebble dyke is indicated by the black line, which at time of the photograph, was buried by sand.

seen in Figure 6) contrasts against ground exposures of greywacke (Fig.14A) and is further supported with petrology in chapter 4.

Alteration: Extensive alteration has destroyed the primary texture, resulting in an almost fine-grained, homogenous character across much of the rock and a significant proportion of the mineralogy is secondary. The rock also appears to have been hardened, even more so than the Central cohesive andesite due to silicification. There is also abundant disseminated sulphides, with individual grains easily visible in hand specimen.

The pebble dyke hosted within the Southern andesite, one of the two bodies found in the southern region of the field map, is the widest at the site. Other evident hydrothermal features are the abundance of sulphide filled veinlets which are a few millimetres wide and occur all over the outcrop, appearing most concentrated at the Rocky Point feature (Fig.14B).

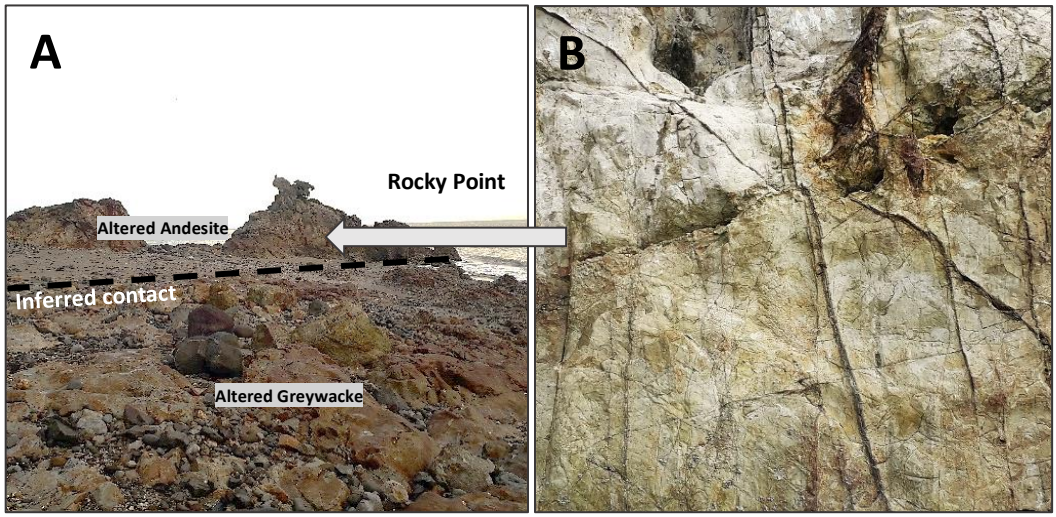

Figure 14: A. The inferred contact between the southern altered andesite and altered greywacke, indicated by the geomorphology of the small Rocky Point peninsula. B. The abundant sulphide filled veinlets on the Rocky Point outcrop. Site of photograph subject in B indicated by the grey arrow.

Volcanic Breccia

This breccia unit, like the cohesive andesite, also belongs to the Coromandel Group Volcanics. Located in the central region of the site, it is well exposed along a substantial length of beach, appearing both north and south of the Central cohesive andesite (Fig.7). A sharp contact occurs between the southern breccia with the Central andesite (Fig.15), whereas elsewhere lithological contacts are not exposed.

Figure 15: Contact between Central cohesive andesite outcrop and the southern volcanic breccia.

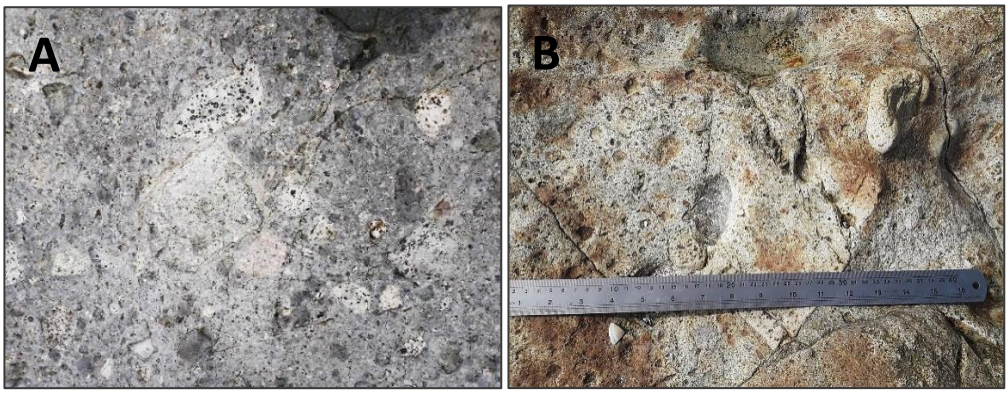

Figure 16: A. Clasts and matrix of the pale blue-grey northern volcanic breccia outcrop. B. Weathered surface of southern volcanic breccia outcrop and its clasts with 40 cm ruler for scale.

Appearance: The northern breccia section is exposed across ~ 50 m, the southern section along ~ 150 m until it is buried by sand and beach debris. Both of these beach face outcrops are similar in that they both display a very high matrix to clast ratio and similar clast size ranges and forms. The most prominent difference is the pale blue-grey colour of the more northern exposure, compared

to pale grey seen in the southern exposure, which also has more significant orange surface weathering (Fig.16).

The matrix of the breccia ranges from sand to silt in size, the northern section with a slightly higher sand proportion. The clasts can reach up to 15 cm in size but generally remain in the range of 2 – 5 cm. They are polymict in composition, the various volcanic and sedimentatry lithologies with varied colours and textures is described in chapter 4. All clast lithologies are sub to well-rounded. No evident flow structures are present in the matrix or clast distributions. There is however an increase in the abundance of clasts away from the central andesite.

Alteration:

The breccias are not notably hardened and are not evidently silicified, no significant colour change is apparent and although sulphides are present, they are low in abundance. There are however apparent hydrothermal features found in the southern section, including two parallel pebble dykes. Another feature of particular interest is where the host breccia unit is fractured and fragmented, in the style of a crackle breccia or jigsaw-fit texture which often form by hydraulic fracturing (Fig.17A). Within the resulting void space there is fine-grained, clay size material. Therefore, this feature represents fragmentation and possible chemical and/or physical milling processes which may be related to the pebble

Figure 17: Hydrothermal features within the southern volcanic breccia outcrop A. Possible hydrothermally-formed fractures which have created voids and infill of clay-sized material. B. Oval shaped concentration of fine sulphides around the mould of a plucked clast

dyke formations located only a few metres away. There is also an oval-shaped concentration of fine-grained sulphides which appear to line the mould of a plucked clast (Fig.17B), suggesting sulphide-bearing fluids percolated and precipitated around the clast surface.

Greywacke

Unaltered: fresh greywacke is exposure along ~ 150 m of the southern end of the beach. The northernmost part of this section is a beach face exposure expressed as a dark grey fine-grained unit (Fig. 18A). It consists of beds of well-sorted, dark grey siltstone (argillite) which is interrupted by occasional beds of lithic supported sandstone (greywacke). These beds are more poorly sorted and contain angular to sub-rounded lithics with a size range of generally 1 – 5 mm. Within the coarser beds, the lithic grains are pale and dark brown or grey in colour, reflecting a variety of lithologies. Farther up the beach face and to the south, this exposure becomes a slightly paler brown, and sandstone becomes more dominant over siltstones.

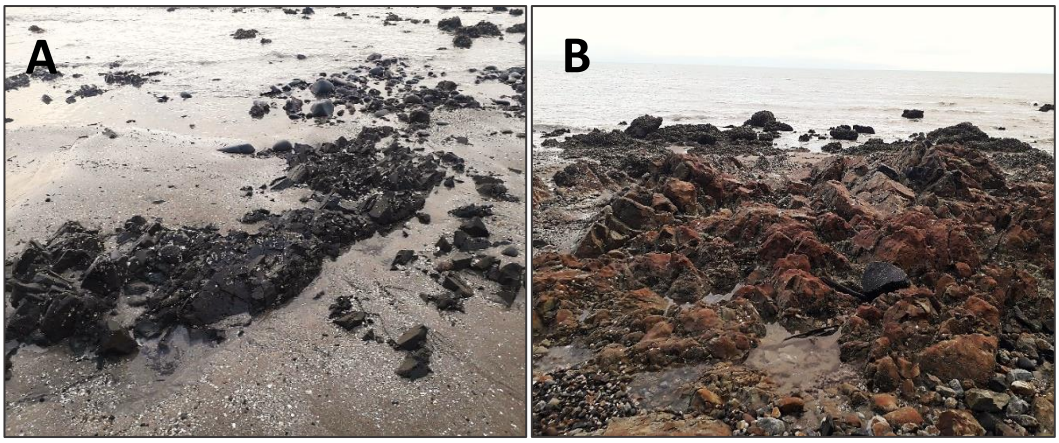

Figure 18: Exposure of unaltered greywacke (A) contrasting to the altered greywacke (B) only a few meters to the south.

Altered: The unaltered greywacke transitions into significantly altered outcrops only a few metres down the beach (Fig. 18B). The surface of these rocks is weathered to an orange colour; however, freshly broken rocks show an internal bleached colour and are visibly abundant in sulphides. Hydrothermal alteration

commonly causes colour changes such as this, typically as a result of lighter minerals replacing the primary assemblage (Schwartz, 1959). The altered rock generally appears very fine-grained, with almost no visible grains or bedding. This massive texture is cut by millimetre-wide veinlets of sulphides, which appear to become more abundant towards Rocky Point (Fig.19a). Farther south, however, sulphides also become less restricted to these veinlets and instead, are scattered within the rock. The unit is more indurated due to possible silicification, however not to the same degree as the Rocky Point andesite.

Characteristics indicative of alteration appears to intensify as the unit continues to the south, possibly linked to a higher intensity of hydrothermal fluid interaction. This includes the appearance of an exposure of a hosted pebble dyke. Samples were taken from increasing distance from the unaltered greywacke as well as towards the pebble dyke (G2 and G3) to recognise the variation in alteration, with one taken from directly adjacent to a hosted dyke body (6-HST-G).

3. 4 Locations and Morphology of Pebble Dykes

There are multiple hydrothermal features along the length of the study site which have been discussed in reference to the units which host them. Their locations have been compiled onto a modified version of the geological strip map (Fig.19a).

Amongst these hydrothermal features are also several pebble dyke bodies. Two clusters of pebble dykes (Cluster A and Cluster B), within which are seven separate bodies, were identified. Their extent can be seen in Figure 19a with more detail at each of these sites in Figures 19b and c. A descriptive summary of each of the major (units >5 cm wide) pebble dykes have been compiled in Table 4 but are discussed in further detail below.

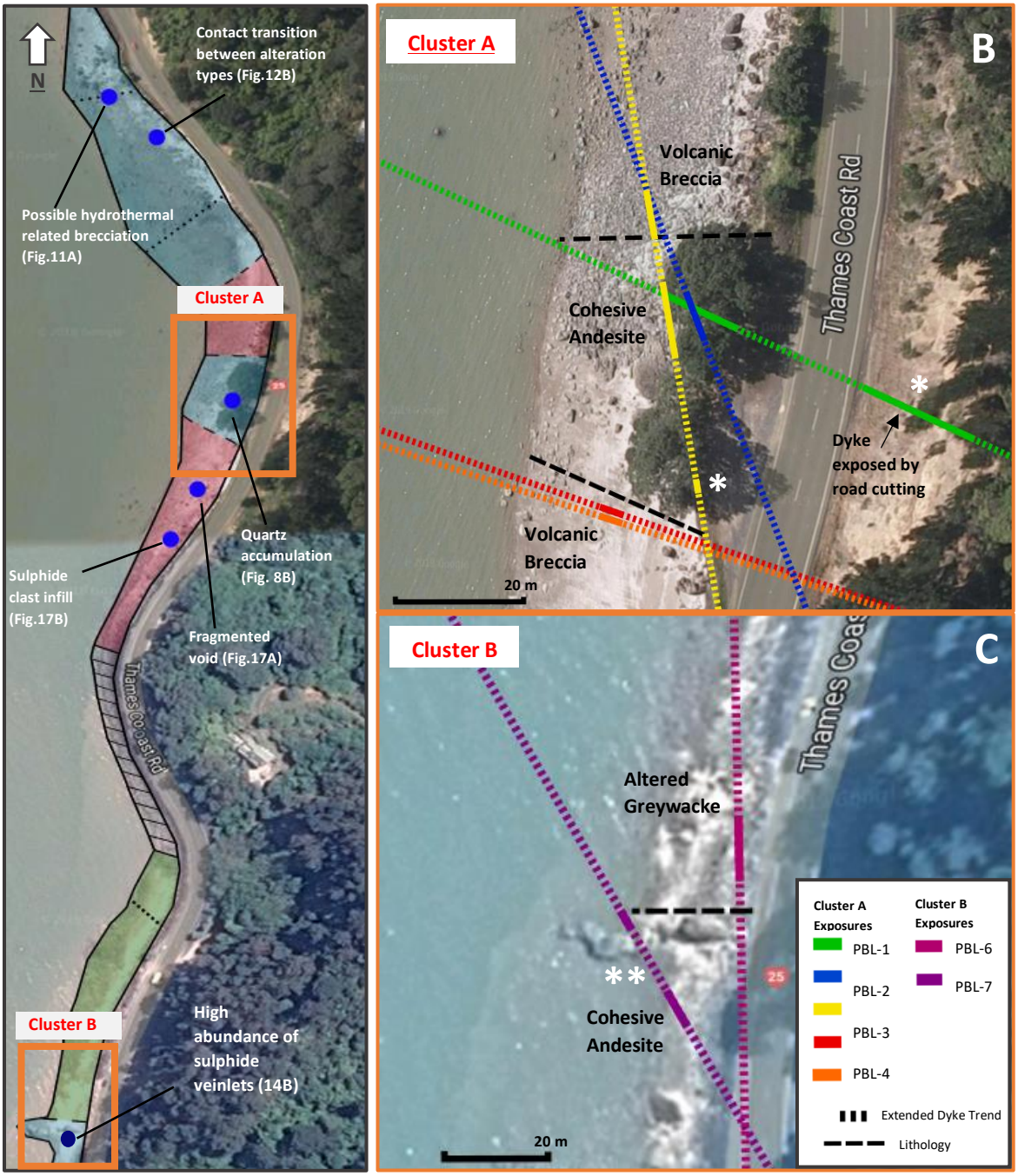

*Figure 19: A. Locations of hydrothermal features detailed in the previous section (3.3). Pebble dykes are located within the boundaries of the areas defined as "Cluster A" and "Cluster B". B&C. Zoomed in views of each of the dyke clusters. Dyke trends have been extended to reflect possible interactions they may have which are not visible on the beach. * Exposures which are inferred to be an extension of dykes within the main beach outcrop. ** The trend for PBL-7 is likely less accurate, due to issues in the field of sand burial when retrieving the orientation.*

Table 4: Summary of the characteristics of each of the major pebble dyke bodies found along the study site.

Pebble Dyke	Cluster[1]	Host Rock[2]	Width Range	Max Clast Size	Morphology[3]	Cross-Cutting[4]
PBL – 1	A	Cohesive Andesite	16 – 27 cm	10cm	Straight	PBL – 2 & 3
PBL – 2	A	Cohesive Andesite & Volcanic Breccia	18 – 52 cm	9 cm	Undulating	N/A
PBL – 3	A	Cohesive Andesite & Volcanic Breccia	2 – 17 cm	5 cm	Straight with major thickness changes	Minor dyke
PBL – 4	A	Volcanic Breccia	8 – 11 cm	3 cm	Straight	N/A
PBL – 5	A	Volcanic Breccia	8 – 23 cm	4 cm	Straight	N/A
PBL – 6	B	Altered Greywacke	3 – 12 cm	4 cm	Straight with branches of smaller dykes (1 – 3 cm width)	N/A
PBL – 7	B	Altered Greywacke & Cohesive Andesite	20 – 40 cm	12 cm	Straight but main body splits in two	N/A

[1]Cluster = The grouping on the beach the pebble dyke belongs to (A or B) (Fig.19).
[2]Host Rock = The lithology the dyke is hosted in.
[3]Morphology = characterises the form of the exposed dyke sections at an outcrop scale.
[4]Cross-cutting = details any cross-cutting relationships they have with other dykes.

Pebble Dyke Clusters

Cluster A – The most prominent cluster of pebble dyke bodies is located at the centre of the study site, focused within the Central cohesive andesite (Fig.20A). These dykes are found within the "Cluster A" section of the map seen in Figure 19B. The three major bodies found here are PBL-1, PBL-2 and PBL-3, with two smaller exposures, PBL-4 and PBL-5 to the south hosted in the volcanic breccia (Fig.20B). Higher up the beach face behind PBL-4 and 5, a wide dyke body is exposed (~20 cm) and is inferred to be a continuation of PBL-3 due to their comparable orientations (Fig. 19B). All exposures within the Cluster A site appear along a ~ 75 m span of the beach, with PBL-3 visible for the longest stretch, almost continuously for ~20 m. Due to this, PBL-3 is hosted within both volcanic breccia and cohesive andesite, and although the transition from one lithology to

the other is not exposed, there are no apparent changes in the dyke character between the two sites.

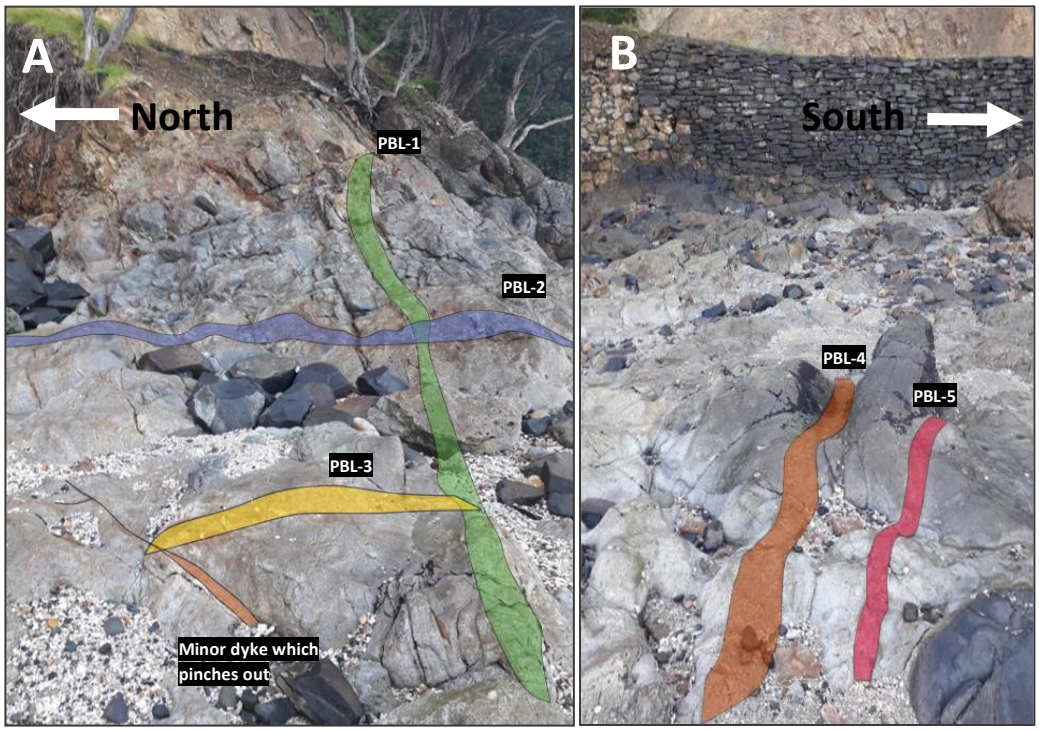

Figure 20: A. The positions, orientations and cross cutting relationships of the largest grouping of pebble dykes within Cluster A. B. Two very similar pebble dyke exposures in Cluster A, a few meters south of the dykes in figure A.

Each of the pebble dykes within the central section of Cluster A have a somewhat similar character. They display very sharp contacts with the host rock, are clast-supported and very indurated. They each display the characteristic rounded pebble components with occasional sub-angular clasts which appear to consist of varied lithologies, which are discussed later in the chapter. Sulphides are also present, appearing as clumps of fine material within the matrix, however, they are not as disseminated as in the case of the host rocks. PBL-4 and 5 are the most similar to one another, orientated in parallel and their morphology, clast sizes and widths are comparable. This likely indicates their timing and formation have a close relationship, possibly even belonging to branches of a larger dyke body from the same formation event.

Dykes differ in their relative orientations. PBL-2 and PBL-3 each run parallel to one another (NNW trend) and cross-cut PBL-1 (NWW trend) (Fig.20A), whereas the trend of PBL-1 is more similar to PBL-4 and 5 (Fig. 19B). The morphologies of

the Cluster A dykes also vary, as in the case of PBL-2 which undulates across the ~4 m length of exposure compared to the straight geometries of the others. Their widths generally range from 10 - 30 cm and PBL-3 can be seen to narrow in the span of approximately a metre to as little as 2 cm. There is also a “minor” dyke < 2 cm in size which cuts across PBL-2 (Fig. 20A). It pinches completely, potentially representing a branch of one of the larger dykes present. Widths also appear to relate to the size and form of the components found within them. In wider dykes, or within wider sections of a body, larger clasts tend to be hosted. Whereas in the narrower features, much finer and compacted clasts are found, often appearing as more sub-angular in morphology than the rounded rock fragments in the wider sections.

- *Adjacent Road Cutting*

Upslope of the beach bank outcrop hosting Cluster A, within a road cutting, a vertical dyke-like feature is also exposed (Fig. 19B). This feature does, however, have a markedly different character to any of the dykes found on the beach, only its orientation and tabular form suggesting it may be an extension of PBL-1. It is much softer, yellow-brown and featureless relative to the beach outcrops with no preserved clast oulines due to a higher degree of alteration and weathering.

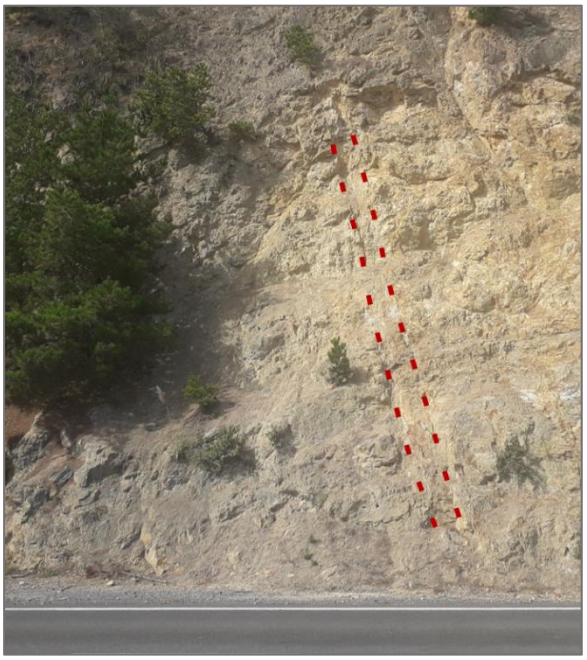

Figure 21: Possible exposure of extension of PBL-1 in road cutting.

Cluster B – At the southern end of the study site, in the area termed "Cluster B", there are two pebble dykes (Fig.19C). These dykes have smaller exposures than those of Cluster A, some less than one metre long. There are however, multiple exposures of the same dykes across a larger area of the beach. Their morphology can be seen to vary more than the Cluster A group, with irregular widths and branching morphologies. PBL-6 is the northern-most of the two, and has many branches of thin, <1 – 2 cm wide dykes which appear to split away from the main body (Fig. 22). The major PBL-6 body narrows from 12 cm to 3 cm, so is smaller than most of the units found to the north. Its clast sizes also reflect this, the largest reaching only a few centimetres.

Figure 22: Pebble dyke (PBL-6) with multiple narrow branches which appear to split from the central main exposed body (pencil for scale).

The southernmost unit on the beach, PBL-7, also displays a branching character, where the 40 cm dyke body splits into two (Fig.23). PBL-7 is one of the largest of the pebble dykes exposed along the beach, contrasting to the much smaller PBL-6. It is possible for these two bodies to be branches of the same dyke, as they display a similar trend and possibly intersect farther south (Fig.19C). If this was the case, they demonstrate irregular thicknesses and attitudes across a relatively small area of ~ 50 m.

Figure 23: The largest pebble dyke in the field site, PBL-7, that splits into two smaller branches (40 cm ruler for scale).

Lithic Quantification

To provide a rough quantification of the different types of lithologies present in a pebble dyke, the simple characteristic of clast colours has been used to indicate different rock types. In the field a 7 x 11 grid with 1 cm intervals was drawn on top of an exposed pebble dyke, then clasts at intersections of the grid were classified providing a count of 87 (the other 9 points fell on host rock due to the non-uniform shape of the dyke). PBL-3 was used as the basis for this as it was the best exposed and had the least weathered clasts in the field (Fig.24). Although this classification only represents PBL-3 components, the proximal dykes at least would be expected to have a similar clast content.

Clasts were separated into three categories of observed colours, identified as dark grey (Dg), light grey (Lg) and white (W) and counted along with the matrix to reflect their proportions. The results are displayed in graph form in Figure 25. Lg is the most abundant clast hosted in PBL-3, accounting for 45% of the components. The proportion of Dg and matrix are present in similar abundance at ~15%, with W present in a marginally less.

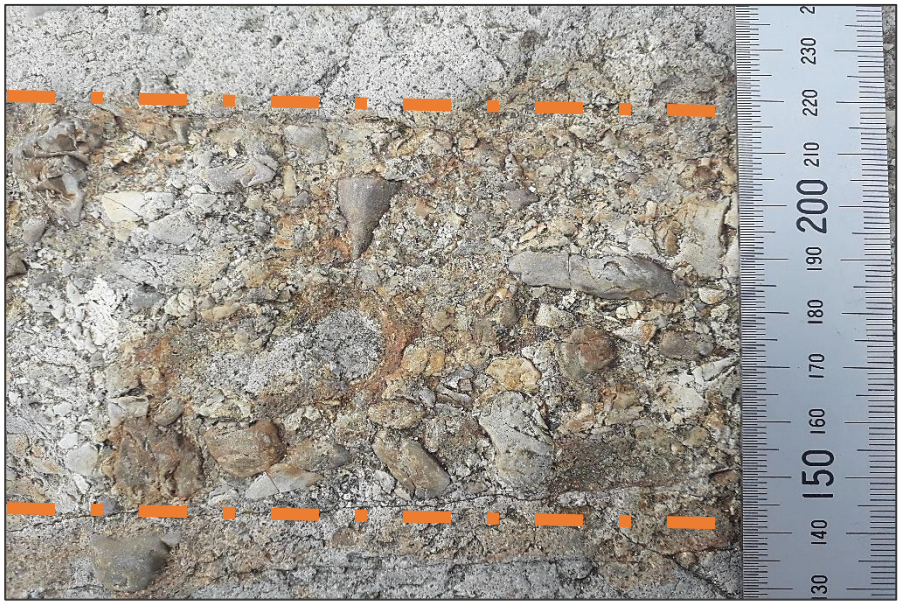

Figure 24: Section of pebble dyke used for lithic quantification (PBL-3) from Cluster A. Components of nearby dykes are not as well exposed as this site, however, they reflect a similar mixture of clast forms and colours as seen within this section.

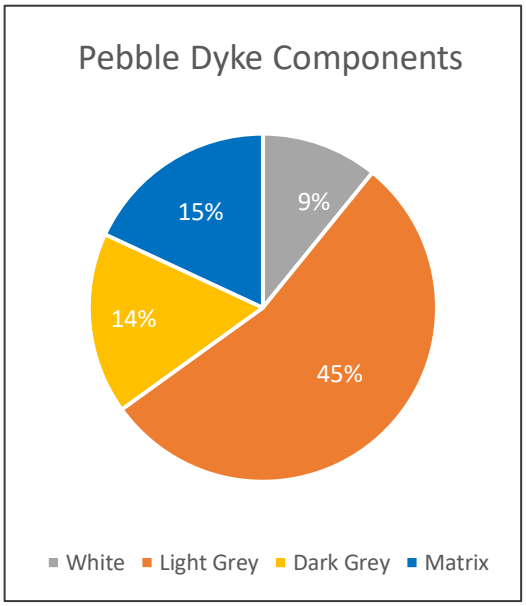

Figure 25: Proportions of clast types classified based on their colouring and matrix.

Petrological observations in the following chapter confirm that clasts are composed of argillite and sandstone with a lesser proportion of volcanics. This is supported by the descriptions of the pebble dyke clasts in the area by Merchant (1978) & Skinner (1967) who describe an assortment of sedimentary and calc-alkaline volcanic and plutonic rocks. This mixture of rock types represents the typical lithologies of the Coromandel Group volcanics and Manaia Hill basement

greywacke. The dark grey clasts (Dg), are the regional basement greywacke. As the proportion of the Lg clasts are so high, together with the Dg clasts they may represent the combination of greywacke argillite and sandstone identified in the dyke. This, therefore, indicates that the volcanic components may be accounted for by the W clast proportions and the matrix likely consists of a fine mixture of each of these present clast lithologies.

4. Host Rock and Pebble Dyke Petrography

Different zones of alteration occur at the study site, reflected in the varying secondary minerals, textures, hardness and colour of the host rocks. Optical mineralogy and electron microscopy allow for mineral identification and the determination of small-scale textural relationships that aid in understanding the fluid-rock reactions and secondary paragenesis of minerals. This too enables a better understanding of the host epithermal system.

Twenty samples were taken from both host rock and pebble dykes and from them twenty-nine polished thin sections were made (Chp. 3: Table 3). These sections were examined by transmitted light microscopy, which was useful for much of the petrographic analysis, however, for identification of the opaque minerals which were more abundant within the rocks with higher alteration intensity, reflected light microscopy was also used. The resulting descriptions were also further supplemented by scanning electron microscopy (SEM), which provided both textural detail through imaging and compositional determinations of minerals through energy-dispersive X-Ray spectroscopy (EDS) within the same polished sections.

Methods

Hand rock samples were cut to fit standard petrographic glass slides, then mounted to them with resin before they were cut and ground down to a thickness of ~30 microns with a Struers Discoplan-TS. For the more porous rock samples, a further step of resin impregnation was included to lessen loss of material during grinding. These mounted thin sections were then polished with a Bueller twin polisher grinder and 0.3 micron grit silica carbon (SiC) powder. As the prepared samples were polished, this also enabled their use with SEM analysis. The SEM instrument for this purpose was a Hitachi S-4700, with both backscatter imaging and EDS detectors used.

4.1 Alteration Texture and Intensity Terminology

Alteration of rocks in a hydrothermal system drives changes in mineralogy, texture and chemical composition. Pre-existing mineral phases become unstable during changing hydrothermal conditions and are replaced by more stable secondary minerals. This modification of minerals can occur via a variety of processes which can create varied alteration textures. Processes which alter textures in volcanic rocks have been described by Gifkins et al. (2005) and are listed in Table 5.

Table 5: Alteration textures of volcanic rocks described by Gifkins et al. (2005).

Replacement	Existing minerals or glass is replaced by one or more new mineral species
Infill	A mineral or minerals are precipitated from solution into open space
Dissolution	Existing minerals or glass is leached and removed by solution with or without replacement
Static Recrystallisation	Recrystallisation of existing minerals to new grains, and/or a change in the morphology of the same mineral species or composition
Dynamic Recrystallisation	Recrystallisation of existing minerals to new grains and/or a change in morphology and/or orientation of the same mineral species or composition
Deformation	Existing component or texture is rotated, milled, broken, compressed, modified, distorted or fractured

Although the processes listed in Table 5 are specific to volcanic rocks, these same processes can also be present in sedimentary rocks, such as the greywacke exposed at the study site. Therefore, these terms have been used when describing each of the samples. Alteration processes cause changes to the shape, form, grainsize and orientation of grains, and may either preserve or destroy pre-existing textures. The resulting textures can be used to recognise the intensity of alteration, which mineral assemblages are in equilibrium with the hydrothermal system and can also reflect overprinting of alteration events indicating a paragenetic mineral succession.

The intensity of alteration experienced by a rock is the measure of how completely it has reacted with the system. It is linked to textural and compositional changes, as it measures the extent of the preservation of pre-

existing rock character. The most effective method of recognising the degree of alteration is by comparing samples with unaltered samples of the same unit. Within the study site, the only lithology that is unaltered is the greywacke so the intensity of the volcanic rocks onsite must instead be inferred from observed changes in mineral assemblage, texture and colour.

Petrographically, the intensity of alteration within the sample rocks can be qualitatively estimated, based on the abundance of new minerals and preservation or destruction of pre-existing minerals and textures. Gifkins et al. (2005) provides a ranking scheme to categorise rocks based on these traits. From this, a rank from fresh/least altered to significantly altered sections has been created, accompanied by brief descriptions of the alteration character of the host rock samples (Table 6).

Table 6: Host rock character of alteration and alteration intensity rank defined on the extent of growth of secondary alteration minerals, destruction of primary minerals and textures and pervasiveness of alteration texture. Classifications based upon criteria described by Gifkins et al. (2005).

Host Rock	Sample	Intensity	Description
Northern Cohesive Andesite	OR-AND	Moderate to Strong	Alteration of phenocrysts and groundmass is pervasive, so volcanic texture has been almost completely destroyed. Feldspar has been entirely replaced by chlorite, sericite and opaques and partial quartz dissolution has occurred. Weak pseudomorphs and outlines of phenocrysts remain visible
	GR-AND		
	UN-AND	Moderate	Alteration has a similar character to OR-AND and GR-AND, however, mafic mineral pseudomorphs are better preserved.
Volcanic Breccia	BRC-2	Weak	Replacement by sericite, calcite and epidote has occurred in a patchy and domainal manner, often centred around existing minerals, clasts and fractures. However, the primary texture has been predominantly preserved.
Central Cohesive Andesite	HST-AND	Moderate	Feldspars have only been partially replaced by carbonate and occasional epidote suggesting weak alteration. However, the mafic minerals have been entirely replaced and the groundmass has been completely recrystallised and is abundant in disseminated opaques.
	HST-TRAN	Moderate to Strong	Feldspars have been almost entirely replaced and most primary textures seen in HST-AND have been destroyed by alteration.
Volcanic Breccia	BRC-1	Weak	Appears more altered than BRC-2 due to the higher abundance of alteration minerals, particularly epidote. However, is not pervasive enough for most original textures to be lost.
Unaltered Greywacke	G1	Subtle	Primary minerals are unaffected by alteration. Any evidence of secondary mineral growth is only present on boundaries of primary phenocrysts and lithic fragments and infilled open space. The primary texture is clearly visible
Altered Greywacke	G2	Strong	Sparse relict clast outlines preserved. The primary phenocrysts and lithics have been completely replaced by sericite and opaques; some relict texture in the form of grainsize grading remains.
	G3		
	6-HST-G		
Southern Cohesive Andesite	RP1	Intense	No primary minerals remain, replaced by pervasive, almost homogenous alteration to sericite and quartz
	RP2		

This guide is also specific to the alteration of volcanic rocks, so the greywacke has been classified broadly based on the pervasiveness detailed by Gifkins et al. (2005). This petrographic summary of alteration intensity is also supported by geochemical representations of hydrothermal mineral assemblages discussed in later chapters. Therefore, these observations will be combined with XRF data for a more comprehensive alteration intensity overview in chapter 6.

4.2 Host Rock Petrography

Note: *The term sericite used throughout is in reference to the definition provided by Velde (2013); a textural term for a highly birefringent, fine-grained, micaceous mineral, which may be muscovite, illite or interbedded illite and smectite.*

Cohesive Andesites

Primary Phenocrysts

The most crystal-rich of the andesite samples is HST-AND taken from the central cohesive andesite outcrop which is abundant in tabular plagioclase phenocrysts (Fig.27A). These crystals display polysynthetic twinning, indicating that they are plagioclase rather than alkali feldspar in composition. Applying the Michel-Levy method, extinction angles measured from multiple twinned crystals average at 45°, suggesting a plagioclase composition of $AN_{75\%}$ of bytownite. Some instances of anhedral plagioclase crystals also display chemical oscillatory zoning, which is an indication of disequilibrium during crystallisation of the plagioclase. This is often a product of volcanic processes related to H_2O content during formation of the magma chamber (Hughes, 2013). Therefore, the zoning related to lava genesis and intermediate plagioclase composition suggests that the plagioclase within HST-AND is of the primary rock assemblage.

The boundaries of plagioclase crystals tend to be relatively well-preserved, with no significant replacement or dissolution textures. They do however have frequent patches of fine-grained cryptocrystalline minerals, displaying a much higher interference colour which is likely early sericitic alteration. This fine-

grained alteration mineral can also be seen infilling occasional fine fractures across the plagioclase, and the alteration generally gives the plagioclase a ‘dusty’ appearance. Quartz grains which have not been affected by alteration (c.f. Browne & Ellis, 1970) are present in much lower abundance and are likely a remaining parent rock phenocryst.

The other samples of coherent andesite from each of the other outcrops differ significantly from the character of HST-AND described above (Fig.27). The most evident difference is the lack of plagioclase crystals. Almost complete dissolution of the feldspars has occurred, modified instead to a very fine-grained alteration matrix in the Northern cohesive andesite outcrop samples (UN-AND, OR-AND and GR-AND), creating a much higher “apparent groundmass” to crystal ratio. Multiple larger quartz crystals are highly resorbed with significant embayment’s reflecting partial dissolution in each of the samples from the northern series (Fig.26). However, this is not a secondary hydrothermal texture, but instead is an artefact of the primary andesites genesis.

The samples from the southern boundary and Rocky Point outcrops (RP1 and RP2) differ in character again, where most of the primary texture and mineral assemblage has been destroyed and extensively replaced by an interlocking “mosaic” of quartz.

Figure 26: Resorbed quartz grain with extensive embayment’s within the UN-AND sample.

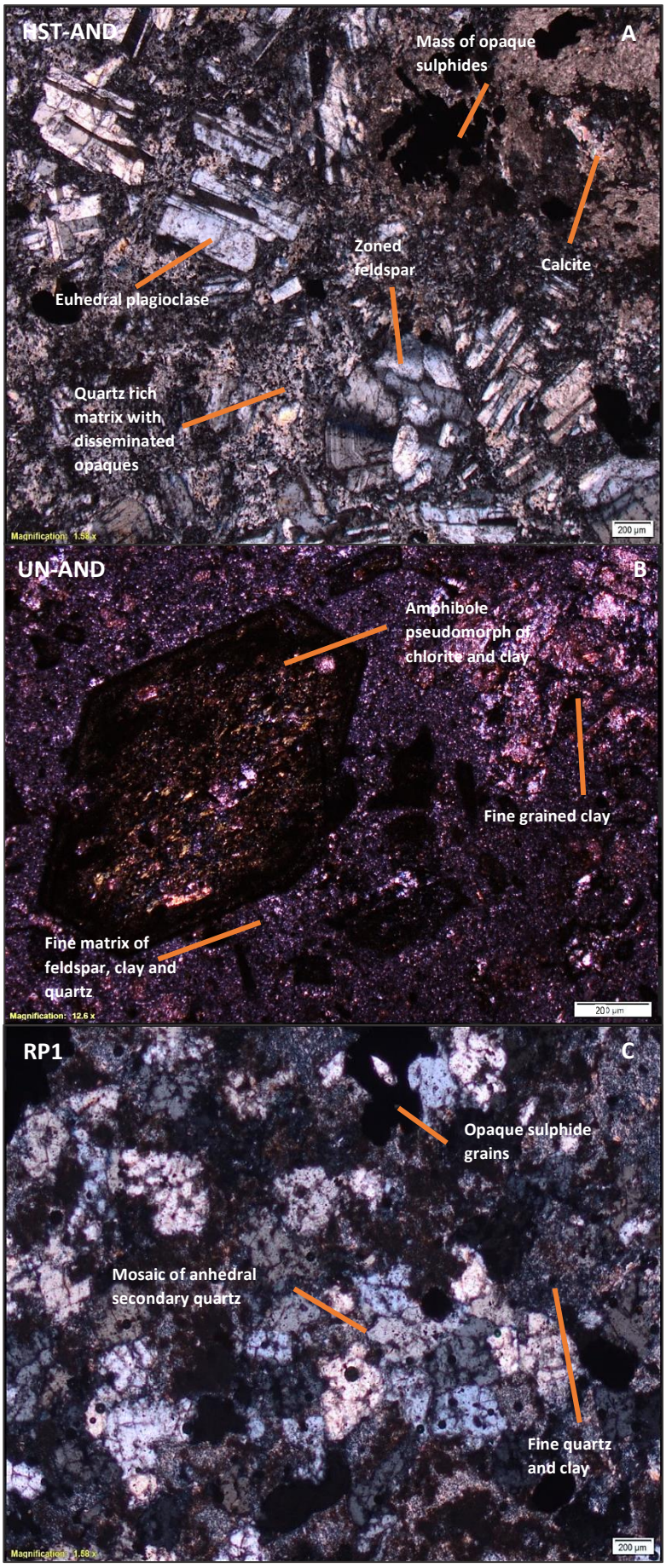

Figure 27: Mineralogy of samples of the cohesive andesites. From top to bottom displaying representative samples from the Central (B), Northern (A) and Southern (C) boundary/Rocky Point site.

Groundmass

The recognised variability in dissolution and replacement of phenocrysts within each of the altered andesites is also accompanied by varied groundmass characteristics. The least modified groundmass is present in the central HST-AND sample, although its groundmass has experienced a moderately higher degree of alteration compared to its feldspar phenocrysts. This alteration has occurred in a generally uniform manner, primarily seen as the addition of fine-grained silica and recrystallised feldspar with a lesser calcite component (Fig.28A), creating an almost cryptocrystalline texture. Also littered amongst the fine quartz and plagioclase feldspar is an abundance of disseminated opaques. With reflected light, the opaques under transmitted light are instead grey-white in colour and are confined solely within the groundmass. SEM-EDS recognises these as flecks of Fe-Ti oxides, which may be titanomagnetite or ilmenite (Fig.28B).

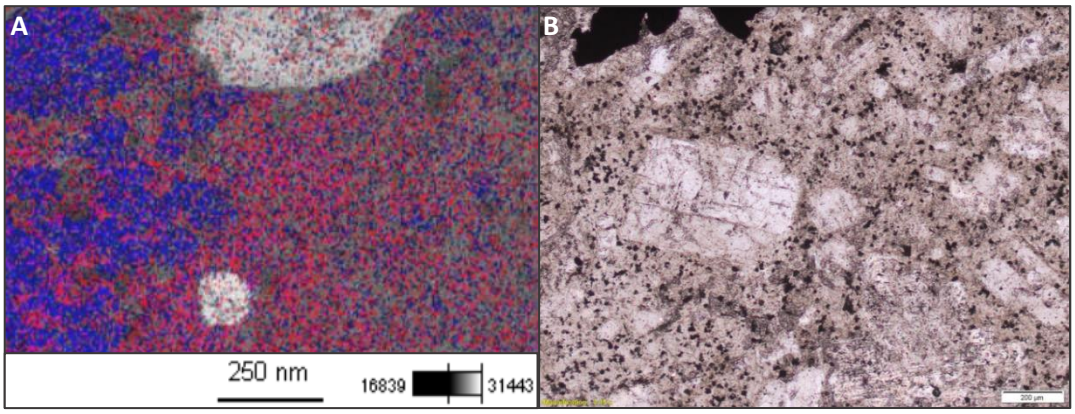

Figure 28: A. SEM – EDS element map reflecting the composition of the groundmass of the sample HST-AND. Areas rich in Si are indicated by blue, reflecting high quartz abundance, and areas abundant in Al are indicated by red, reflecting feldspar. White sites are masses of sulphides. B. Disseminated opaques of Fe-Ti oxides amongst the groundmass of sample HST-AND under transmitted light.

The groundmasses of the Northern cohesive andesite sample reflects a similar cryptocrystalline character, however there is some variation in texture between samples. UN-AND and OR-AND display a marginally coarser texture compared to the almost glassy texture present in the GR-AND sample. This is due to a higher abundance of recrystallised plagioclase and quartz.

As with HST-AND, due to a fine groundmass/alteration matrix, the mineralogy of the northern cohesive andesites is difficult to determine with optical microscopy, hence this was complemented by secondary electron SEM imaging and EDS point

analyses. This reflects that the groundmass is composed significantly of aluminosilicates, predominantly plagioclase accompanied by chlorite and clay (Fig. 29). The flooding of plagioclase, also seen in HST-AND, is likely a result of the static recrystallisation of the feldspar phenocrysts which had previously experienced dissolution due to the disequilibrium of primary plagioclase. There is variability in the chemistry of this plagioclase with both Ca and Na bearing members present, reflecting variability in the $An_{\%}$. This was also seen in the HST-AND sample matrix; however, Na-rich plagioclase is present in higher proportions in the northern samples indicating this recrystallised material is closer to the albite endmember.

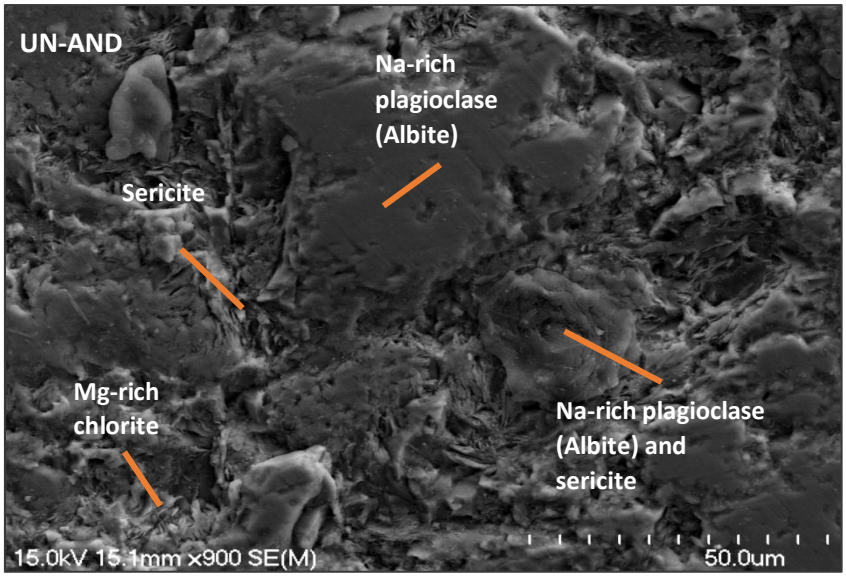

Figure 29: SEM image showing groundmass alteration matrix texture and minerals identified in the northern cohesive andesite sample UN-AND through EDS spot analysis.

The fine, unoriented, platy clays (Fig.30) that accompany the feldspar occur as both chlorite (predominantly Mg-rich clinochlore) and K-rich fine white mica or muscovite which will be referred to as sericite due to its fine texture. Both minerals are very characteristic secondary minerals of low-sulfidation epithermal environments. Therefore, their pervasiveness indicates such alteration has occurred extensively within the groundmass. Within the Rocky Point samples, there is very little primary groundmass due to replacement by silica. However, where groundmass is present, pervasive replacement has occurred solely as

sericite. Therefore, the groundmass of the associated samples (RP1 and RP2) have the finest character of all the cohesive andesites, having been extensively altered and losing much of its primary crystalline igneous texture.

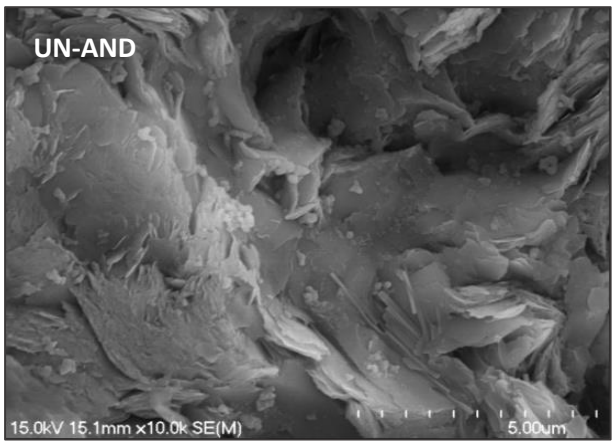

Figure 30: Texture of fine white mica, or sericite, within the alteration matrix of sample UN-AND.

Pseudomorphs

Evidence of original host rock minerals and textures of the cohesive andesites are reflected in numerous pseudomorphs. Pseudomorphs are instances of original reacted mineral shapes being preserved by the secondary mineral or minerals which replaced them. These textures are most clearly present in both the UN-AND, GR-AND and OR-AND samples, and present but in lower abundance in HST-AND (Fig.31). Even in the southern Rocky Point samples, which have been intensely altered, there are also possible tabular forms composed entirely of sericite, but they are not as well preserved as those found at the other sites. Feldspar pseudomorphs in these cohesive andesite samples are not uncommon, however pseudomorphs of mafic minerals are the most abundant, determined by the preserved outlines of their euhedral pyroxene and amphibole shapes. Where present, this links their parent rock type as being a pyroxene-hornblende andesite which is known to dominate the Coromandel Group (Edbrooke, 2001).

The UN-AND pseudomorphs are the best preserved, primarily composed of chlorite with lesser sericite clay and sulphide replacement. Disseminated amongst the pseudomorph alteration are inclusions of the same fine plagioclase

that makes up the groundmass of the rock. The pseudomorphs are present as “iso-alteromorphs” where the volume, shape and size of the original mineral has been preserved (Delvigne, 1998). These pseudomorphs vary in the extent of replacement, however. Some are entirely replaced (Fig.32B), whereas others appear to maintain a rim of the original mineral (Fig.27B), where it is assumed partial dissolution and replacement has occurred. Descriptions of the UN-AND outcrop in chapter 3, described the rock as appearing relatively unaltered. This is likely due to the quality of preservation of the pre-alteration porphyritic texture. However, it is apparent with microscopy that this sample is much more extensively altered than is recognisable at the outcrop scale.

Chlorite pseudomorphs in the GR-AND sample are common, however, pseudomorphs are more often composed of predominantly sericite compared to UN-AND. This develops even more so in the OR-AND sample, where sericite becomes the primary pseudomorph mineral accompanied by extensive Fe-oxide staining. The pseudomorphs, after mafic minerals, remain most abundant within both samples, seen as well preserved iso-alteromorphs. There are also however, instances of tabular feldspar forms which have also been well preserved.

Within the central andesite HST-AND sample, pseudomorphs are far less abundant than seen in the previous samples of the northern outcrops. As previously described, sulphides are a major alteration mineral present in HST-AND, and they along with calcite are the most evident pseudomorph replacement minerals (Fig.31A). They are not as well preserved as elsewhere however, taking on the form of “kata-alteromorphs” where the shape and volume have been altered resulting in an outline which is no longer clear, but their original position can still be recognised (Delvigne, 1998). Due to these modifications, the form of the original minerals is less evident, but appear to have been pyroxenes, as seen in the northern samples.

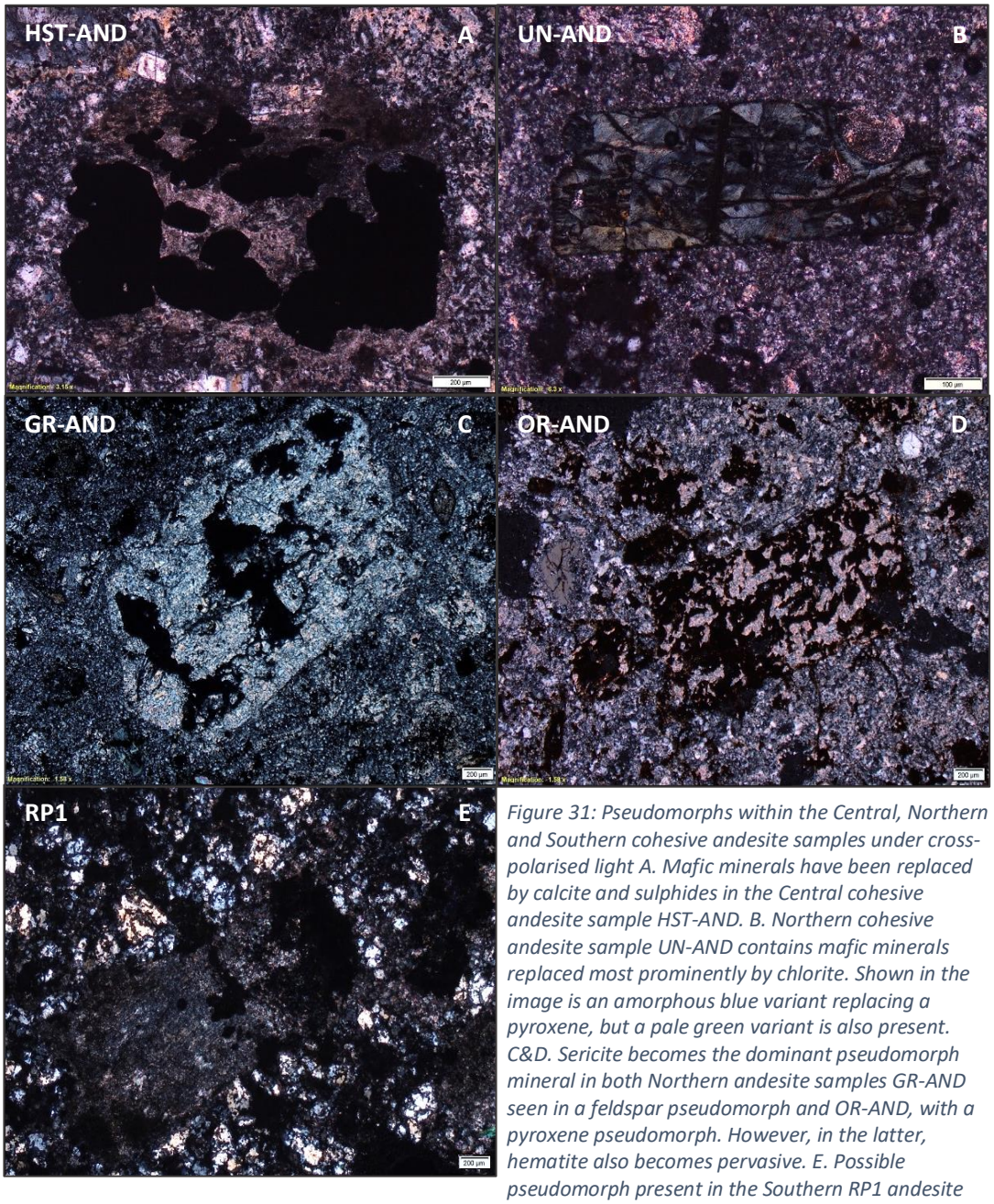

Figure 31: Pseudomorphs within the Central, Northern and Southern cohesive andesite samples under cross-polarised light A. Mafic minerals have been replaced by calcite and sulphides in the Central cohesive andesite sample HST-AND. B. Northern cohesive andesite sample UN-AND contains mafic minerals replaced most prominently by chlorite. Shown in the image is an amorphous blue variant replacing a pyroxene, but a pale green variant is also present. C&D. Sericite becomes the dominant pseudomorph mineral in both Northern andesite samples GR-AND seen in a feldspar pseudomorph and OR-AND, with a pyroxene pseudomorph. However, in the latter, hematite also becomes pervasive. E. Possible pseudomorph present in the Southern RP1 andesite sample, composed solely of sericite.

Variations in Colour across the Northern Cohesive Andesite

The alteration of the northern cohesive andesite varies significantly in colour across rock exposures. This is seen in variation from orange (OR-AND sample) to green (GR-AND sample) and dark green-grey (UN-AND sample). These colour changes are a result of the addition of particular secondary minerals in high abundance.

- **Hematite:**

The orange colour of the outcrop from which the OR-AND sample was taken can be attributed to the presence of a fine-grained amorphous Fe-oxide which has developed within grain boundaries and along fractures (Fig.31D). Its occurrence has also made the boundaries of phenocrysts less well defined and masked the primary porphyritic texture. Hematite, which varies from dark to reddish orange in colour in thin-section, is a form of Fe-oxide which may have developed due to the alteration and weathering of the chlorite which is present in the neighbouring outcrops of UN-AND and GR-AND (Allen, 1996), therefore, suggesting this section has experienced an overprinting of alteration that the others have not.

- **Chlorite:**

The presence of secondary chlorite has caused the green colour seen most strongly in the GR-AND sample and to a lesser degree UN-AND. As described, chlorite is significant in mafic mineral replacement, but it is present as two different colour varieties (Fig.32). A lighter green variant appears to dominate pseudomorphs of pyroxenes and a blue/green variety with more irregular "anomalous" interference colours has replaced more variably across the rock as pseudomorphs of both pyroxene and hornblendes (Fig. 31B).

Chlorites are a group of phyllosilicate minerals which, based on their substitution of Mg, Fe, Ni, and Mn into a silicate lattice can chemically be described as one of four endmembers. Therefore, the two different coloured chlorites present in the samples are likely to be variants of these endmembers. The most likely variation is in Mg and Fe abundance. SEM compositional analysis recognises that the light green variant has a marginally higher Mg content (+1.98 wt. %) than the blue-green. The Fe content detected was similar between the two, however, dark blue tends to be indicative of Fe rich varieties (Schwartz, 1959). These two variations therefore represent chlorite species of varied compositions between clinochlore

(Mg-rich) and chamosite (Fe-rich). As the rock has a higher abundance of the light green species, it is therefore dominated by clinochlore.

Figure 32: Two variants of chlorite present in the UN-AND sample under crossed polarised light. The left is the blue-green variant, the right is the light green.

Volcanic Breccia

The components of the volcanic breccia have been classified as two separate classes; clasts and matrix. The clasts have been considered rock fragments upwards of 2 mm, the matrix as anything sand sized and smaller (<2 mm).

Clasts

Despite the high matrix to clast ratio of the volcanic breccia, some clasts reach tens of centimetres in size, they therefore represent a significant feature of the rock. The BRC-1 and BRC-2 matrix samples provide a broad characterisation of the lithics present, but little detail of their individual lithologies and alteration character. Therefore, three separate clast samples from both the northern and southern exposures were also retrieved to better establish the lithologies which have been incorporated into the unit and their relationship with alteration.

From the volcanic breccia (BRC-1) south of the central andesite, two of the three clasts were recognised as sedimentary, the other as volcanic. The volcanic clast has a fine crystalline groundmass which has experienced silicification and contains feldspar phenocrysts that have experienced partial dissolution and replacement by sericite. Therefore, this suggests more intense seritisation has occurred than seen in the adjacent Central cohesive andesite in which the plagioclase feldspars were predominantly unaffected. The two sedimentary clasts alteration character is similar to one another, resembling that seen in the BRC-1 matrix, with sericite, sulphides and epidote addition apparent. One of the sedimentary clasts however has experienced silicification as well, causing significant alteration to its texture. However due to the abundance of lithics, which are moderately sorted with poorly rounded forms, this enabled its classification as a sedimentary clast

The samples associated with the BRC-2 outcrop again display varied lithologies, two volcanic and one sedimentary. The sedimentary rock is recognised as greywacke argillite, which is similar in character, if not slightly finer grained than the siltstone bedding in the unaltered greywacke sample (G1) described later in the chapter. The alteration character is more aligned with the associated matrix of BRC-2 than the unaltered G1 however, due to the presence of occasional small epidote grains and sulphide content. The two volcanic clasts reflect a similar mineralogy to the Central cohesive andesite HST-AND sample, with abundant plagioclase phenocrysts and a fine quartz and feldspar rich groundmass. However, there are two apparent classes of plagioclases, larger crystals as seen in HST-AND, and smaller crystals. The intensity of alteration experienced by these two groups vary, where dissolution and replacement of the larger by calcite and sericite is evident, whereas the smaller grains are minimally affected. This is a possible indication of the presence of secondary feldspars which were more stable under the changing hydrothermal conditions.

Matrix

Representative samples of the volcanic breccia from both outcrops (BRC-1 and BRC-2) were taken from the matrix which makes up a large proportion of the unit (Fig.33). The most distinctive feature within the matrix is the abundance of small lithic fragments which have a comparable character between the two samples. They are present in a variety of shapes and sizes, very angular to rounded and from 15 µm up to 200 µm in size with no orientation preference. Boundaries of these lithics are generally poorly defined, appearing weathered and altered, with slightly more intense weathering present within the BRC-2 sample from the northern exposure. There are also a variety of lithologies present, including both fine-grained sedimentary fragments and volcanic fragments with recognisable porphyritic textures.

Finer-grained interstitial matrix is found in similar abundance to the matrix lithics and appears to consist of the same material which has been ground finely to a clay. Apart from occasional small and rounded primary quartz grains, there are no other crystals present. The interstitial matrix alteration character is stronger than that of the lithic fragments, but the character of alteration is the same, where replacement by sericite and epidote has occurred in a patchy manner accompanied by sparse disseminated sulphides. This alteration seems more abundant in some areas across both interstitial matrix and lithics within BRC-2 however, whereas marginally weaker and more uniform alteration is present within the southern BRC-1 sample.

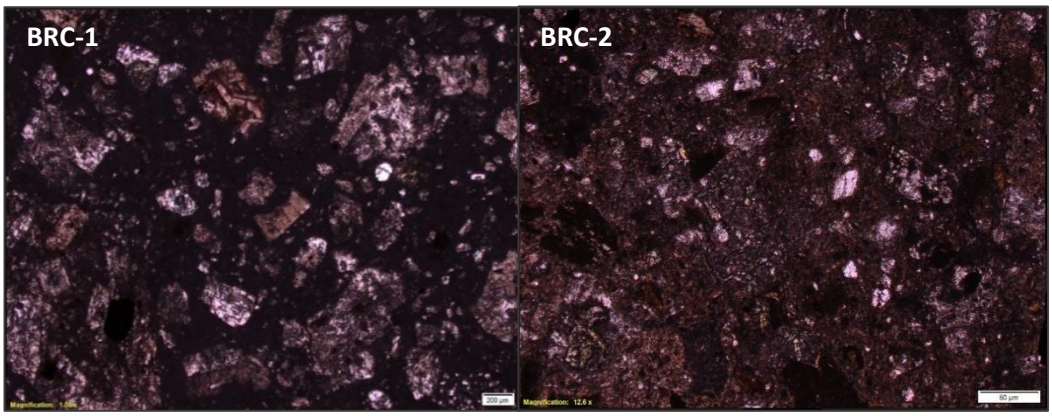

Figure 33: The southern volcanic breccia outcrop (BRC-1) and northern outcrop (BRC-2) matrix samples under plane polarised light. They each have an abundance of lithic fragments amongst a finer interstitial matrix of the same material.

Epidote

Epidote is an alteration product and accessory mineral that is most abundant in the volcanic breccia and its occurrence in volcanic breccia is unique amongst the other host rocks present. Under plane polarised light they appear as equant, pale green crystals, likely reflecting a Fe-rich pistacite epidote member (Fig.34A). They are present in both the lithics and finer interstitial matrix of both samples (BRC-1 and BRC-2) and are often proximal to sulphide masses, although they are higher in abundance in the BRC-2 sample. It is apparent that much of the epidote developed post deposition due to crystals having grown between and over top of multiple lithic fragments.

Some lithics are free of epidote entirely, whereas others have been significantly replaced by large masses of epidote crystals often accompanied by sericite replacement. (Fig. 34B).

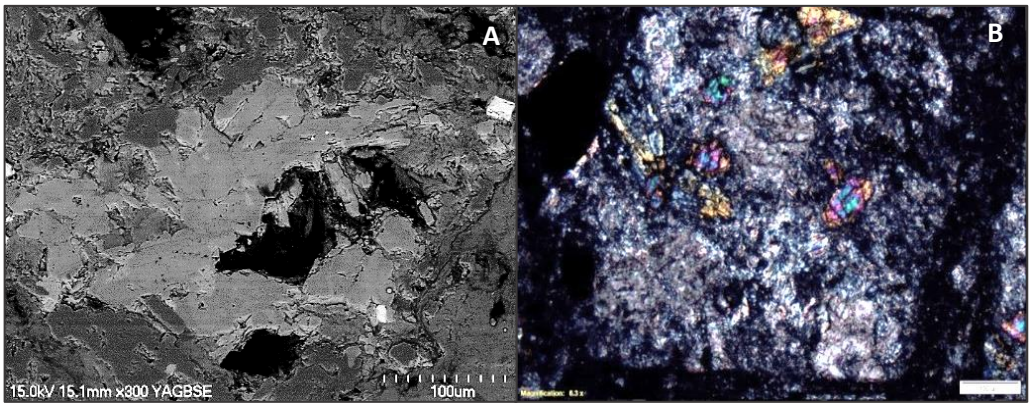

Figure 34: A. Close up SEM backscatter image of epidote within the volcanic breccia, occurring commonly as clusters of equant crystals. B. Clusters of epidote accompanied by sericite within a lithic fragment under cross polarised light displaying high but zoned interference colours.

Greywacke

Unaltered Greywacke

The bedding within the unaltered greywacke was observed in thin section (sample G1) as interbedded fine and coarse sandstone layers separated by a sharp boundary (Fig.35). The bedding of the greywacke is likely a result of its origin, forming from sub-sea turbidity currents during its deposition (Suggate,

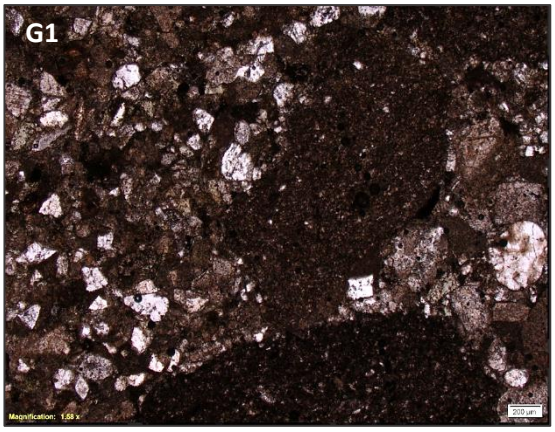

Figure 35: Unaltered greywacke (G1) sample with the fine sand (left) separated from coarse sand(right) by a sharp, undulating bedding plane.

1978). This has results in creating the varied grainsizes and bedding planes reflected in the G1 outcrop and sample. The grains of both beds are well compacted, with little interstitial matrix, associated with the deep burial of greywackes due to their position in the regional stratigraphy as a basement rock. There is no preferred orientation of grains and the lack of deformation features in the coarser fraction indicates minimal compaction deformation (Fernandes, 2016).

The finer grained of the two beds is composed of lithic fragments, quartz and plagioclase with occasional fine, elongated, dark green chlorite deformed around the lithics. The coarser bed has a similar composition, however its ratio of lithics is much higher, resulting in a lower matrix and crystal component. These lithics are sub-angular to rounded in form and their larger size allows for their lithologies to be recognised as predominantly greywacke and argillite with a lesser proportion of volcanic lithics which have varied porphyritic textures. The presence of alteration minerals within both beds is very minimal, where there is partial replacement of some of the argillite lithics and matrix by sericite and calcite, however, this is mainly evident in the coarser bed. The replacement textures of these minerals make it evident they are secondary. Unlike every other sample observed in thin section, the unaltered greywacke is completely void of any sulphides.

Altered Greywacke

South of unaltered greywacke, multiple samples (G2, G3, 6-HST-G) were retrieved at intervals of a few meters to reflect successive alteration of the same greywacke parent rock. Each of the altered samples are finer grained than G1, displaying an argillic texture, and their grain size fines further to the south (Fig.36). However, this may be a factor of sampling bias, as the altered exposures were sampled higher up the beach face than the G1 sample. If it is the result of alteration, however, primary textures in the form of gradational bedding and primary grainsize has been predominantly retained. The most evident change is the increasing homogeneity of grainsizes and gradational bedding contacts in the altered greywacke, contrasting to the poorly sorted grains and sharp contact seen in G1. Due to these observations, it is likely alteration has modified the texture but has not completely destroyed it.

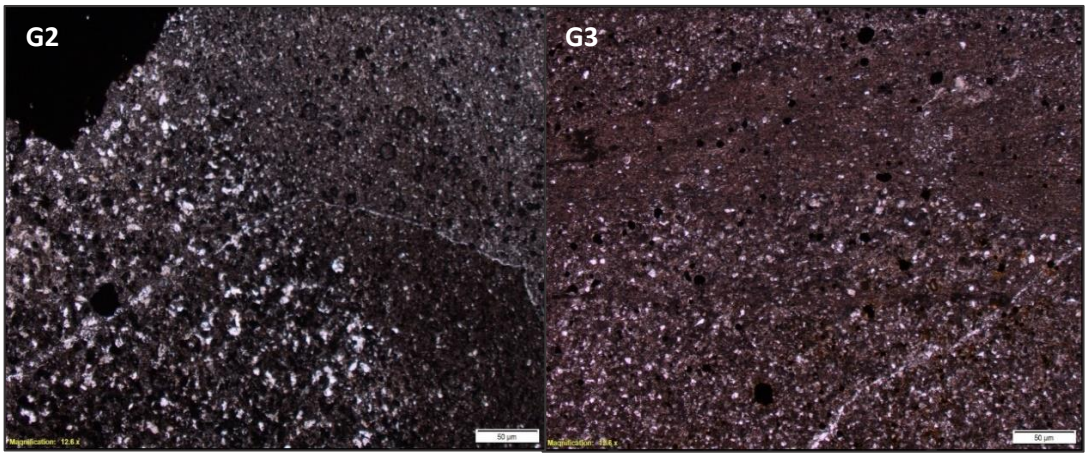

Figure 36: Changes in grainsize within samples G2 and G3 which are successively farther from the predominantly unaltered G1 sample. Fine veinlets or seams of quartz are also in both. Alteration has affected grainsize and matrix, but the primary grainsize has been retained.

The fine grained altered rocks have developed a bleached bronzy colour, through the pervasive addition of both microcrystalline quartz and sericite (Fig.37). The proportion of sericite and quartz in the successive samples of greywacke to the south is generally consistent, however the proportion of sulphides does vary. In the sample collected closest to the unaltered greywacke outcrop, G2, has abundant sulphides. They are present as irregularly shaped blebs and are disseminated across the sample, but they are primarily confined to veins up to 1 mm wide. Closer to Rocky Point, these sulphides become marginally more

abundant, but the sulphides are less restricted to veins, and are more disseminated.

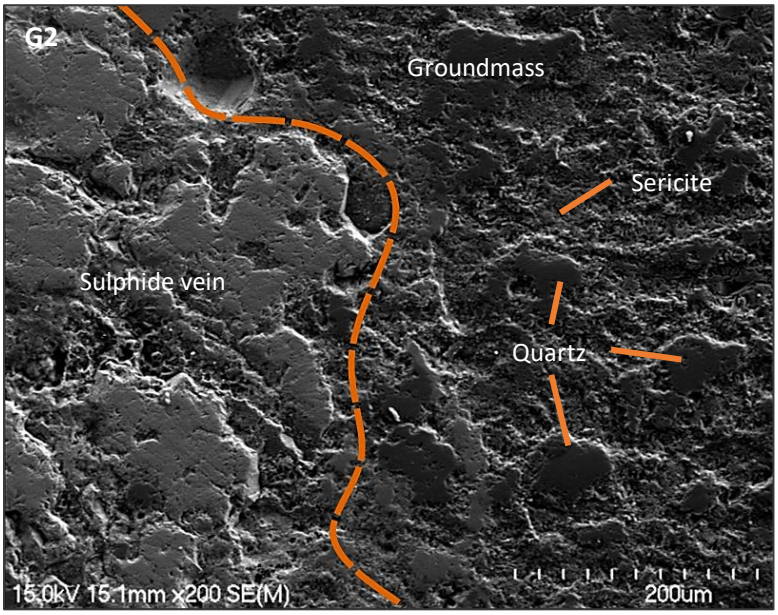

Figure 37: Sample G2 of altered greywacke with quartz and sericite rich replacement and a sulphide vein cutting across the groundmass.

4.3 Pebble Dyke Petrography

Matrix

Within each of the pebble dyke samples, the clast to matrix ratio varies broadly. Some are clast supported, whereas others are more loosely compacted and supported by a very fine grained dark grey-brown matrix which is difficult to resolve optically.

Amongst the matrix, flow banded patterns are not apparent, which were recognised in the El Salvador pebble dykes (Gustafson & Hunt, 1975). There are however, varied orientations of fine rock material and although there are angular fragments, many also reflect the sub-rounded character of the larger pebble dyke clasts which supports the interpretation of formation under turbulent conditions. In the pebble dykes with less matrix (e.g. PBL-7), void spaces are also abundant between the clasts. The boundaries of these void spaces have an

accumulation of fine, clay sized minerals and sulphide blebs, the growth of these secondary minerals likely due to the permeable pathway they provide.

There appears to be a correlation between the clast-matrix ratio and observed thickness of the dykes measured in the field. The thinner dyke represented by the PBL-3 sample (2 – 17 cm wide) has a much lower matrix content compared to the much thicker PBL-1 dyke (16 – 27 cm wide) (Fig.38). Despite the PBL-3 sample reflecting a higher degree of compaction, the clasts remain generally well defined and sub-to well-rounded, indicating little deformation has occurred.

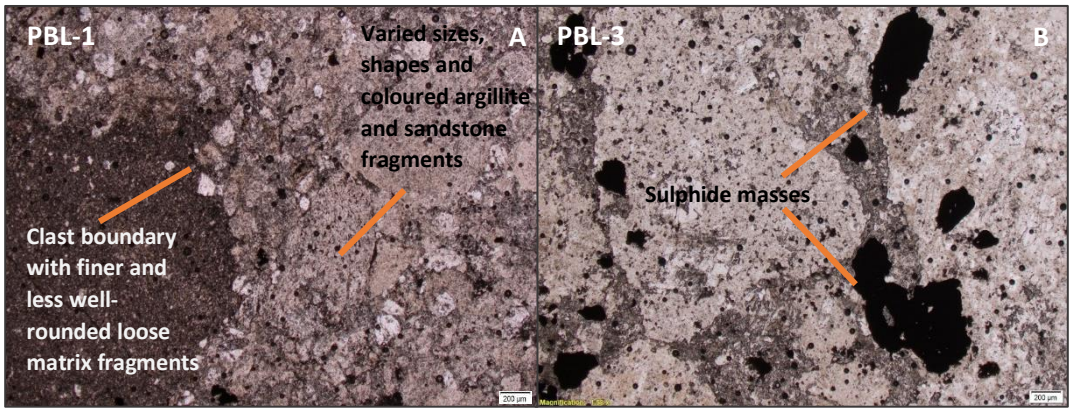

Figure 38: Images of two pebble dyke samples under plane polarised light. The PBL-1 (A) sample displays more compaction compared to the wider dyke body of PBL-3 (B).

Clasts

The pebble dykes each contain assorted lithic clasts which are variable in size and lithology. As with the matrix to clast ratio, there is also an association with clast size and pebble dyke width where the wider dykes are associated with coarser material. The lithic clasts generally have a sub-to well-rounded morphology with only occasional sub-angular fragments.

There is a dominance of sedimentary lithics within each of the dykes. These range from coarse grained sandstone clasts to the more dominant fine-grained siltstones which occur in various colours, pale to dark shades of brown and grey. Amongst these lithics are also occasional crystals of quartz and a few feldspars with the quartz mirroring the rounded character of the clasts. There are however

a few occurrences of volcanic lithics present, some dykes hosting more than others. Despite their commonly altered character, pseudomorphs of feldspars and pyroxenes enable their identification even when there has been significant secondary mineral replacement. Fragments of fresh unaltered volcanic rock were not at all present. The dyke that is most abundant in volcanic lithics is PBL-4, where they account for a little under half of the clast components. PBL-5 which is from the dyke neighbouring PBL-4 has a similar abundance, whereas PBL-1,2 and 3, which are hosted slightly north of these, have only occasional volcanic lithics. The southern dykes PBL-6 and 7 both host an even lesser abundance of volcanic clasts; however, their clasts are extensively altered so this may possibly be intensified by texture destruction.

Greywacke Clasts

Multiple greywacke lithic clasts occur within the pebble dykes. Their source is either from deep basement rock, the depth which is unknown locally, or from much shallower depths associated with the adjacent outcropping greywacke. To further constrain their source, samples were taken from two different pebble dykes to compare their mineralogy with the observed samples taken from the beach outcrop. One from the Cluster A site, the other from Cluster B.

The PBL-1 lithic clast (Cluster A) has a similar grainsize to the finer-grained bed of the unaltered greywacke sandstone (G1). It is predominantly composed of lithics and quartz with a lesser abundance of feldspars. Secondary alteration minerals are present as epidote and sericite, however neither are present in significant abundance. This alteration character is comparative to the greywacke clast taken from the northern volcanic breccia outcrop (where BRC-2 was sampled). The clast has a very sharp boundary with the surrounding pebble dyke matrix.

The PBL-6 lithic clast (Cluster B) has an even finer grain size with zoning of slightly coarser material toward the edge of the sample, indicating possible gradational bedding. It displays a similar grainsize to altered greywacke of sample G3, but it is a pale grey colour rather than pale bronze. There appears to be a general

alteration through addition of sericite and silica, again similar to the altered greywacke outcrops. It has a similar sulphide content to the 6-HST-G greywacke sample, with a general abundant spread of irregular pyrite forms. There are also many fine quartz and sulphide filled veins. However, there are no veins filled only with sulphides as in the host rock samples.

Host Rock Alteration Near Pebble Dyke Contacts

From the pebble dyke PBL-7, a representative sample (of the same name) of the contact between the dyke and its host rock of altered andesite (RP1) was collected. A sharp contact between the two, was seen in the field and also in thin section (Fig.39). There is however slight undulation at this scale, but the host unit does not appear to be deformed in any way. Within the pebble dyke along the contact, the texture is dominated by very fine matrix material. Alteration on either side of the contact does not appear to be significantly different to alteration further out from the contact. The only notable feature is that the margin within the pebble dyke appears paler than the surrounding rock creating a halo, this may possibly be due to the fining of material outwards. There is also a slightly higher sulphide abundance near the contact compared to the centre of the pebble dyke.

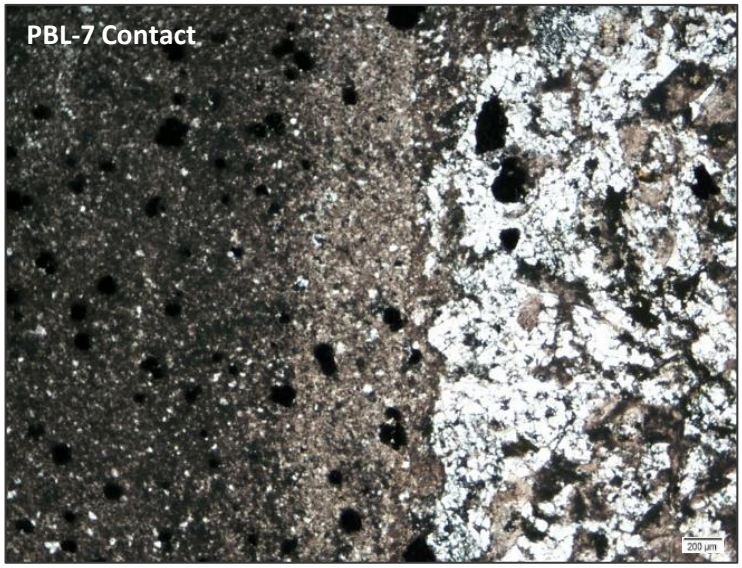

Figure 39: Contact between PBL-7 (left) and heavily silicified host rock (right) of altered andesite as seen in sample RP1 under plane polarised light.

Alteration Within Pebble Dykes

Compared to the degree of alteration observed in the most altered host rocks across the beach section, alteration within the pebble dykes is relatively weaker. Although secondary minerals are present, they are not pervasive in their replacement, with many primary textures remaining. Generally, the alteration character of the pebble dykes does not differ significantly between bodies or even between the central and southern sites (Clusters A & B). Alteration is most evident as the addition of sericite, seen most prominently within lithics and as silicification in each pebble dyke sample. Epidote is also found in the matrix of some of the dykes, appearing as small, infrequent sub-euhedral grains similar to epidote occurrence in the volcanic breccia host samples. In PBL-3 epidote is hosted within clasts of varied volcanic and sedimentary lithology, their abundance however varies between them. Calcite is also sometimes present, often associated within only partial replacement textures. In PBL-4 calcite is most abundant, seen to have replaced both clasts and matrix in a dominal nature similar to what was seen in HST-AND. Alteration has also caused texture changes, where primary clast texture has been partially destroyed in some cases (Fig.40A)

and instances of pseudo brecciation is apparent in some of the pebble dykes due to propagation of sericite. This has not occurred extensively, but some sites appear more fractured as a result of progressive dissolution and infill.

Sulphides are also present, both clast and matrix hosted, typically occurring as disseminated grains. They appear to infill void space rather than as a preferential replacement texture as they are more abundant in areas of matrix where voids were available (Fig.40B). Seams of sericite, quartz and sulphides are present in most of the pebble dyke samples but not in abundance. These seams or veinlets cut across multiple clasts and matrix, which is a possible confirmation that alteration occurred post deposition (Fig.40C).

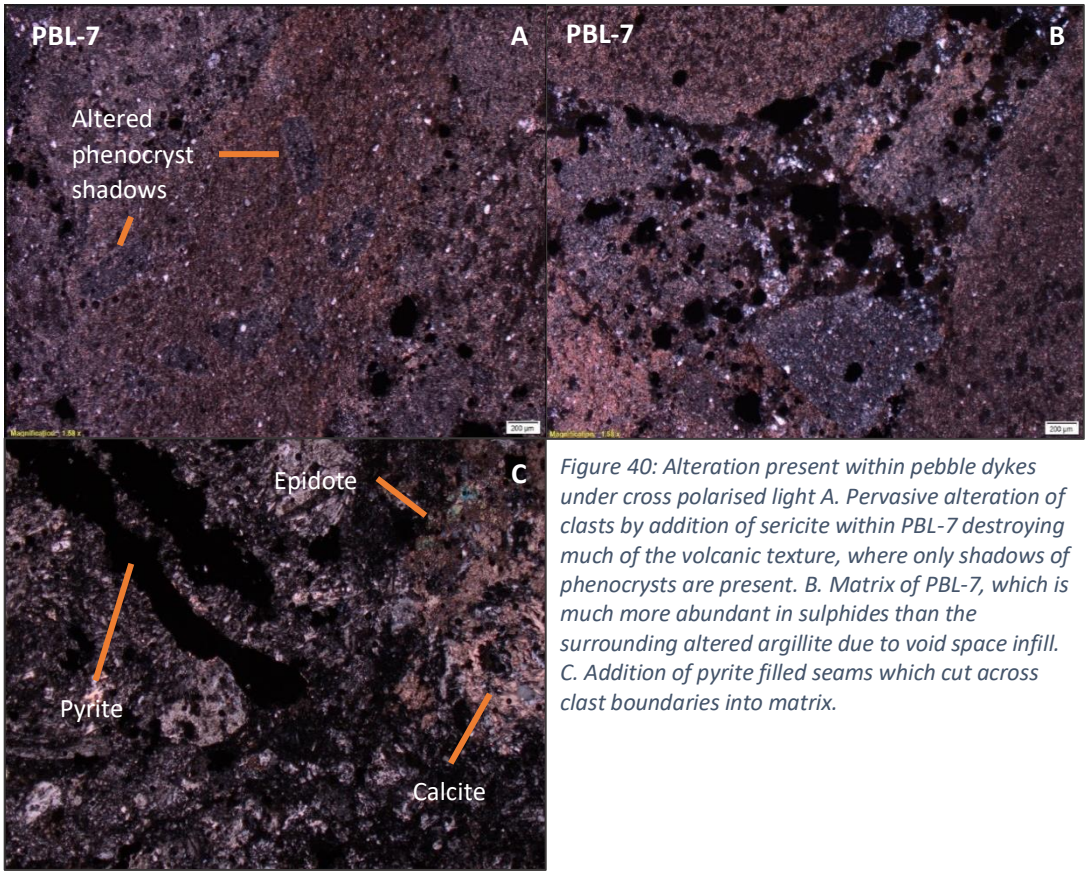

Figure 40: Alteration present within pebble dykes under cross polarised light A. Pervasive alteration of clasts by addition of sericite within PBL-7 destroying much of the volcanic texture, where only shadows of phenocrysts are present. B. Matrix of PBL-7, which is much more abundant in sulphides than the surrounding altered argillite due to void space infill. C. Addition of pyrite filled seams which cut across clast boundaries into matrix.

Proximal Alteration Influence on Host Rock

Two samples were taken from the main central andesite outcrop to observe any effect that the presence of the proximal pebble dykes may have had on the host rock (Fig.41). The sample HST-TRAN was taken adjacent to the pebble dyke PBL-1, and HST-AND was sampled ~1.5 m away from the dyke body which has previously been described (Chp. 3: Fig.8A). The "transition" sample, HST-TRAN, has lost much of the original character of an andesite. The texture and colour of groundmass has been clearly modified to a higher extent and much of the original crystal forms have experienced considerable dissolution and are more difficult to distinguish, particularly in the case of the plagioclase phenocrysts. The presence of clay is also now evident, associated with the loss in definition of phenocryst boundaries. Epidote is present in higher abundance, however like HST-AND, often occurs proximal to large masses of sulphides. Sulphides are also found in higher abundance but again also appear to primarily occur as an infill texture. Large pseudomorphs have formed with replacement by sulphides, epidote, calcite and chlorite.

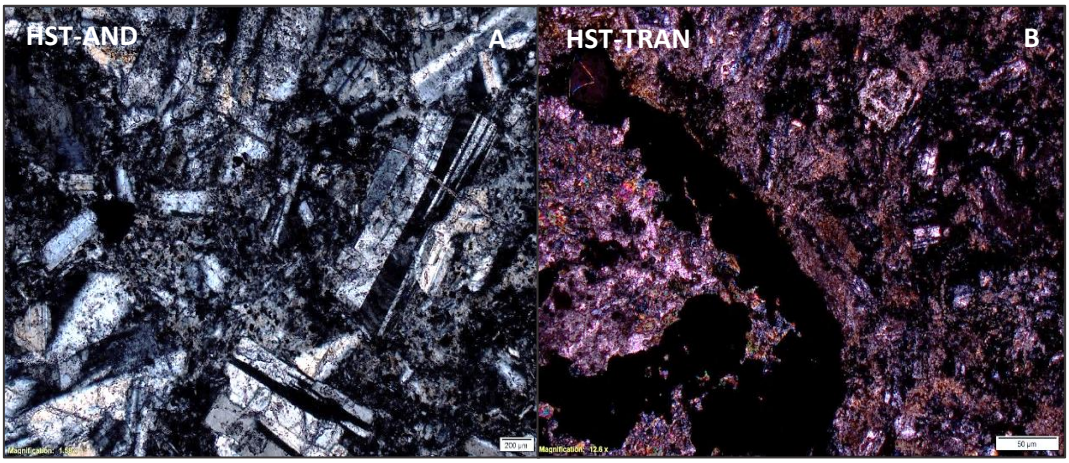

Figure 41: Rock samples from the central cohesive andesite which hosts multiple pebble dyke bodies. A. Sample taken from a ~1.5 m away from pebble dykes. B. Sample from the same rock type take from directly adjacent to a pebble dyke body, reflecting a much higher degree of alteration.

4.4 Sulphides

Reflected light microscopy allows for opaque sulphides to be recognised based upon their colour, reflectivity and anisotropy. The main sulphide present is pyrite which has a pale-yellow colour, moderate reflectivity and is isotropic under reflected light (Fig.42). Solely within the central andesite sample HST-AND sample, small and infrequent masses of darker yellow, chalcopyrite was also found.

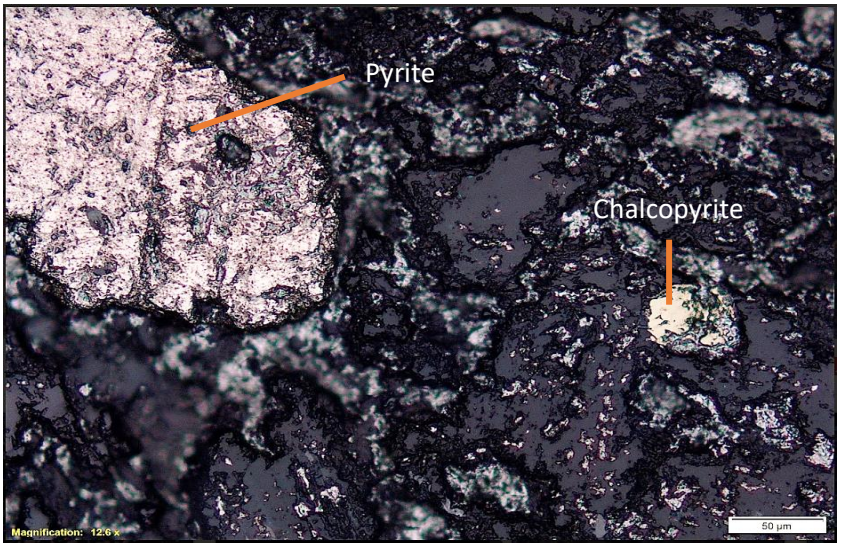

Figure 42: Pyrite and chalcopyrite visible under reflected light within the central cohesive andesite sample HST-AND.

Estimated proportions of sulphides observed within each of the main samples from each of the outcrops are shown in Figure 43. Samples on this plot are listed with spatial reference of their location from north to south along beach section and can be seen to vary considerably in sulphide abundance.

The sulphide proportion is associated with proximity to pebble dykes and there is weaker correlation to the intensity of alteration. The largest cluster of pebble dykes, Cluster A, is hosted within the cohesive central andesite (samples HST-AND and HST-TRAN). Samples from the central andesite reflect the first major increase in sulphide abundance from north to south along the beach; HST-TRAN, taken directly adjacent to a dyke represent a peak of up to 10% sulphides. The Cluster B site of pebble dykes is hosted in the southern most altered greywacke, with 6-HST-G proximal to one of the bodies, and the Rocky point cohesive

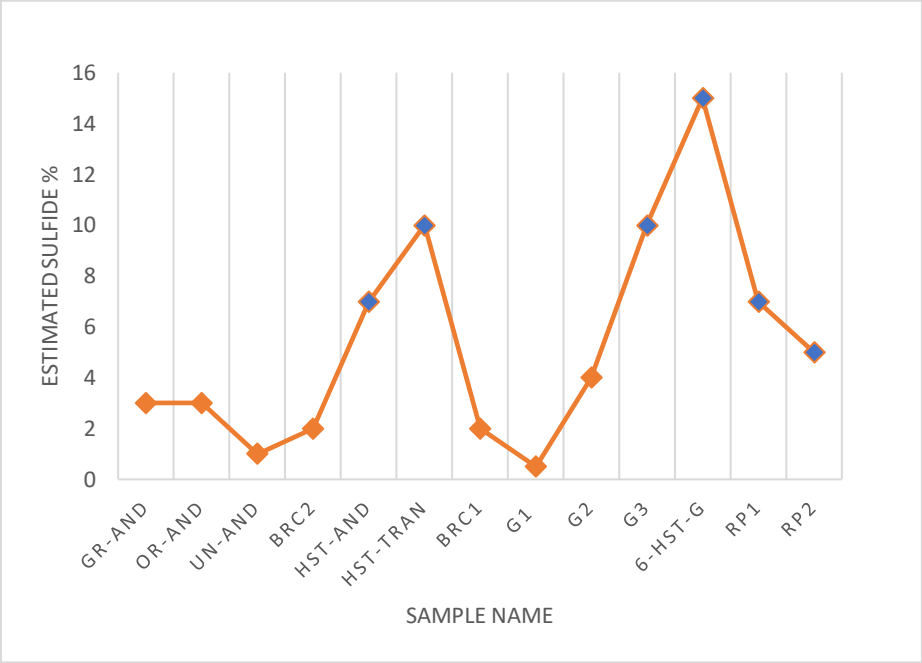

Figure 43: Estimates of sulphide percentage observed in each of the major samples from host rocks from north to south along the beach section. Pebble dyke hosts are represented by blue squares.

andesite samples of RP1 and RP2. These samples again reflect an increase in observed sulphide proportions, creating another peak of up to 15% sulphides. The association of sulphides in pebble dyke-bearing rocks contrasts to the observations within the pebble dyke samples themselves which reflect a much lower sulphide abundance comparatively.

The trend of observed sulphides may also be linked to the intensity of alteration. The samples associated with the southernmost sulphide peak are the most intensely altered (Table 6). However, the northern series of altered andesites (UN-AN, GR-AND and OR-AND) have experienced more intense alteration than the HST-AND sample, therefore limiting the association. The lack of sulphides in the orange coloured andesite of the Northern cohesive andesite in particular may relate to the abundance of hematite which may be a weathering product after pyrite.

Sulphide Textures

Pyrite, the major sulphide present, occurs predominantly as disseminated flecks within the alteration matrix or volcanic groundmass of host rock. Within some samples it is also present as masses of irregularly formed blebs through to well-formed anhedral to euhedral grains which can reach 0.3 mm in size. Not uncommon in these larger grains are also occasional small inclusions of the same matrix/groundmass within the andesite samples (Fig.44). In the cohesive andesites it is sometimes apparent, particularly with larger pyrite masses, that they have preferentially infilled pre-existing void space. Pyrite is also a replacement of mafic minerals, contributing to the creation of pseudomorphs.

Pyrite is frequently accompanied by other replacement minerals, sometimes in higher abundance than seen elsewhere. This may be a factor of their growth coinciding with focal points of permeability in the host rock (e.g. fractures) and local availability mineral forming elements. Epidote, as previously described, is frequently found in association with pyrite where present, often occurring in the immediate vicinity of large pyrite grains. Around the perimeter of pyrite crystals, in the altered andesite sample GR-AND, there is modification of pyrite boundaries in some crystals (Fig.45A). The centre of the crystal is pyrite, hosting

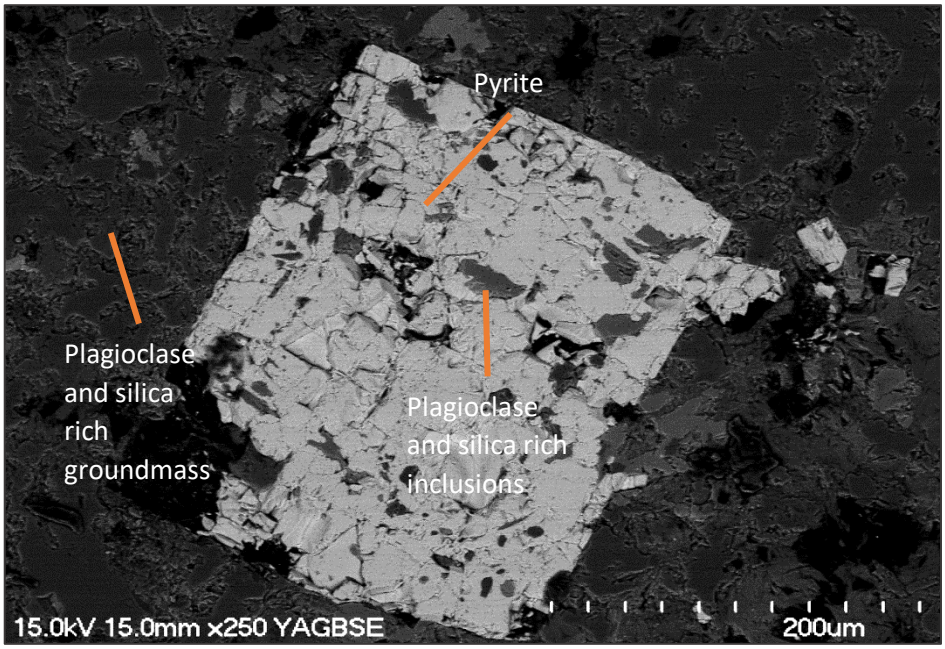

Figure 44: SEM backscatter image of euhedral pyrite grain within the cohesive andesite sample UN-AND, with inclusions of groundmass material.

an abundance of both S and Fe, however outwards to the darker grey boundary, the S content decreases significantly but the Fe content remains. This suggests mobility of the S as the pyrite is being replaced, possibly oxidised to hematite or a Fe-hydroxide. This occurrence is also associated with some of the pyrite veins in the altered greywacke sample G2 (Fig.45B), reflecting S-poor boarders. Sample G2 does not have a peak in the observed sulphide abundances (Fig. 43), but has a moderate presence, suggesting pyrite is not likely to have been significantly lost.

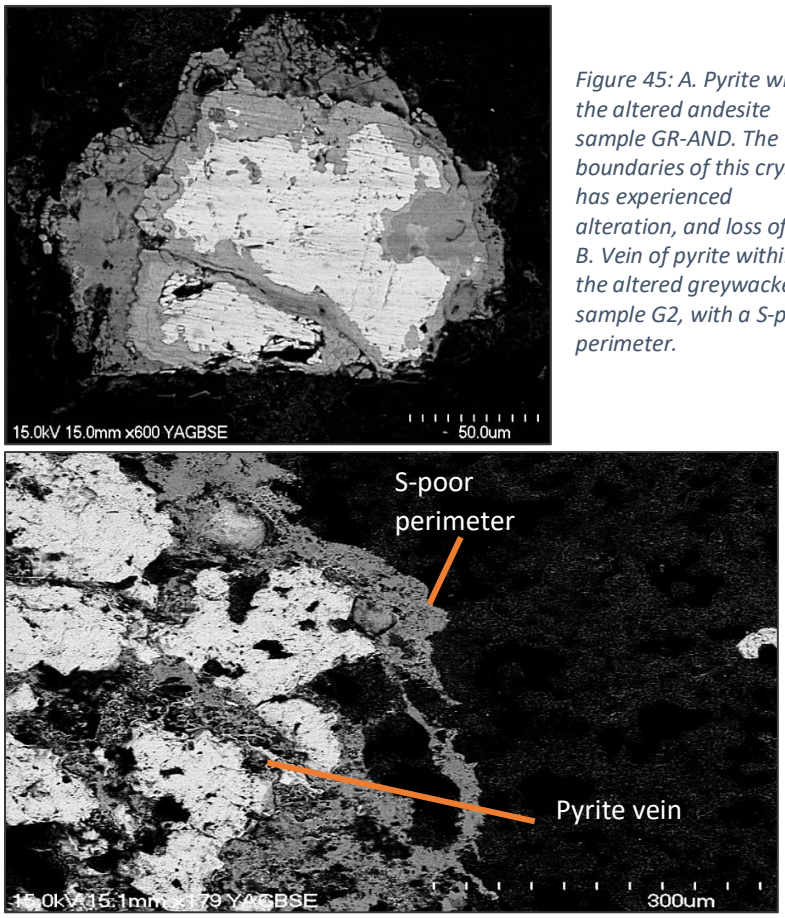

Figure 45: A. Pyrite within the altered andesite sample GR-AND. The boundaries of this crystal has experienced alteration, and loss of S. B. Vein of pyrite within the altered greywacke sample G2, with a S-poor perimeter.

Veins of pyrite are a significant feature in some samples, particularly within the altered greywacke series and Rocky Point andesites. Some of these veins are seams (<0.1 mm) of fine material which may pinch off to nothing. Whereas, others are larger (0.5 mm) and appear to have formed weak alteration halos around them. In an example from the altered greywacke G2 (Fig.46) the halo appears finer grained and brighter in polarised light compared to more distal material.

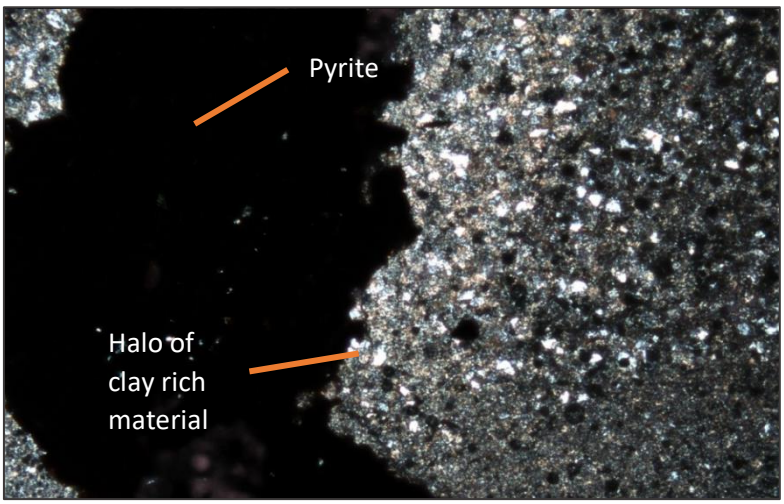

Figure 46: Altered greywacke sample G2 under cross polarised light, with an alteration halo around a pyrite filled vein.

Pebble Dyke Sulphides

Within the pebble dykes, the sulphide content is considerably less than in the surrounding host rocks (HST-AND, HST-TRAN, 6-HST-G, RP1 and RP2). However, the abundances across each dyke sample seem to be similar at a proportion of about ~5 %. The pyrite within the pebble dyke matrix is often very fine-grained and disseminated but some larger masses have developed within what appear to be void spaces within the unit. Pyrite occurs in higher abundance within some lithics of the pebble dykes, particularly in fine-grained argillite lithics. This may indicate some pyrite mineralisation may have occurred prior to brecciation or may just be an effect of some lithologies providing more permeability allowing for more extensive infill.

5. X-Ray Diffraction

Due to the hydrothermally altered nature of the rock, mineral identification through microscopy is often not comprehensive enough to recognize the complete assemblages present due to the destroyed and varied textures. To aid this, X-ray diffraction (XRD) analysis was implemented, a method which analyses the crystalline structure of powdered homogenized rock samples to identify alteration phases present. The result is a qualitative and semi-quantitative means for identification of minerals (Lagat, 2007). This non-destructive analysis is performed with the use of X-rays directed at the sample, where the angle and intensity of diffracted rays creates a signature pattern unique to each mineral type based upon Braggs law. Comparisons of the positions and intensities of measured diffraction peaks against a library of known crystalline materials enables the identification of the mineral phases present. 15 samples were chosen for XRD analysis, of both clay fraction and bulk rock alteration mineralogy. From the hydrothermal alteration minerals identified, the alteration style and epithermal setting which acted within the study site can be further defined.

5.1 Alteration Styles

Alteration style can be used as an aid in describing the overall characteristics of a zoned alteration setting, as well as acting as a useful vector towards zones of mineralisation. An alteration style or mineral zone is often defined by diagnostic mineral assemblages of silicates, carbonates and/or sulphates (Velde, 2013). Therefore, they can be divided by the mineral assemblages based upon their dominant mineralogy and chemical changes produced as the result of fluid-host rock interaction (Gifkins et al.2005).

Meyer and Hemley (1967) stated that there are five core alteration styles commonly associated with hydrothermal alteration: argillic, advanced argillic, phyllic, propylitic and potassic.

Argillic alteration, synonymous with intermediate argillic, can be characterised by the formation of clay minerals as a result of intense H^+ metasomatism and acid leaching (Pirajno, 2009). The associated temperature setting is typically low (>200-250°C), sometimes occurring in atmospheric conditions, and at a pH of approximately 4-5. The assemblages are dominated by kaolinite and smectite, and the bleaching of feldspars due to the abundance of clays is common. Clay minerals can also replace mafic silicates (e.g. hornblende, biotite).

Advanced argillic alteration is a subcategory of argillic alteration which forms due to intense acid interaction, and near complete leaching of the alkali cations causing the destruction of feldspars and mafic silicates (Pirajno, 2009). It is common in low pH environments and high temperatures (<220°C) and is characterised by the presence of kaolinite, pyrophyllite, or dickite (depending on the temperature) and alunite together with lesser quartz, topaz, and tourmaline.

Rose and Bart (1979) indicate that the phyllic type can also be referred to as sericitic, both defined by the dominant assemblage of quartz-sericite-pyrite. This style forms at similar pH ranges as argillic mineral assemblages but higher temperatures (>200-250°C) and is one of the most common forms of hydrothermal alteration. Mineral phases usually associated with this alteration style are K-feldspar, kaolinite, calcite, biotite, rutile, anhydrite and apatite.

Propylitic alteration, also termed saussuritization forms with near neutral to alkaline conditions and is characterised by the presence of epidote and/or chlorite (Meyer and Hemley, 1967). In lower temperatures (<200-250°C), zeolites may be present in the place of epidote, where the alteration style would then be termed sub-propylitic. At higher temperatures (>280-300°C) secondary amphiboles form characterising an inner-propylitic zone.

Potassic alteration is more typical at depth in the hydrothermal system, with characteristic high temperature and pressures compared to the other styles. The alteration assemblage is typically biotite and adularia. It is more common of neutral to alkaline conditions.

The full mineral assemblages associate with each of the five alteration styles are listed in Table. 7

Table 7: Hydrothermal alteration style terminology and associated mineral assemblages, modified from Gifkins et al. (2005).

Alteration Style	Associated Mineral Assemblage	Alteration Setting
Argillic	Kaolinite (or halloysite, or dickite) + montmorillonite ± sericite (or muscovite) ± chlorite	Porphyry Cu, high-and low-sulfidation epithermal, geothermal
Advanced argillic	Pyrophyllite + kaolinite (or dickite) ± quartz ± sericite ± andalusite ± diaspore ± alunite ± topaz ± zunyite ± enargite ± tourmaline ± pyrite ± chalcopyrite ± hematite	Porphyry Cu, high-sulfidation epithermal, geothermal
Phyllic (or sericitic)	Sericite + quartz + pyrite ± biotite ± chlorite ± rutile ± leucoxene ± chalcopyrite ± illite	Porphyry Cu, low-sulfidation epithermal, geothermal, VHMS, sediment hosted massive sulphide
Propylitic (or saussuritization	Epidote (or zoisite or clinozoisite) + chlorite + albite ± carbonate ± sericite ± montmorillonite ± septachlorite ± apatite ± anhydrite ± ankerite ± hematite ± pyrite ± chalcopyrite	Porphyry Cu, high-sulfidation epithermal, low-sulfidation epithermal, geothermal
Potassic	K-feldspar (orthoclase) + biotite + quartz ± magnetite ± sericite (or muscovite) ± albite ± chlorite ± anhydrite ± apatite ± rutile ± epidote ± chalcopyrite ± bornite ± pyrite	Porphyry Cu

5.2 Method and Instrumentation

To prepare the samples for XRD analysis, they were first crushed to a fine powder to create a homogenous sample. For the pebble dyke samples, the matrix was cut from around the clasts to prevent the clast lithologies from dominating the analysis. The powder was then pressed into sample holders and analysed by XRD using a Panalytical Empyeran instrument with a Cu anode. The resulting profiles were then able to be matched known mineral peak arrangements, which was done with aid from Panalytical High score plus software. The peak profiles were interpreted between the 5-35° 2θ range, as this is where the significant peaks for all mineral components of interest are found.

Based upon the results from the bulk rock analysis, the samples indicated a clay component due to peaks present below 10°. As their profiles are predominantly obscured by the other mineral peaks in bulk analysis, for the purposes of identifying which clay species are present, analysis of the clay fraction was necessary. The clay content was therefore first separated by gravitational settling

which enables the division of material based on particle size to create a purer clay sample, minimising the contamination from non-clay minerals. The standard technique to enable the identification of clay species is commonly based upon the basal spacings of the major clay XRD reflections in four different conditions: air-dried, treated with ethylene glycol and heated to 300, then 550°C (Środoń, 2006). However, only the first two separate treatment runs of analysis are required for the identification of illite/smectite interstratification which was the main relationship of interest. This is due to a special property of smectite; its ability to absorb water molecules or other polar ions into its structure causing swelling (Velde, 1992), which cases a migration of peaks after treatment of glycol. It reacts this way due to a larger attraction between the interlayer cations to water than the small interlayer charge between sheet layers (Moore & Reynolds, 1989). The application of glycol rather than water is preferred as it creates a more intense reflection and is more useable at room temperature (Środoń, 1980). This phenomenon does not occur with non-swelling clay types like illite, therefore, to identify interstratification, it must be determined whether the clay separate samples display a swelling character.

Mineral assemblages determined by XRD are listed in Table 8, each bulk rock and clay separate profile can also be found in Appendix 3. There are also minerals which were identified in thin section but were not recognised during XRD analysis, due to the low abundance, or due to superimposition of peaks hiding their presence. Epidote in particular is a mineral which is present in small amounts, as seen in chapter 4, however, its trace is not seen. Therefore, it has been added to the sample mineral assemblages where it was recognised petrologically.

Table 8: Mineral assemblages within each of the sample rocks identified through bulk rock and clay separate XRD analysis in order of abundance, supplemented by microscopy. Samples are listed in reference to their location from north to south. Pebble dyke samples listed last. Minerals identified by microscopy alone are indicated by italics.

Rock Type	Sample Name	Mineral Assemblage	Alteration Style
Northern Altered Andesite	GR-AND	Clinochlore + Illite + Quartz + Albite + *Pyrite*	*Propylitic*
	OR-AND	Illite +*Hematite* + Kaolinite + Quartz + *Pyrite*	*Argillic*
	UN-AND	Illite + Clinochlore + Albite + Quartz	*Propylitic*
Volcanic Breccia	BRC-2	Quartz + Illite + Clinochlore + Albite + *Epidote* + *Pyrite*	*Propylitic*
Central Altered Andesite	HST-AND	Anorthite + Quartz + Calcite + *Pyrite* + Clinochlore + Chalcopyrite	*Propylitic*
	HST-TRAN	Albite + Quartz + *Pyrite* + Calcite + Clinochlore + Illite	*Propylitic*
Volcanic Breccia	BRC-1	Quartz + Illite + Clinochlore + Albite + Calcite + *Pyrite* + *Epidote*	*Propylitic*
Greywacke	G1	Quartz + Calcite + Illite + Clinochlore	*Phyllic*
	G2	Quartz + Illite + *Pyrite* + Albite + Clinochlore	*Phyllic*
	G3	Quartz + *Pyrite* + Albite	*Phyllic*
	6-HST-G	Quartz + Illite + *Pyrite* + Albite + Clinochlore	*Phyllic*
Southern Altered Andesite	RP1	Quartz + Illite + *Pyrite*	*Phyllic*
	RP2	Quartz + Illite + *Pyrite*	*Phyllic*
Pebble Dykes	PBL-1	Quartz + Albite + Clinochlore + *Pyrite* + Illite + Epidote	*Propylitic*
	PBL-2	Quartz + Albite + Clinochlore + *Pyrite* + Calcite+ Epidote	*Propylitic*

5.3 Bulk Rock XRD Analysis

With reference to the styles in Table 7, the bulk rock mineral assemblages allow for the identification of alteration styles in the samples listed in Table 8. The epithermal environment (low-versus high sulfidation) can also be determined by the mineral assemblage's present, according to the definition of White &

Hedenquist (1995) (Table 9). The abundance of sericite in the form of illite and calcite within the samples of each lithology suggests a low sulfidation (adularia-sericite) setting, the only deviation from this is kaolinite (sample OR-AND) which is more common of high sulfidation environments but can occur in low sulfidation settings as the result of overprinting. Both the alteration styles recognised and the low sulfidation epithermal environment reflect the broader character of the Hauraki Goldfields hydrothermal system.

Table 9: Gangue mineral assemblages associated with low sulfidation and high sulfidation epithermal settings (White & Hedenquist, 1995).

	LOW SULFIDATION	HIGH SULFIDATION
QUARTZ	ubiquitous (abundant)	ubiquitous (abundant)
CHALCEDONY	common (variable)	uncommon (minor)
CALCITE	common (variable)	absent (except as overprint)
ADULARIA	common (variable)	absent
ILLITE	common (abundant)	uncommon (minor)
KAOLINITE	rare (except as overprint)	common (minor)
PYROPHYLLITE-DIASPORE	absent (except as overprint)	common (variable)
ALUNITE	absent (except as overprint)	common (minor)
BARITE	common (very minor)	common (minor)

Mineral Assemblages in Host Rocks and Pebble Dykes

The altered andesites within the site have varied secondary mineral assemblages and alteration styles. Most have assemblages reflecting propylitic alteration, with chlorite in place of epidote. These propylitic assemblages also host plagioclase, which although is associated with the primary rock is likely to be secondary albite. This is not only due to its identification during microscopy, but also because of the presence of calcite in the central andesites which is a by-product of albitization (Blatt, 1982). Argillic alteration is recognised in the northern OR-AND andesite sample due to the presence of kaolinite indicating either possible overprinting of hydrothermal alteration styles due to kaolinization or from supergene weathering (Schwartz, 1959). The southern andesite samples (RP1 and RP2) differ from the other andesites also due to their intense phyllic character of alteration, having much more in common with the assemblages of the neighbouring altered greywacke that has quartz-sericite-pyrite assemblages.

The epidote content within the volcanic breccia is the strongest indication of its propylitic alteration, supported by the presence of chlorite, illite and pyrite. This reflects the alteration styles of surrounding central altered andesite, which is also propylitic in nature.

The altered greywacke in the study is similar to the other greywackes within the region, all having been intensely altered to phyllic quartz-sericite-chlorite-pyrite assemblages (Brathwaite et al., 2001b). The unaltered G1 sample has some secondary illite present, however, only in minimal quantities. Calcite is also present and may be an alteration product. However, it is more likely that it is a primary mineral from the sandstone cement (Blatt, 1982). It has been lost with the subsequent alteration of greywacke along the site.

The matrix samples of the pebble dykes reflect alteration of propylitic style due to the presence of illite and epidote. As these dykes are located within the central andesite, this mirrors the same alteration style as the rock they are hosted in. Despite the lack of analysed samples from the southern Cluster B pebble dykes, their alteration character observed during microscopy appear to have a higher abundance of sericite and illite, therefore possibly reflecting the phyllic style of their host rock alteration.

5.4 Clay Separates

The use of XRD is particularly necessary in the identification and quantification of the mineralogy of fine-grained and structurally diverse alteration products, particularly with clays and phyllosilicates (Allen, 1996). Their small particles and similar optical properties require the use of X-ray diffraction to analyse the rocks made possible when concentrations of clay minerals are substantial (>10%) (Blatt, 1982). In hydrothermal settings, clays are produced by interactions of rocks with acid to neutral solutions (Velde, 2013). The form of clay produced is dependent on the chemistry of reacting fluids, time exposed and temperature. Identifying clays present in samples is therefore useful in interpreting the geological history due to these controlling variables.

Clays can be particularly useful when used as an indicator of paleotemperature, the most important of which is the transition zone between discrete and interstratified smectite and illite, common in low sulfidation ore bodies where there is a clear upward and outward zonation of minerals (Velde, 1992). Although this transition of smectite to illite clay can be the result of several factors, the process is most strongly controlled by temperature (Pollastro, 1993; Moore & Reynolds, 1989). Under increasingly elevated temperatures, water from the smectite structural interlayer space is released, causing alteration to illite. As a result of this process, illite is more stable than smectite at higher temperatures, pressures and to different chemical environments. Within active New Zealand hydrothermal systems, illite is abundant and can be found at temperatures as low as 10°C (Ji & Browne, 2000), however, it is most common without smectite at temperatures above 230°C (Muffler and White, 1969). With decreasing temperatures, the transitional zone of interbedded illite/smectite can be found stable at <220°–150°C, with discrete smectite present at <150°C in New Zealand (Reyes, 1990; Simpson, 2011). This is a result of increasingly heightened temperatures favouring the stability of increasingly dehydrated species (Crobett, 1998). These recognised ranges in discrete versus interstratified occurrences can therefore provide an immediate identification of the temperature range involved in the alteration of a rock when illite ± smectite is present.

Identification of Illite/Smectite Interstratification

After two XRD runs with air-dried and ethylene glycol treated samples, two profiles enable identification of possible illite/smectite interstratification. These peak positions in both profiles are related to the proportion of clay species layers, their ordering, thickness and thickness of the glycol layers. Therefore, if there is disorderly migration of the glycol reflection away from the expected sites of the illite peaks, variable broadening and an increased valley to peak ratio, this indicates mixed-layering with expandable layers (smectite) is present (Moore & Reynolds, 1989; Velde, 1992). Otherwise, if peaks remain immobile, the assemblage only hosts discrete illite (Fig.47).

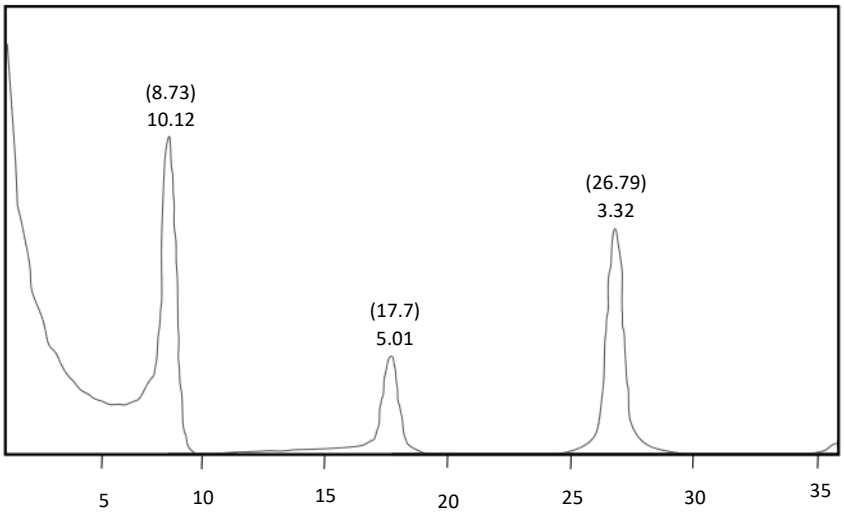

Figure 47: Locations of illite peaks in XRD diffractogram (Cuk anode). If discrete illite is present, these peak positions will not migrate.

Within each of the samples hosting illite (Table 8), there is evidence for the presence of discrete illite. There was no irregular broadening of the major illite peaks due to a swelling character, which would have been seen most notably as a broadening to a lower angle in the 18° illite peak due to the influence of a smectite peak at 16°. Not all samples host illite however, as in the case of the central andesite sample HST-AND. Despite this, the sample HST-TRAN from the same host rock does contain illite, only differing within the site as it was sampled more proximal to a pebble dyke. The sampled pebble dykes from the central Cluster A also show variability. PBL-1, the largest dyke at this site has an illite content, however, the dyke PBL-2 which cross-cuts it does not.

Results of Clay Fraction XRD Analysis

Illite and chlorite are the major minerals present within the northern andesite, volcanic breccia, and altered greywacke samples (Table 8). Within the samples clay fraction, the illite accounts for the sericite content described in previous chapters. A representative XRD profile for the analysis of the clays can be seen in Figure 48, from northern altered andesite sample GR-AND. This figure shows the key peak positions of illite and chlorite present as clinochlore. Although they are

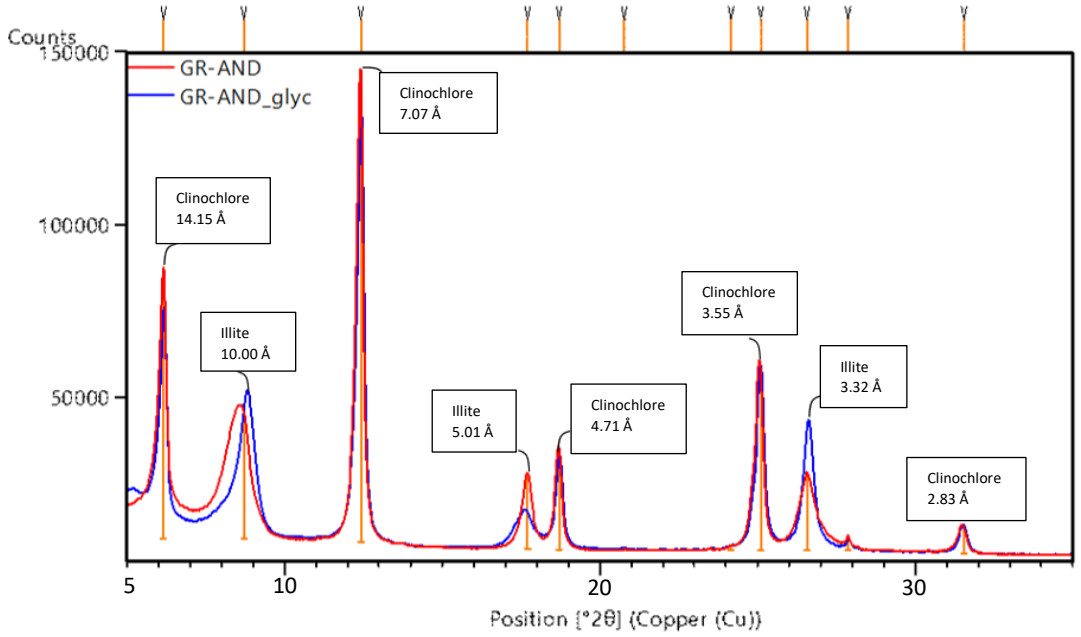

Figure 48: Clay separate XRD analysis of altered andesite sample GR-AND. This sample contains illite and chlorite (in the form of clinochlore), their major peaks *and associated angstrom (Å) positions are labelled. The untreated profile is in red and the secondary XRD run with the sample treated with ethylene glycol is in blue. Peak Å values from Moore & Reynolds (1989)*

not present within all samples, they are often present together, particularly within the samples taken from the centre and north of the field site. The peaks are narrow and sharp in the profiles which suggests that there are no other mineral signatures superimposed behind the clinochlore and illite peaks. The 10 Å illite peak does narrow with treatment, however this may be the result of the glycol creating a more intense peak. Between the untreated and ethylene glycol treated profiles from the GR-AND sample, there are also no significant deviations in peak positions. Although illite and smectite interstratification tends to be common in low sulfidation environments, due to the absence of smectite in each sample the temperature conditions were likely to have been too elevated for smectite to remain stable. Rather, the environment must have been in the temperature range to support the formation of both discrete illite and chlorite.

The only deviation in the character of the illite peak positions is seen in the sample taken from the orange outcrop of altered andesite (OR-AND) in the north of the site. In this particular sample, the key illite peaks have a broader character compared to the illite seen in the other traces (Fig.49). The broad peaks are

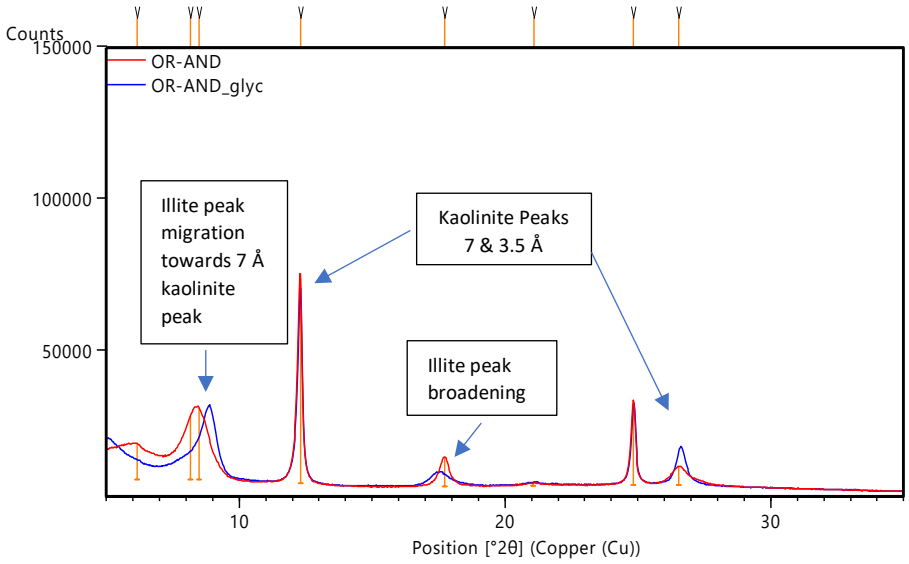

Figure 49: The profile of the clay fraction of the altered andesite OR-AND sample hosting illite and kaolinite but lacking the clinochlore present in the previous figure. The illite peak positions are broader than seen in other samples (e.g. figure 50), indicative of the presence of kaolinite. This is supported by the presence of the kaolinite primary peak at 7 Å.

present in both treated and untreated traces, therefore indicating this is not a factor of swelling but is instead the result of the influence of another clay species on the illite peak. Kaolinite has likely caused this trace effect, its major peak positions (7 Å and 3.5 Å) present in the place of the missing chlorite (Fig. 50). Due to the strength of the kaolinite peaks, this has resulted in the broadening of the illite peaks, where the illites 10 Å peak migrates to the 7 Å kaolinite peak, and its 5 Å peak widens towards both of kaolinites peaks situated either side. This has

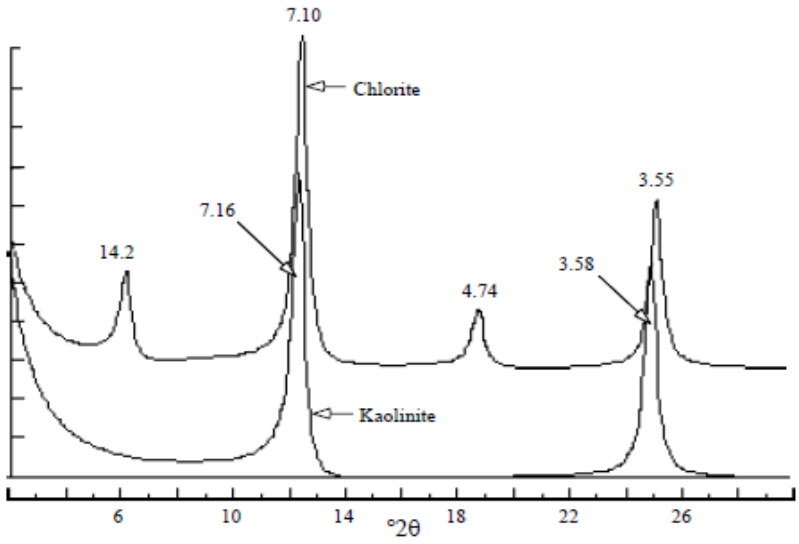

Figure 50: Chlorite and kaolinite peak positions, Moore & Reynolds (1989)

caused a broadening of the illite peaks by ~ 0.5° compared to the peaks seen in other sample traces.

Of all the samples analysed, clay fractions were present in all but the southernmost altered greywacke sample (G3) and the altered andesite sample from the southern boundary (RP2). For RP2, due to significant addition of silica rather than clay seen with microscopy, this is not surprising. However, for the G3 sample, due to the trend in phyllic alteration seen in the preceding altered greywacke samples, this is unexpected. It may also be the result of an increase in the addition of quartz, versus sericite which is also a major component in the phyllic mineral assemblage.

Crystallinity Index

Further interpretation of illite XRD profiles for use as a paleothermometer indicator is possible due to the crystallinity of illite relating to the temperature conditions (Ji & Browne, 2000). With increasing temperature, likely with proximity to the heat source driving the hydrothermal system or towards a local zone of mineralisation, illite becomes increasingly crystalline. A useful indicator of this crystallinity of the clay crystallinity is the width of the major XRD illite peaks. Width is controlled predominantly by two factors, the scattering domain size or crystal size and the percent of expandable layers (Eberl & Velde, 1989). Therefore, by recognising change in peak width, there has been a change in the crystal size as illite does not host expandable layers. The width of the peak is expected to be broader for smaller illite grains and narrower for larger grains as the sample becomes more crystalline (Fig.51).

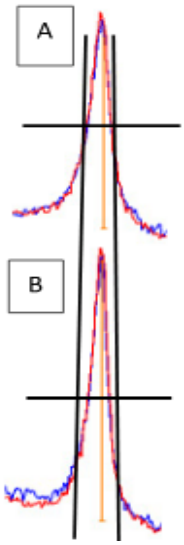

Figure 51: The narrowing of illite peak from figure A to B due to an increase in crystallinity and therefore the increase in thermal conditions.

To quantify this peak narrowing, a crystallinity index can be used. The major illite peak 001 (10 Å) is the

most commonly measured to find the full-width half maximum (FWHM) value, also known as the Kubler index (Eberl & Velde, 1989). The peak is measured at half of the peak height which is used to estimate particle size (Moore & Reynolds, 1989). The more crystalline the material, the sharper and narrower the peak will appear, providing a larger half-height value for poorly crystalline material.

For each of the samples with an illite content, the FWHM was calculated. The results are reflected in Figure 52 with samples plotted with spatial reference to the study site to show a comparative analysis of crystallinity. From north to south along the study site, although not a uniform trend, there is an apparent general increasing crystallinity with decline in FWHM values.

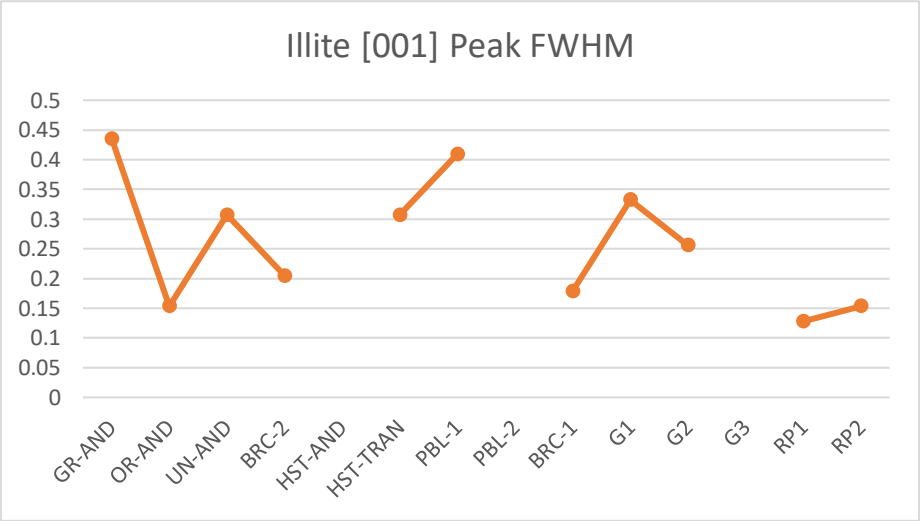

Figure 52: The FWHM or crystallinity of illite in the samples down the study site. Samples not plotted lacked clay content.

6. Geochemistry

Hydrothermal solutions introduce a variety of elements into altered rock. This interaction varies in nature due to the evolution of the temperature, chemistry, pH, and the volume of fluid interacting with rock from the core to the margin of the system (Schardt et al., 2001). The dispersion and mixing of magmatic and meteoric fluids, exsolved salts, magmatic volatiles and metals with circulating solutions results in zoned alteration around mineralisation centres (Corbett, 1998). The resulting signatures of this activity can be recognised in bulk rock chemistry which is a reflection of the rock mineralogy. Geochemical data is fundamental in recognising alteration processes that have occurred, enabling its use as a vector towards focal sites of alteration and mineralisation. Trends in alteration associated chemistry within the study site can be used to locate the local alteration zones within the larger epithermal system.

Lithogeochemical analysis is necessary to determine the material transfer involved in alteration, allowing for alteration process reconstruction associated with mineral and chemical zoning. Major, minor and trace element data provides an integrated signal of all alteration which would have acted within the site, reflecting the once dynamic interactions.

Methods

The same 15 samples analysed with XRD were also analysed for their geochemistry. Crushed bulk rock samples were made into pressed pellets for trace element analysis and fusion beads were made for major element analysis via X-ray fluorescence (XRF). The XRF instrument used was a Spectro X-Lab 2000. This provides a representation of mineral assemblages and geochemical signatures associated with host rock volcanics and greywacke and the two central pebble dykes which were sampled.

The fusion beads were also then used for LA-ICP-MS analysis, using an Elan 6100 DRC II ICP-MS (Perkin Elmer Sciex), with particular interest in the sample's

tellurium content. The data was processed using Iolite v 3.32. (Paton et al. 2011). The standards that were analysed on the day are from Jochum et al. (2011) (NIST610 and NIST612). Full instrument and laser setting are included in Appendix 4.

Precursor Samples

Alteration can affect certain minerals or phases preferentially, such as the preferential modification of feldspars during sericitisation (Mathieu, 2018). Fluids may interact variably with different minerals and therefore host rock types, which means that parent rock plays a large role in the character of replacement and leaching. The result is the amount or type of elemental mass gained or lost can rely greatly on the composition of the precursor rock. Therefore, having the representative chemistry of unaltered host rock can be extremely beneficial.

Obtaining unaltered rock compositions is often difficult in hydrothermal environments. Fresh or least altered samples of the altered rocks can instead be gathered from more distal sites if difficulties arise. A subtly altered greywacke sample was collected within the field site (sample G1), however, all of the igneous host rock was too pervasively altered to obtain the equivalent. To address this, whole-rock geochemical data from Booden et al. (2012) of a similarly described hornblende + pyroxene andesite (sample R12415), described as being fresh Kuaotunu subgroup andesite from Maumaupaki ~ 30 km from the study site, has been used as the andesite proxy.

6.1 Major Element Alteration Geochemistry

For alteration products to be useful for either indicating proximity to base and precious metal deposits or for characterising a hydrothermal system, alteration styles need to be both summarised and quantified. Due to the complexity of chemical changes accompanying alteration, this can make generalising the processes involved difficult. The alteration styles of propylitic, phyllic and argillic

alteration have already been classified within the site and provide a basis for the expected chemical changes with their associated alteration character. For this purpose, the full geochemical dataset from XRF analysis is displayed in Table 10.

During progressive hydrothermal fluid interaction with host rocks in a system, some elements are more prone to forming new minerals during alteration. Major elements are recognised as being mobile during alteration, this means they are involved in many of these mass change interactions between host rock and circulating fluids. Mass transfer represents the gains and losses resulting from the conversion of primary minerals to secondary (Leitch and Lentz, 1994). Therefore, with expected mineral assemblages and processes associated with these alteration zones, there are associated expected chemical changes. Table 11 summarises the expected chemical changes within the study site.

Table 11: Alteration types recognised within the study site and associated chemical changes and alteration minerals. Modified from Mathieu (2018).

	Mass Changes	**Example of Assemblages**
Sulfidation	+S, +metals	+ sulphides
Silicification	+Si	+ quartz
Carbonatisation	+C, (+Ca)	Carbonates ± quartz-white mica-chlorite Talc + chlorite + carbonate
Sericitisation	+K or -K, -Na, -Ca, +H	White mica +quartz +pyrite
Chloritisation	+Fe, +Mg, +H, -Na, -Ca, -K	Chlorite + pyrite + white mica ± quartz
Propylitisation	+H, +C	Epidote + chlorite + albite ± carbonate
Albitisation	+Na, -K	Albite + hornblende ± biotite-quartz

Table 10: XRF geochemical data of host rock and pebble dyke samples. Sample R12415 geochemical data sourced from Booden et al. (2012), representative of fresh Kuatounu subgroup andesite.

Rock Type	**Altered**			**Volcanic**	**Altered**		**Volcanic**	**Unaltered**	**Altered**			**Altered**		**Pebble Dyke**			**Unaltered**
	Andesite			**Breccia**	**Andesite**		**Breccia**	**Greywacke**	**Andesite**			**Andesite**		**(Cluster A)**			**Hbl + Px Andesite**
Sample	GR-AND	OR-AND	UN-AND	BRC-2	HST-AND	HST-TRAN	BRC-1	G1	G2	6-HST-G	G3	RP1	RP2	PBL-1	PBL-2		R12415 *
Major Elements (XRF, wt%)																	
SiO2	64.11	62.51	63.16	59.03	54.49	51.80	63.06	62.66	69.40	64.63	63.12	62.92	64.11	67.54	62.85		61.18
TiO2	0.61	0.67	0.59	0.61	0.77	0.95	0.51	0.96	0.63	0.81	0.78	0.53	0.56	0.66	0.52		0.71
Al2O3	18.72	18.05	18.05	17.15	18.28	19.68	17.50	16.91	15.21	17.32	19.32	16.30	17.38	13.93	15.68		17.35
Fe2O3	5.07	6.39	6.03	6.71	7.48	6.60	4.44	6.92	4.86	6.03	5.57	8.90	6.51	4.48	4.38		1.85
MnO	0.07	0.17	0.07	0.25	0.20	0.16	0.24	0.09	0.23	0.01	0.01	0.01	0.01	0.10	0.13		0.14
MgO	2.18	0.93	2.83	3.69	3.23	4.68	4.03	2.70	1.13	0.73	0.60	0.49	0.69	2.78	4.27		1.99
CaO	0.26	1.14	0.58	3.72	8.05	6.50	2.43	0.53	0.23	0.07	0.13	0.09	0.06	2.87	3.55		6.17
Na2O	2.80	0.45	2.51	2.90	2.41	2.93	3.89	3.16	0.36	0.30	0.59	0.35	0.33	0.43	0.24		3.25
K2O	2.85	2.44	2.50	0.86	0.14	0.52	0.67	3.08	2.59	4.65	4.25	4.27	4.98	0.34	0.30		1.82
P2O5	0.19	0.21	0.16	0.15	0.17	0.19	0.14	0.32	0.19	0.13	0.19	0.09	0.12	0.27	0.14		0.14
LOI	3.49	7.31	3.93	4.84	4.84	5.47	3.63	3.15	5.24	5.17	5.65	6.27	5.38	3.45	5.02		
Total	100.95	101.49	100.87	100.78	103.13	102.93	101.23	100.90	101.39	102.76	102.85	104.16	103.44	102.89	102.16		
Trace Elements (XRF, ppm)																	
F	416.00	627.00	249.00	129.00	331.00	425.00	47.00	543.00	387.00	896.00	1063.00	1034.00	1237.00	292.00	289.00		
S	1648.00	7036.00	607.00	6248.00	29007.00	32122.00	3924.00	1160.00	9468.00	24545.00	22248.00	36746.00	29644.00	21033.00	18931.00		
Cl	2675.00	3469.00	2603.00	1073.00	248.00	360.00	1578.00	871.00	2092.00	2067.00	1252.00	531.00	1106.00	309.00	294.00		
Sc	18.00	24.00	16.00	22.00	34.00	35.00	21.00	17.00	10.00	18.00	13.00	24.00	18.00	14.00	17.00		21.50
V	170.00	193.00	152.00	168.00	278.00	316.00	203.00	156.00	91.00	132.00	125.00	177.00	152.00	131.00	173.00		156.00
Cr	52.00	40.00	63.00	118.00	49.00	150.00	53.00	22.00	17.00	35.00	64.00	25.00	27.00	17.00	55.00		26.00
Co	20.00	23.00	24.00	18.00	21.00	19.00	20.00	21.00	20.00	19.00	10.00	42.00	28.00	25.00	16.00		21.40
Ni	11.00	12.00	12.00	22.00	14.00	16.00	27.00	16.00	12.00	11.00	11.00	15.00	9.00	14.00	13.00		6.30
Cu	23.00	36.00	20.00	25.00	149.00	5.00	19.00	37.00	127.00	66.00	13.00	6.00	6.00	7.00	10.00		25.80
Zn	67.00	67.00	76.00	93.00	80.00	82.00	212.00	73.00	289.00	13.00	14.00	15.00	12.00	57.00	85.00		59.00
Ga	18.00	20.00	18.00	17.00	21.00	22.00	18.00	21.00	17.00	23.00	26.00	14.00	19.00	15.00	17.00		21.00
As	10.00	16.00	4.00	15.00	31.00	8.00	11.00	43.00	24.00	34.00	46.00	32.00	46.00	9.00	43.00		
Rb	108.00	86.00	98.00	29.00	8.00	14.00	29.00	97.00	99.00	143.00	122.00	97.00	128.00	10.00	12.00		61.00
Sr	103.00	35.00	171.00	178.00	259.00	268.00	363.00	153.00	31.00	42.00	242.00	29.00	35.00	354.00	322.00		266.00
Y	24.00	17.00	14.00	16.00	16.00	18.00	16.00	18.00	14.00	18.00	21.00	12.00	9.00	15.00	13.00		20.70
Zr	112.00	105.00	107.00	94.00	94.00	101.00	93.00	182.00	178.00	193.00	217.00	92.00	99.00	136.00	104.00		124.00
Nb	5.00	4.00	5.00	3.00	2.00	2.00	3.00	6.00	5.00	6.00	6.00	2.00	2.00	3.00	2.00		5.60
Mo	4.00	4.00	4.00	4.00	4.00	4.00	4.00	4.00	4.00	4.00	4.00	4.00	4.00	4.00	4.00		
Sn	1.00	1.00	3.00	2.00	0.00	0.00	3.00	3.00	5.00	0.00	8.00	6.00	11.00	0.00	1.00		
Sb	2.00	2.00	2.00	2.00	0.00	0.00	2.00	3.00	0.00	0.00	0.00	0.00	0.00	0.00	1.00		
Cs	7.00	2.00	3.00	1.00	2.00	4.00	0.00	7.00	0.00	5.00	5.00	3.00	4.00	2.00	0.00		1.97
Ba	535.00	371.00	435.00	379.00	109.00	489.00	165.00	823.00	275.00	699.00	654.00	587.00	515.00	177.00	170.00		298.00
La	10.00	5.00	1.00	0.00	0.00	3.00	0.00	4.00	5.00	12.00	16.00	0.00	0.00	0.00	0.00		16.50
Ce	36.00	26.00	20.00	13.00	19.00	24.00	16.00	41.00	43.00	51.00	50.00	5.00	7.00	14.00	15.00		35.20
Nd	15.00	13.00	14.00	9.00	11.00	17.00	10.00	22.00	17.00	26.00	24.00	5.00	5.00	12.00	9.00		15.80
Tl	0.00	0.00	0.00	0.00	1.00	0.00	1.00	0.00	0.00	1.00	0.00	0.00	1.00	1.00	1.00		
Pb	8.00	7.00	10.00	4.00	12.00	9.00	17.00	7.00	5.00	11.00	6.00	3.00	12.00	13.00	13.00		7.40
Th	7.00	8.00	9.00	4.00	6.00	4.00	5.00	10.00	9.00	14.00	12.00	3.00	4.00	8.00	4.00		

Sericitisation

The deposits within the Hauraki goldfield are quartz ± calcite ± adularia ± illite type (Simmons et al. 2005), the equivalent of adularia-sericite type settings. For aid in characterising such epithermal systems, a whole rock geochemical approach presented by Warren et al. (2007) can be implemented. This method uses chemical compositions using molar element ratios (MER) for typical fresh volcanic rocks and main alteration minerals (illite, smectite, kaolinite and calcite). This provides a means for confirmation of mineral assemblages and determining alteration trends in the volcanic rock samples (Fig. 53).

The volcanic samples cluster into groupings based upon their spatial relationships, with the central andesites plotting in association with their higher degree of albitisation versus the northern and southern samples which bear significant illitic (sericitisation) alteration. The unaltered andesite proxy plots

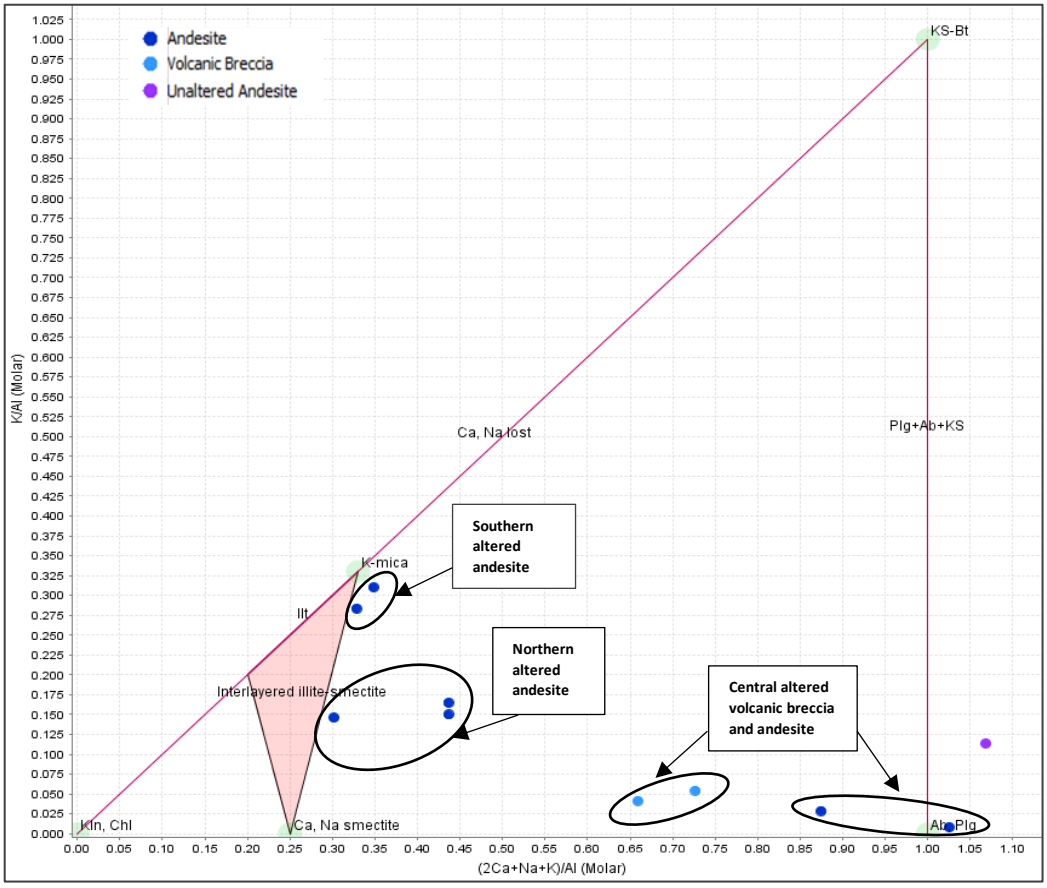

Figure 53: Molar element ratio plot for volcanic rock alteration, showing samples of this study (blue dots) After Warren et al. (2007). Kln – Kaolinite, Chl – Chlorite, Ilt – Illite, Plg – Plagioclase, KS – Potassic Feldspar, Ab – Albite, Bt – Biotite.

close to the central series, reflecting that albitisation has caused far less chemical deviation in the central samples compared to the seritised samples.

Silicification

Silicification has led to increasing silica concentrations in many of the altered samples relative to the protolith rocks. From the predominantly unaltered greywacke (G1) with a 62.66 wt.%, the proximal altered greywacke sample G2 increases to 69.40 wt.%. However, this value is seen to then decline by 6.28 wt.% again in southern greywacke samples across ~20 m. This may reflect the increasingly pervasive sericitisation, which often occurs simultaneously with silicification but can replace quartz in extreme cases (Schwartz, 1959; Schwartz, 1939). Due to the intensity of alteration recognised in these samples this may be the case or otherwise be the result of variations in host rock composition.

The volcanic host rock samples from the north and south of the site also see an increase from the unaltered andesite proxy. The central cohesive andesite and volcanic breccia however reflect a decline, with the largest loss seen (-9.38 wt.%) in the sample taken most proximal to the pebble dyke cluster it hosts. This is reflected in the presence of plagioclase feldspar noted with aid of microscopy within these rocks, as silica addition is often achieved partly by dissolution of feldspar not only from fluid. This therefore reflects the likely dominance of albitisation instead. The pebble dykes themselves also vary in their concentrations, with the larger of the two dykes sampled (PBL-1) at 67.54 wt.% and the smaller (PBL-2) at 62.85 wt.%. Both values higher than their host rock Si abundance.

Chloritisation and Carbonatisation

On the periphery of hydrothermal systems, Mg and Ca metasomatism occurs (Warren et al. 2007). This results in the addition of MgO and CaO to the rock, which is associated with the addition of calcite and chlorite and loss of K into

fluids. Plotted together (Fig.54), MgO and CaO reflect similar trends within the samples, with the central site showing the largest increase in their concentrations. This abundance declines both to the north and south due to the increase in seritisation and silicification which typically causes loss of both Ca and Mg (Mathieu, 2018), seen to be associated with phyllic alteration. The addition of MgO, often accompanied by the gain in FeO and H_2O, results in chlorite group mineralisation which is a product of propylitization. Therefore, this supports the propylitic alteration style classification assigned to central host andesite and associated pebble dykes.

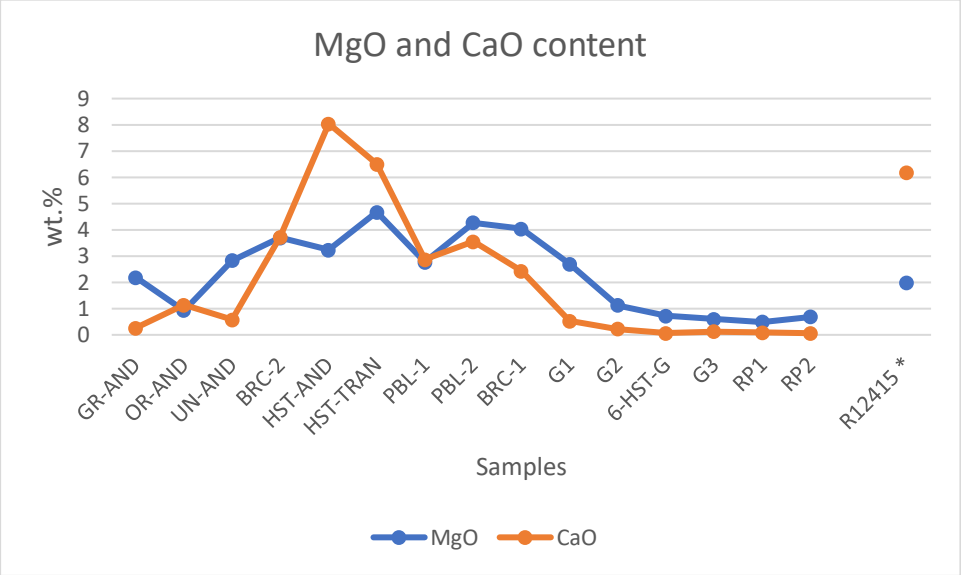

*Figure 54: MgO vs CaO wt.% concentrations within samples with spatial reference to their positions from north to south along the study site. * Unaltered andesite chemistry from Booden et al. (2012).*

Sulfidation

Although not treated as a major element, the sulfur content within many of the samples is significant, reaching minor levels of abundance (minor elements or elements are defined as occurring in concentrations of 0.1 – 1 wt.%). The sulfur within the samples are likely a result of the varied but often significant abundance of pyrite (FeS_2). The presence of pyrite in the broader Hauraki goldfield region is often associated with proximity to mineralisation (Christie et al., 2007). Low concentrations of sulfur lie within the distal areas of the system,

whereas increasing sulfur indicates more proximal distances from the central system. Such samples become associated with dominant adularia close to bodies of mineralisation (Barker et al. 2019).

Using total Fe vs S (wt.%) plot (Fig.55) the variance in the presence of pyrite within the study site can be demonstrated. Values toward the upper right of the plot indicating an increased pyrite abundance. The andesites plot across the full range, however, fall into clusters based on their position along the study site. The southernmost samples record the highest values, and northernmost samples with the lowest values. The central andesite is divided into two groups, high and low S and the subgroups of Central, Northern and Southern andesite and volcanic breccia clustering separately higher and lower respectively. The altered greywacke samples host moderate concentrations, with the least altered greywacke protolith (indicated by a red boarder) demonstrating S-poor chemistry. Amongst these host rock samples, the two pebble dyke samples plot lower than their host central andesite, central to the other values.

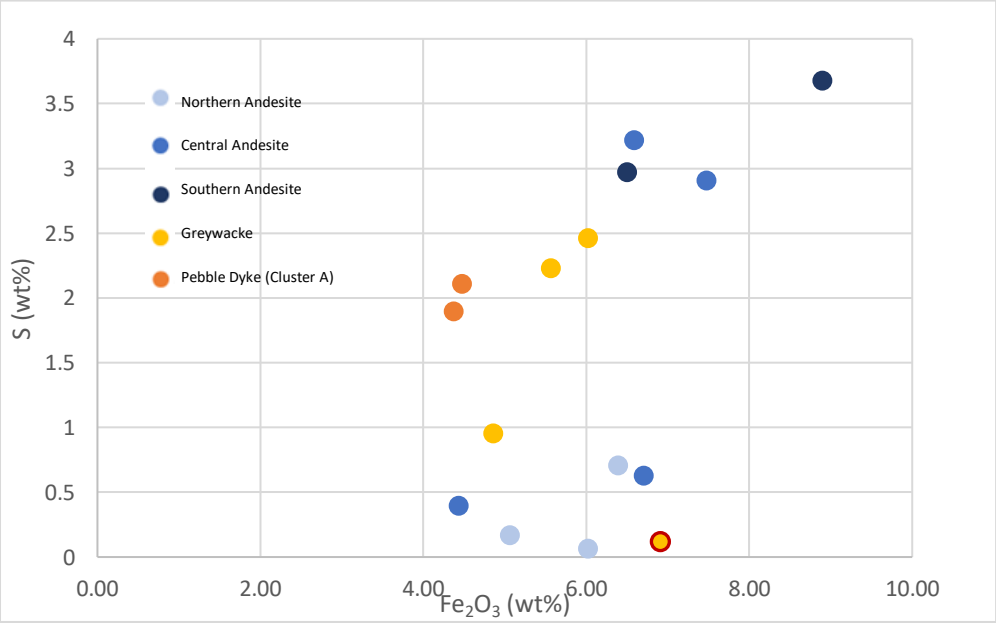

Figure 55: S vs total Fe (wt.%) reflecting pyritization of samples. Yellow point with red outline is "unaltered" greywacke sample (G1).

These observations are consistent with microscopy observations and reflect that the presence of pyrite varies across the site but not notably with alteration style. Instead degree of alteration appears to have an equivalent relationship.

6.2 Chemical Vectors

Pathfinder elements are elements associated with a target element (the commodity/orebody in explorative ventures) but are more widely dispersed and/or easier to detect (McQueen, 2006). They therefore reflect the concentrations of Au-Ag in the system and are able to be used as a vector towards them. Pathfinder concentrations can be controlled both by the solubility of an element within hydrothermal fluids and the growth of minerals which incorporate them. Barker et al. (2019) recognised As and less significantly Sb as being most enriched in rocks classified as dominant in illitic alteration, which would progress towards increasing As, Sb and Tl enrichment in adularia-dominant rock more proximal to ore bodies.

Split probability plots of the relationship between As and Sb with the samples classified by alteration type show this zoned enrichment (Fig.56) The As plot reflects a stronger association to the samples which experienced a dominance of sericitic alteration, those belonging to the phyllic alteration zone. This relationship weakens in relation to the samples associated with propylitic alteration. This would indicate the phyllic alteration has a more proximal relationship to ore bodies. The argillic sample relates closest to the propylitic samples, however, with only one plot point the relationship is not evident. In contrast, the Sb probability plot demonstrates a weak relationship with each sample, with very low values (ie. <2 ppm) which could be at or below the XRF detection limits. Therefore, its concentrations appear less beneficial, possibly due to how small of a scale the site encompasses.

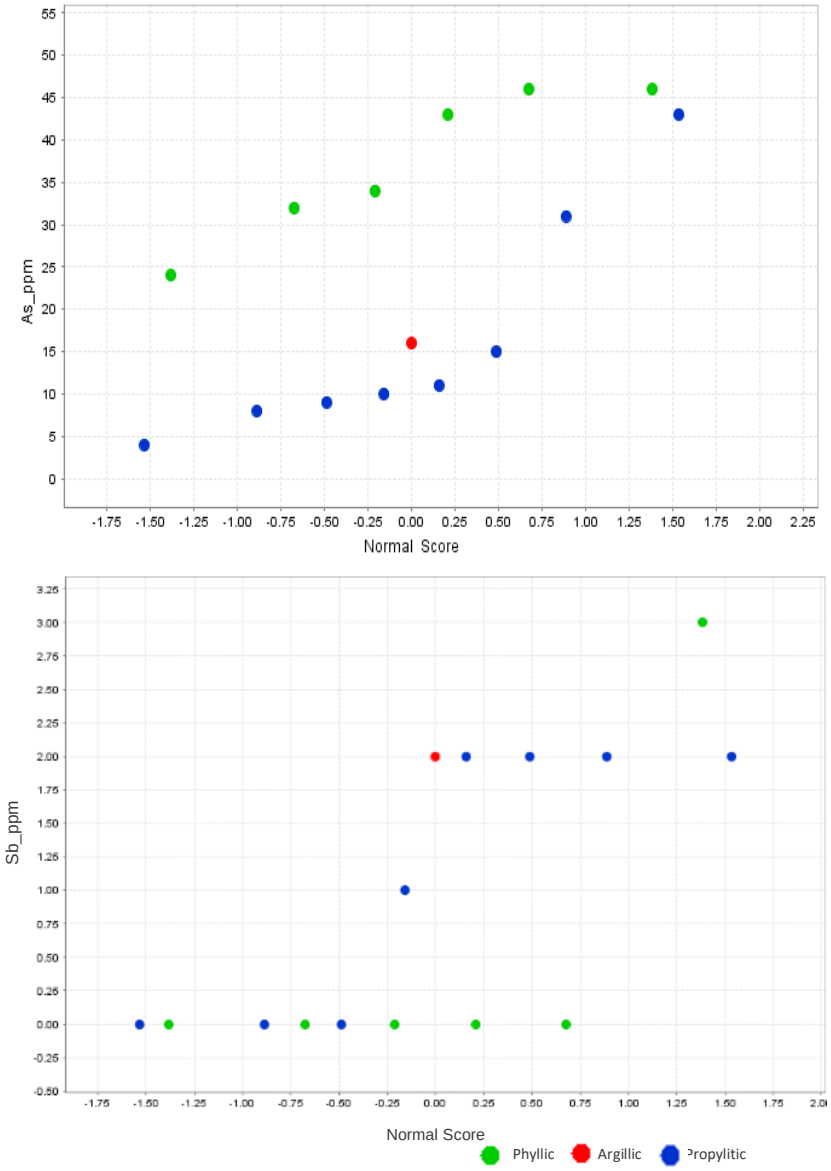

Figure 56: Split probability plots for arsenic (As) and antimony (Sb), showing their distribution within the different alteration styles present in the study site.

6.2 Alteration Intensity

From petrological observations, samples have been classified into degree of alteration intensity based upon alteration texture criteria (see chapter 4). Geochemical data can also be used to supplement and support this scheme, important as quantification of intensity is necessary for positioning the sample within the system (Mathieu, 2018). A simple method for this is use of the loss on ignition (LOI) values.

Figure 57 combines both the alteration intensity of each sample classified in chapter 4 (subtle to intense) based on thin section observations and the chemical LOI values. The resulting plot demonstrates the two methods predominantly mirror one another. The only significant anomaly between the two is the major LOI peak in the altered cohesive andesite sample OR-AND.

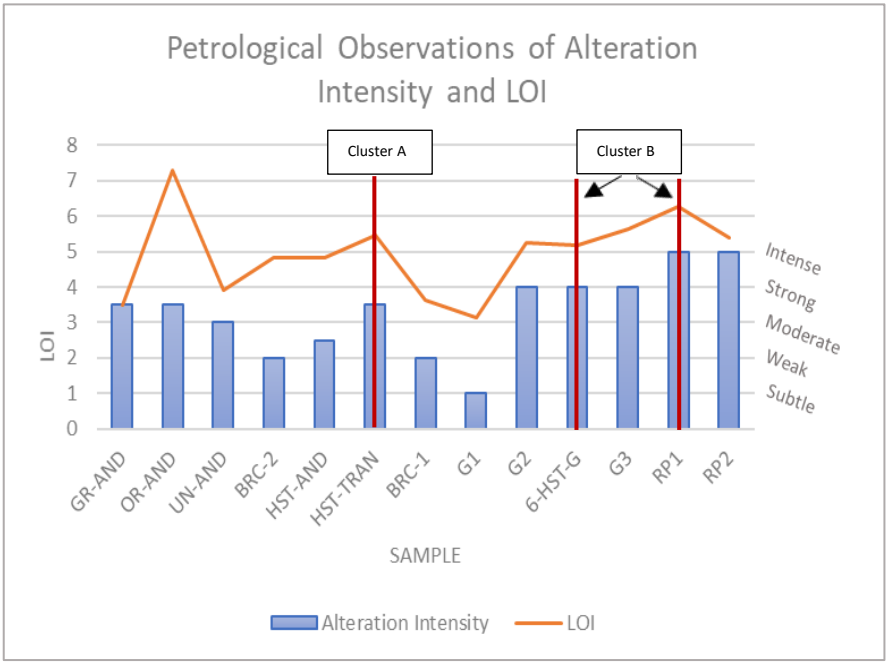

Figure 57: LOI values and alteration intensity classifications from petrological observations of host rock samples. Samples are arranged in relation to their positions down the study site from north to south. The most proximal samples to pebble dyke clusters A (central) and B (southern) are indicated by red markers.

The general trend of alteration intensity remains consistent within the northern andesite samples (with exception of OR-AND), declining within the central site to a minimum in the much more weakly altered greywacke sample G1. G1 has a LOI higher than 2%, a threshold used by Browne & Ellis (1970) to recognise fresh rock, which is an indication of the subtle alteration reflected in the petrological classification. With the increasing intensity of the alteration of greywackes, this trend continues to the southern boundary altered andesites where the LOI values again come to a peak.

Rocks which host the identified pebble dyke clusters (A and B) are indicated by the red markers in Figure 57. Their positions, although not always associated with the plots significant peaks, appear to correlate with localised peaks within

the study site. For example, the Cluster A pebble dykes are hosted in the central cohesive andesite, which was sampled twice with the HST-TRAN sample more proximal to the dyke bodies than the HST-AND sample. Between these two samples there is an increase in LOI of 0.63 wt.% despite the proximity of their sample sites (~1 m).

6.4 Fluid Source

As solutions percolate up through a hydrothermal system they are modified. Ascending fluids of magmatic origin mix with overlying meteoric fluids and interact with wall-rock, acting to further neutralise and modify its chemistry. These interactions therefore make identifying the fluid source difficult, especially due to the long-lived and ancient nature of the hydrothermal system with the possibility of direct chemical measurements impossible. However, trace bulk rock element data can aid recognising possible sources. These fluids are a dominant constituent of the processes involved in alteration, therefore comprehension of the significance of these fluids is fundamental in understanding the mineralising system.

Meteoric water can be an abundant fluid source in epithermal deposits, this can be indicated by high concentrations and fluxes of tellurium which is a reflection of direct fluid input from igneous intrusions (Simmons, 2016). Therefore, its presence can be an indicator of influence of magmatic fluid in an epithermal system. Te values (ppm) outlined by LA-ICP-MS analysis are displayed in Figure. 58 (the full ICP-MS data set can be found in Appendix 4). Overall, values exist within a range between 0.1 to 0.3 ppm, reaching a maximum in the most altered of the greywacke samples G3. However, even at its maximum the Te values are very small as low Te concentrations recognised as <5 ppm (Simmons, 2016). Therefore, it is not a noteworthy elemental component within the site, particularly so in the case of a number of samples with amounts too negligible to detect (lacking points in Fig.58). Even the pebble dykes reflect similar concentrations to their host rocks, which are inferred to have had more deeply

circulating water involved in their formation due to their vertical ascent. Although not a conclusive indicator, these low concentrations do suggest minimal magmatic influence overall, possibly resulting from significant shallow meteoric water dilution.

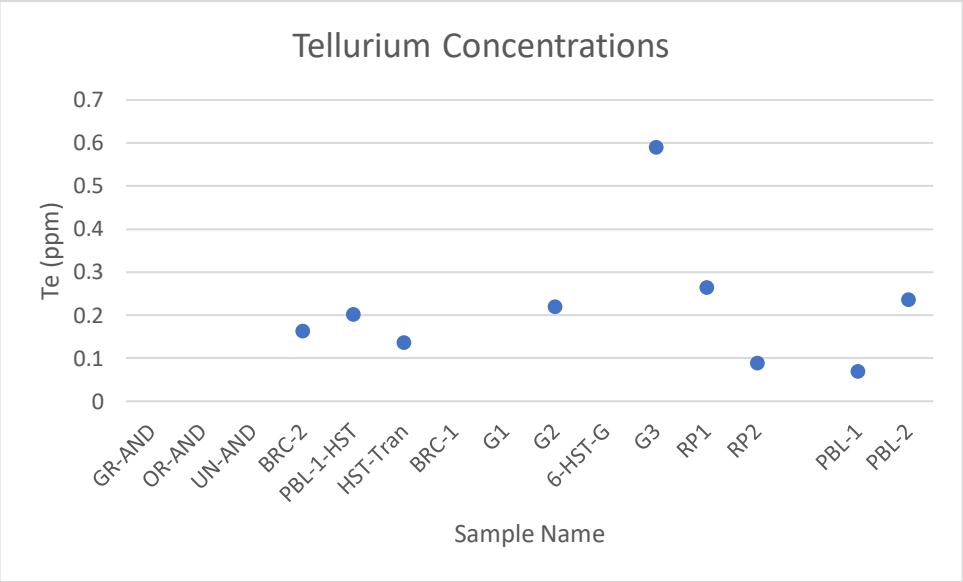

Figure 58: Tellurium concentrations of host rock and pebble dyke samples. Samples without plot points reflect where Te concentrations were too small to be measured by LA-ICP-MS.

7. Discussion

7.1 Zones of Hydrothermal Alteration

Regional alteration has been described as propylitic, phyllic and argillic in nature (Fraser, 1910; Brathwaite, 2001b; Christie, 2007). Each of these zones have been recognised at the study site. Alteration zones provide a means for assessing where, within the broader hydrothermal system, the host rock and pebble dykes are situated in space and time. The zones recognised have been summarised in Figure 59, providing a strip map representation of the hydrothermal character of the site.

- **Propylitic alteration zone** –

Propylitic alteration is common in the Coromandel district, particularly so within andesitic host rocks (Christie et al., 2007; Merchant, 1978). These zones are often present outside of major hydrothermal conduit zones, therefore are indicative of low water-rock ratios meaning the alteration mineralogy is more strongly controlled by the host rock lithology (White & Hedenquist, 1995). Within distal host rock associated with Hauraki Goldfield veins, up to hundreds of metres away, weak propylitic alteration occurs (Christie et al., 2007). Therefore, its presence doesn't necessarily reflect proximity to focal hydrothermal sites. However, the presence of chlorite and epidote identified within the facies assemblages suggests this zone is inner propylitic. Although epidote is only present within exposures of the central volcanic breccia, chlorite remains present across the breadth of the site. Chlorite within these settings also compositionally becomes more Fe-rich away from mineralisation (Barnes, 1997), so the presence of the Mg-rich member of the chlorite group, clinochlore, further justifies locating this field alteration within the inner zone.

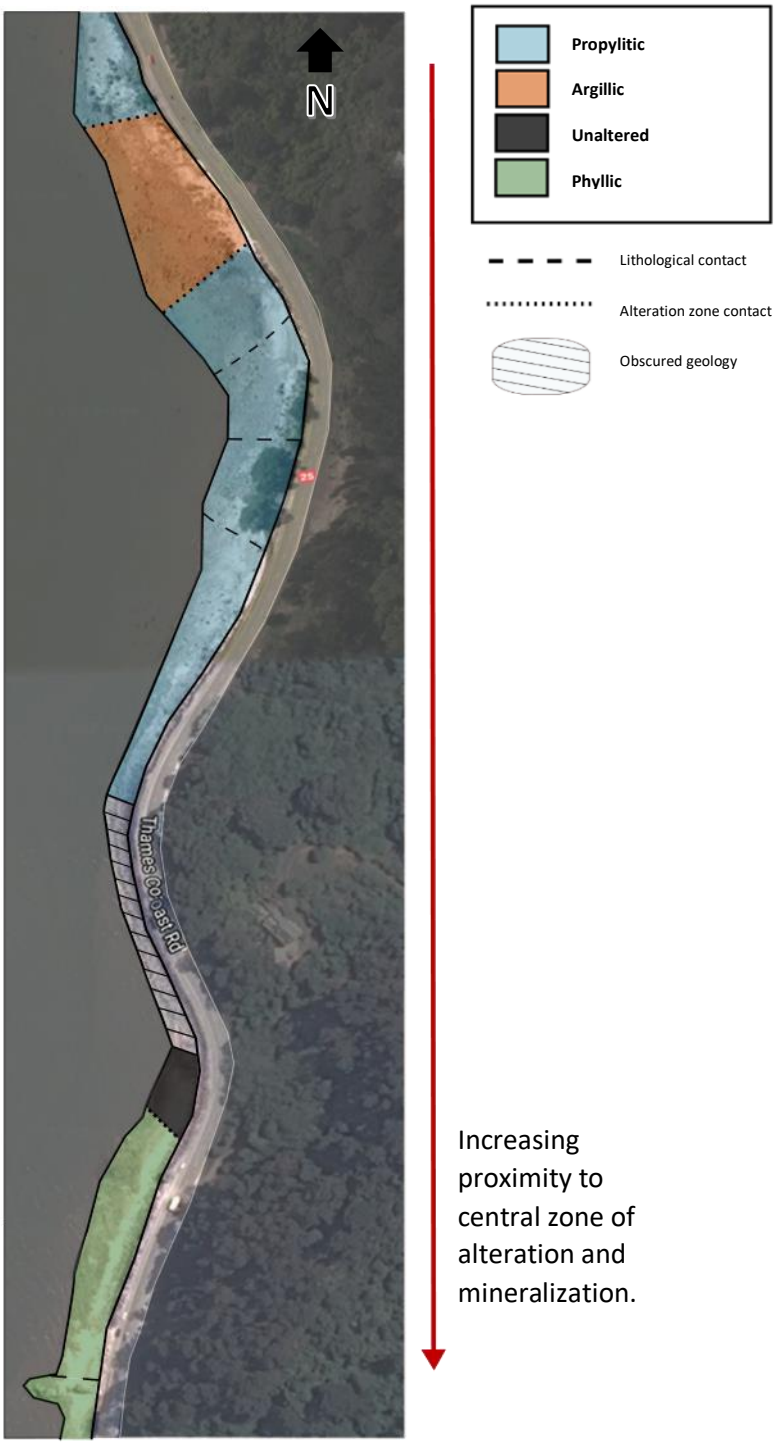

Figure 59: Alteration zones present within the study site. Alteration intensity and alteration zones reflect a likely southern trend in proximity towards focal sites of hydrothermal mineralisation.

Alteration textures of clinochlore pseudomorphs from parent rock minerals pyroxene and hornblende, weak to pervasive alteration of plagioclase by illite and the presence of pyrite due to alteration of magnetite are also recognised by Christie et al. (2007) in proximal propylitic assemblages within the Hauraki Goldfield. These features are not uniform in their occurrence within the full scale of the propylitic zone, however. Central alteration is dominated by albitisation, accompanied by pyritization, and epidote and calcite pseudomorphs. Farther north, the propylitic alteration is characterised, by clinochlore pseudomorphs and a higher abundance of illite which becomes more pervasive towards the northern site boundary. The only variance, however is the loss of pyrite in assemblages, almost entirely lacking in the northern cohesive andesites. Therefore, this may reflect a northern grading towards the inner propylitic zone which corresponds to increasing alteration intensity.

- **Phyllic alteration zone** –

Phyllic alteration zones are located more centrally to hydrothermal mineralisation than propylitic zones, commonly found adjacent to major structures or vein systems where fluids have a less than neutral pH (Corbett and Leach, 1998). Phyllic alteration is present within the field site to the south, with altered greywacke and cohesive andesite mineral assemblages abundant in illite, quartz and pyrite. Coinciding with the presence of phyllic alteration is also a notable increase in the intensity of alteration (Chp 6: Fig.57), which becomes described as strong-to-intense in character within southern altered greywacke and andesite. This is seen in the extensive seritisation and near complete replacement of all feldspar, epidote and chlorite. This therefore infers that a higher fluid-rock ratio was involved. Merchant (1978) recognised zones of pervasive phyllic quartz-sericite alteration in the area to likely represent the lower portions of an original hydrothermal reservoir localised above old heat sources. This correlates to the presence of discrete illite present nearer to veins and with increasing depth (Simpson et al., 2001), therefore, supporting the

association of this phyllic zone as a more focal site within the broader hydrothermal system.

- **Argillic alteration zone** –

Within the Thames area, some associated epithermal alteration occurrences have an affinity for argillic alteration (Chrisite et al., 2007). This character extends within the study site in a section of northern cohesive andesite. In low-sulfidation deposits kaolinite does not occur, except in the case of overprinting (Vikre, 1985). This is due to its stability in more acidic conditions, derived from moderately low pH fluids (pH 4; Reyes, 1990). Therefore, it has occurred as an overprint of the more neutral propylitic assemblage, likely formed separate from the neutral alteration zones. This has resulted in the replacement of chlorite and albite to create an assemblage of quartz, illite, kaolinite, pyrite and hematite.

White & Hedenquist (1995) recognise three possible origins of alteration minerals that are associated with acidic conditions such as kaolinite. This includes: 1) hypogene acidity due to magmatic HCl and SO_2, 2) steam-heated acid-sulfate waters formed near the surface, and 3) post-hydrothermal weathering of sulfide minerals. It is important to recognise which of these processes were involved to determine its association with the system. Magmatic-hydrothermal argillic alteration is unlikely as it occurs within acidic, high-sulfidation environments. The neutral, low-sulfidation setting associated with the study site eliminates this source. Steam-heated sources are a common introduction of acid minerals within low-sulfidation epithermal environments, occurring above the water table at ~100 °C due to boiled off hydrothermal gases. Supergene weathering instead occurs as a post-hydrothermal mechanism, under conditions lower than 40 °C as a result of descending surface waters and oxidation (Simmons et al., 2005).

Although steam-heated argillic alteration is common in the area, also recognised in the shallowest parts of the system as overprinting of propylitic zones (Christie et al., 2007), this site instead has most likely been affected by later weathering.

The strongest indicator of a weathering origin is the presence of hematite within the assemblage. Accompanying kaolinite in supergene weathering mineral assemblages are iron-oxides, which are indicative of a near surface setting. At lower temperatures and pressures at the surface and with an excess of water and oxygen, sedimentary residues become enriched in hydrous minerals and contain polyvalent elements in their most oxidised state (Blatt, 1982). Clay and ferric iron-oxide then become dominate phases, which is seen in the orange zones assemblage in the field. Hematite likely developed through alteration of both chlorite and pyrite, where a change in redox waters stabilised hematite over pyrite (Vaughn & Craig, 1997). As hematite dominates along grain boundaries, this further supports late stage-alteration coatings (Blatt, 1982). Steam-heated argillic alteration may however, have also introduced argillic alteration in conjunction with post-hydrothermal weathering. The presence of fracture patterns within the rock (Chp3: Fig 11B) are likely attributed to high pressure hydrothermal fragmentation, which could have arisen due to steam-heated activity. Therefore, this argillic zone is not indicative of the main phases of local hydrothermal environment but does indicate a near surface paleodepth.

Spatial Relationship to Mineralisation

Adularia-sericite type epithermal deposits display elemental mass changes which are associated with K metasomatism and H metasomatism (Warren et al., 2007). With increasing distance from epithermal Au-Ag mineralisation in near neutral pH systems, minerals grade from adularia to illite as the primary K-bearing mineral, corresponding to gradients of decreasing K (Fig. 60). This results in K acting as a vector towards focal sites of mineralisation. The clay transitions associated with this gradient (smectite -> illite-smectite -> illite) can be recognised with an increasing K/Al molar ratio. Barker et al. (2019) used this relationship within the Waihi extension of the CVZ, recognising that values greater than 0.33 cannot contain illite, and therefore must contain a proportion of hydrothermal potassium feldspar. Within the volcanic samples, the ratios support the lack of adularia reflected in the XRD analysis, with a maximum value

of only 0.32 (Chp 6: Fig.53). This locates the site within the epithermal setting, situating them in the illite division of the K-bearing gradient.

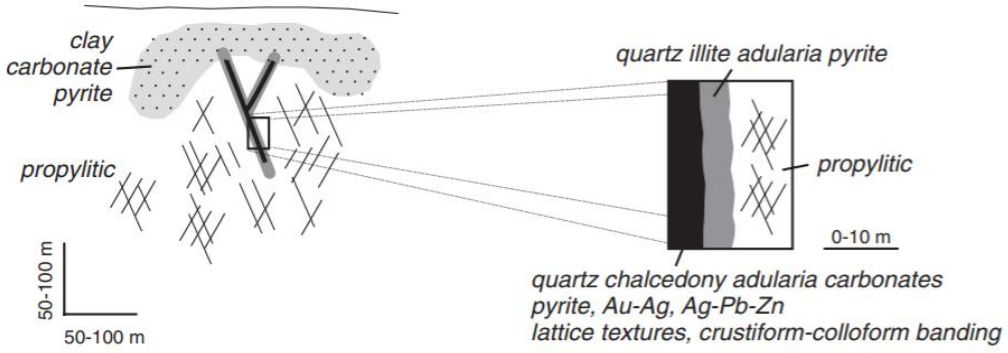

Figure 60: Mineral alteration zoning around Au-Ag mineralisation in a near neutral pH system (Simmons et al., 2005).

7.2 Hydrothermal Conditions

Temperature and fluid pH are the most important factors involved in influencing alteration mineralogy. Host rock lithology locally may have a more minor role in forming alteration assemblages (Corbett & Leach, 1998). Therefore, the mineral assemblages and alteration zones present are particularly useful in reconstructing these characteristics of the past system.

pH

Based upon the gangue mineralogy, the pH of hydrothermal system acting on the site reflects that of the larger Hauraki Goldfield system, dominantly neutral in nature. The two major alteration zones support this, as propylitic assemblages form under near neutral to slightly alkaline conditions, whereas phyllic occurs under slightly more acidic. From north to south across the field site, chlorite was found within a majority of the rock samples. Its presence is associated with slightly acid to near neutral conditions, but when accompanied by illite, as was most frequently the case, indicates conditions of a of pH 5 – 6 (Leach & Muchemi, 1987). It is expected that the alteration involved in creating both phyllic (seritisation) and propylitic (propylitisation) styles are due to similar

solutions but more intense alteration preferentially forms phyllic zones (Reber, 1916; Kirk, 1912). The argillic alteration is the only indication of acid conditions. As kaolinite coexists with illite, it likely signals that interacting fluids had a pH of 4-5 if it was the result of steam-heating (Hemley et al., 1980; Reyes, 1990). Otherwise, the evidence of dominantly near neutral fluids support the location of the site within the up-flow zones of the hydrothermal system (Browne, 1978).

Temperature

Many minerals within hydrothermal environments are temperature sensitive and provide the ability to determine the likely thermal conditions that acted upon a rock (Fig.61). Not all minerals are helpful however, as some are found across a wider range in temperature than others. Useful geothermometers include minerals which fall into the categories of clays, zeolites and calc-silicates (White & Hedenquist, 1990). The best paleoindicator available across the study site is the clay species. With XRD analysis, it was determined that clay bearing samples hosted discrete illite, which is indicative of temperatures above 230°C (Muffler and White, 1969). With the use of microscopy and SEM imaging, the clay textures within the propylitically altered andesite was recognised as sericitic. This means the illite texture is very fine-grained which forms at >200 – 250 °C, rather than the coarse-grained variants which form at a higher temperature range of >250 to 300 °C (Allen, 1996).

The sericitic texture of illite appears consistent across the study site, but its crystallinity was seen to have a general increase down the study section (with use of FWHM values; Chp 5: Fig. 52). This is a factor of increasing temperature during its formation, therefore a possible marginal increase in the temperature of the active hydrothermal system may have occurred down the site towards increasingly intense phyllic alteration. It is not likely to be significant however, with phyllic assemblages commonly forming at a similar range of >200 to 250 °C (Corbett & Leach, 1998).

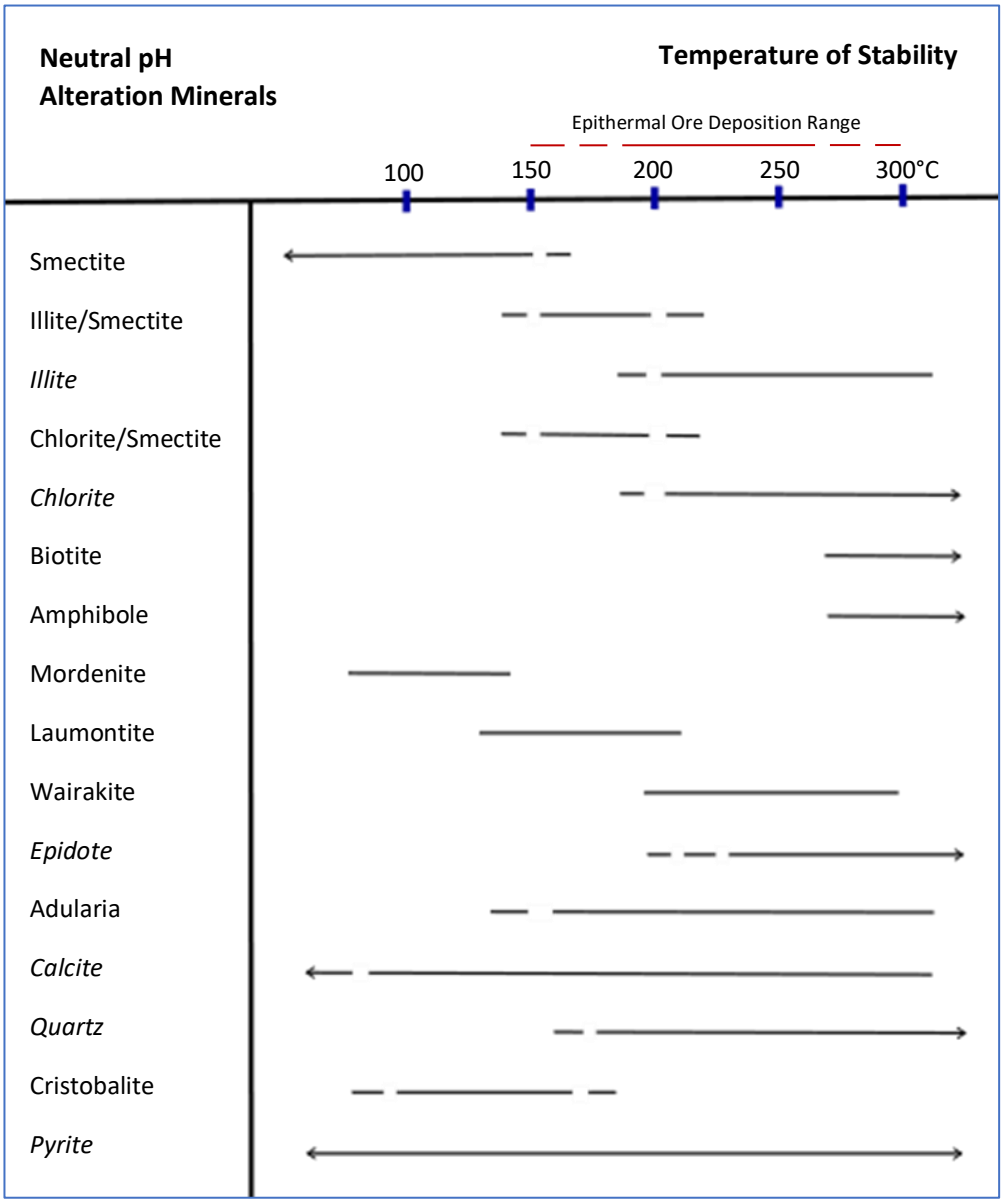

Figure 61: Chart of minerals which are commonly found within neutral pH epithermal settings with their associated temperature ranges of stablity. Minerals which are present within the host rock and pebble dyke assemblages within the study site are italicised. Modified from White & Hedenquist (1990).

The southward trend in increasing temperature may also be reflected in the presence of pyrite across much of the site, except within the unaltered greywacke and andesite to the north. Despite the broad temperature range expected for the formation of base metal sulphides, fluid inclusion data from the broader CVZ indicate that they were deposited from fluids with a high temperature range of 260° - 320°C equivalent (Brathwaite & Faure, 2002). Due to how pervasive pyrite becomes in the samples towards the southern site

boundary dominated by phyllic alteration, this also suggests a higher temperature range is associated with the phyllic style of alteration.

Therefore, across the study site, the minimum temperature expected to have acted to alter rock is at least 230°C, where propylitic alteration is expected within the range of <200-250 °C (Corbett & Leach, 1998). This would increase to 240°C with the introduction of epidote in the central zone of propylitic alteration (Simpson & Mauk, 2011). Towards the phyllic alteration zone to the south, accompanied by an increasing abundance of pyrite, a temperature of ~260 °C is likely. It is possible for minerals to be present outside of their expected range of temperature stability depending on host rock, fluid chemistry and mineral metastability. However, with the multiple mineral phases present contributing to the assessment, this range is well supported.

7.3 Paragenetic Sequence

Based upon knowledge of the setting, the minerals identified, and microtextures, a paragenetic sequence has been created for the hydrothermal activity within the field site with aid from mineralisation sequences described by Christie et al. (2007) (Fig.65).

Early stages of alteration would have involved propylitic alteration introducing albite, calcite, chlorite, epidote, pyrite and to the host andesite, replacing primary plagioclase, pyroxene and hornblende as pseudomorphs in the andesite. As the system developed, progressively intense silicification would have occurred, also introducing seritisation across the site. This modified early propylitic assemblages, introducing illite through partial replacement of chlorite and albite. The weakest and likely earliest seritisation occurred within the central section of the site, indicated by the selective character of replacement (Schwartz, 1959), whereas later, more intense seritisation and silicification occurred within the southern phyllic zone. Pyritisation occurred over much of the hydrothermal history but is most related to early stages of mineralisation in the area (Christie et al., 2007). Post-hydrothermal supergene weathering then would have

introduced the kaolinite and hematite as replacements of chlorite and pyrite within the argillic zone.

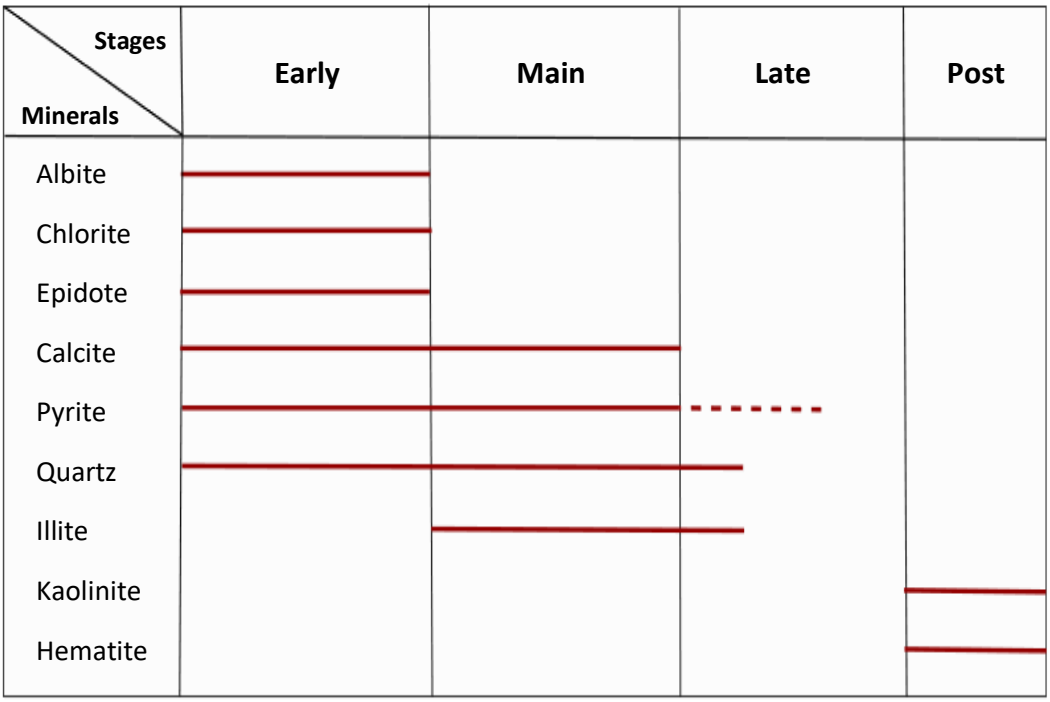

Figure 65: Paragenic sequence of alteration minerals present within the study site.

7.4 Pebble Dykes

Morphology

The location of the Thames coast pebble dykes, as in the case of similar examples globally (see chapter 2) has likely been controlled by pre-existing faults within the host rock. It is thought that the orientations of faults and hydrothermal veins within the Coromandel Peninsula are strongly influenced by the faults in the basement rock, inferred to strike at NNW and NE-NNE (Skinner, 1967; Sporli et al., 2007). The measured orientations of the pebble dykes within the field are aligned between NW and NNW (Chapter 3: Fig.19B & C).

This relationship to pre-existing faults would also mean that the thicknesses of the pebble dykes are also, at least in part, controlled by these faults. This is not to say however, that the processes involved in the dyke formation does not influence the morphology of the pebble dykes. The incorporation of wall rock

into dyke fluid flow may be suggested within the field by the undulating form of some of the dykes. The initial surface expression of the fracture has been modified by erosive dyke-forming processes. However, despite this, contacts with host lithologies remain consistently sharp. On a larger scale, the fractured conduits have also likely experienced wall rock stoping, which would act to enlarge the host conduit through mass collapse of wall rock as the activity of the thermal fluids dissolve and physically remove structural support (McCallum, 1985). This mechanism would have also contributed to more fragmented rock incorporated into flow.

Modification of the fracture network is also apparent. Rather than occurring as a single dyke, as seen at Mt. Emmons (Colorado; Thomas & Galey, 1982) , they instead mirror the character of the dykes recognized at El Salvador (Gustafson & Hunt, 1975), taking on the form of major bodies splitting into minor branches. These offshoots all display irregular thicknesses and attitudes. Therefore, rather than being limited to major fault fractures, it is likely that other weaknesses within host rock; fissures, contacts or structural intersections, have also been utilised for pebble dykes to expand into. A likely feature may include a contact between the unconformably exposed greywacke adjacent to the much younger volcanic breccia and cohesive andesite units.

The thickness of pebble dykes from the Thames coast site range between <1 cm and 40 cm. It is apparent that the character of the pebble dyke components change with this variability of widths. Within the larger dykes, larger pebble clasts are hosted within a matrix of fine material. As dykes narrow to ~ 10 cm, they begin to appear more compact, with matrix and clasts tightly packed together. Narrowing of dykes limits the size of the clasts able to move through the void space. Therefore, they are dropped out of flow. As this continues, the clast components continue to become compacted, resulting in a higher intensity of clast emplacement and causing a lower matrix-clast ratio. At the < 2 cm scale observed in the field, only small < 1 cm-sized fragments and fine clay sized material are able to continue along the flow path until the dyke pinches out.

Clasts

The range of lithologies within pebble dyke deposits have either settled near their host stratigraphy or have travelled unknown distances from depth. They are a representation of the host rocks in the subsurface of the system which the flow of material has travelled through, incorporating fractured rock as it travels. Often to identify the history of a breccia unit, observations of the characteristics and ranges in shapes, sizes and composition of clast can be used (Weisheit et al., 2013).

Lithologies express the extent of fracture and ascent involved in pebble dyke formation. A number of the dyke components have been classified as volcanic, unsurprising due to the region having been heavily influenced geologically by volcanism. However, an even larger volume has been recognised as greywacke sandstone and argillite which most rationally can be assumed to be sourced from the Manaia Hill basement. If sourced from the Coromandel basement depth (>1000 m; Edbrooke, 2001), its presence would reflect significant pressures involved to allow for the fragmented material to ascend vertically to the epithermal system. However, due to the presence of the greywacke as beach exposures, it must also be acknowledged that faulting in the area may have resulted in a far shallower depth of source greywacke.

The morphologies of the clasts also express transport mechanisms. With vertical transport, the clasts become more rounded. This occurs due to hydrothermal milling during transport within the fluid flow, grinding down and shaping rock fragments through abrasive erosion, and to a lesser extent corrosion from hydrothermal gases and fluids (Bryner, 1961; Cornelius, 1967). The well-rounded and wide range in sizes and lithologies of clasts are likely a result of their transportation by turbulent fluidisation (Oliver et al., 2006). Therefore, this provides a means of assessing the distance the greywacke may have been transported.

The milling of material evolves the clasts with longer durations of transport, so subangular fragments would reflect a shorter distance of transportation than the

well-rounded fragments (Bryant, 1968). Due to the limited vertical extent available to measure clasts, it was not possible to recognise whether they become more well-rounded further away from source as was seen in Tintic (Farmin, 1934) and El Salvador (Gustafson & Hunt, 1975). However, the greywacke clasts reflect a similar character as the volcanic clasts, both predominantly present with a sub-rounded character. Therefore, indicating a similar extent of vertical transport. This may however be due to limitations on the degree of rounding possible under these conditions with the extended duration of the greywacke not enabling a well-rounded morphology.

Of more note is the size of both pebble lithologies. Although the largest were frequently volcanic, the greywacke clasts had the same scale as the average volcanic clasts hosted. This is again a possible indication of similar transport distance as extended duration would decrease their size. Therefore, indicating the greywacke being incorporated into flow above basement depths, comparable to the volcanic host rock stratigraphic depth. This observation may also be undermined however, as it may instead be a factor of the durability of the greywacke, able to withstand a higher degree of chemical and physical weathering during transport. Ultimately, the morphologies would indicate a shallower than expected incorporation depth of the greywacke. However, due to the limited extent of the field site, the depth of the greywacke clast source is difficult to define.

Pebble Dyke Alteration

Across the field site, the locations of the pebble dyke clusters did not directly correlate to the sites of highest alteration intensity. This is displayed best with the central Cluster A pebble dyke assemblage, which is hosted within some of the least altered rock in the site. They are hosted within a propylitic zone of alteration which becomes more intense to the north. However, within outcrop scale, directly proximal to the bodies, a marked intensification of alteration degree was recognised. Two samples, one taken neighbouring a dyke and the

other a few metres away display this (Chp 3: Fig.8). Primary textures are significantly modified and there is an introduction of higher temperature minerals (epidote and illite). Therefore, although at alteration zone scale they have not contributed to alteration intensification, at this scale, they have likely acted as a permeable pathway.

Despite this correlation with alteration intensity, the pebble dykes themselves are not altered as strongly as many host rock exposures. Both clusters appear to mirror their host rock style of alteration, Cluster A with propylitic alteration and Cluster B with phylllic. This may be a factor of the pebble dyke adopting the same style as the source rock alteration assemblage of its fragmented material, as the dyke matrix is likely a cement of the fragmented clasts as is often the case for breccias in general (Bryner, 1961). However, the pebble dykes also host clasts with varied alteration character. Volcanic fragments appear with propylitic and phyllic style mineralisation, the greywacke with phyllic. Therefore, they dykes likely experienced alteration at the same time as the local host rock to adopt the same style. As most clasts, including greywacke fragments, have therefore been altered independently prior to incorporation into the pebble dykes, this suggests shallower source depths of fragmentation is more likely. Therefore, the source stratigraphy must occur at depths within the epithermal alteration zone.

The timing of the pebble dyke emplacement is able to be approximately inferred based upon the alteration textures present both in clasts and matrix. Due to the presence of the previously altered clasts, this indicates that they cannot be pre-hydrothermal. Its initiation must have occurred after the source rocks of the clasts had already been modified. This timing can be further confined by the presence of pyrite. Although many of the clasts host varied abundances of pyrite, indicative of alteration prior to fragmentation and incorporation into the dyke flow, pyrite also has developed within the matrix and across clast boundaries. This reflects pyritization must have occurred post-emplacement. The pyritization but lack of ore may indicate that the pebble dykes formed after the early surge of pyrite but prior to ore mineralisation (Bryner, 1961). This therefore

confines the timing of the pebble dyke formation to early stages of alteration (Fig.65).

7.5 Fluidisation Model

With the leading process attributed to transport of material driving to pebble dyke formation being fluidisation, many characteristics of those involved in this study support its involvement. Fluidisation, described in greater detail in chapter 2, transforms the rock material into a fluidised state with the introduction of buoyant gases and fluids. The pebble dyke bodies display features reflective of turbulent, fluidised flow. This includes varied clast orientations, geometries of rounded pebbles and continuity of bodies as material is transported as aggregates rather than individuals (Leva, 1959). Evidence of hydrothermal alteration also provides support for fluidised flow, reflecting the system interacting with associated hydrothermal solutions. At microscopic scale void spaces between larger clast fragments were also common, however amongst the finer matrix material, no form of flow banding patterns are apparent which were recognised in the El Salvador pebble dykes (Gustafson & Hunt, 1975).

The source of fluid leading to this mode of transport was generated at an unknown depth, but deep enough to incorporate the greywacke clasts, with the convection initiated by magmatic heat allowing the ascent to the surface. The ability for the fluids to transport this mass would have initiated by either an increase in fluid density or a change in the flow pathways from low permeability small shear zones to open extension fractures (Bryant, 1968). The pressure gradient would have created the fluid flow along fracture zones, and the transportation may be further aided by the process of wall rock stoping (McCallum, 1985). Due to the higher abundance of greywacke clasts, versus the regional volcanic stratigraphy, this means that the majority of processes (initial fracturing and transport) was initiated deeper than the volcanics which dominate the upper stratigraphy. As stated however, there remains uncertainty as to

whether this was at basement depth or possibly instead at shallower levels from an uplifted greywacke source block.

If initiation was from much shallower depths, fluidisation would be even more plausible. A major limitation of a fluidisation model of formation is the volume of fluid necessary for this form of transport (Bryant, 1968). The flow pathway voids must be entirely filled with hydrothermal fluids to create enough pressure for the upward motion of the fragments. Therefore, with a less extensive system, lower volumes would be necessary. The void spaces requiring flooding relate to the width of the dykes, which measured in the field range between <1 – 40 cm where visible. This scale is modest in comparison to pebble dykes from other global sites which can reach up to 10 m wide. Therefore, further diminishing the volumes of fluid necessary.

Field measurements of pebble dyke clasts reached 12 cm in size, which consist of lithologies from various stratigraphic depth. The mixing of lithologies may be a result of the fluidisation process, spouting. Spouting is the action of a non-uniform pressure gradient circulating material up and down in the channel way, allowing thorough mixing of clasts from many different depths (McCallum, 1985). The strength of flow would have therefore needed to have been able to transport these sizeable clasts and allowed for their mixing. This would have however been alleviated by the presence of fine-grained fragments, seen as the matrix in the pebble dyke deposit. During flow this material would have likely reduced the viscosity of the transporting flow and increased its specific gravity or density allowing for larger clast transport over longer distances (Bryant, 1968). In a transect of a pebble dyke-host rock contact, a band of fine clay material was apparent within the dyke body. This may also suggest transport occurred with a boundary of clay, aiding in suspension during transport of clasts.

It is also apparent that the pebble dykes did not form with a single event of passing fluid, further addressing the limitation of fluid volume (Weisheit et al., 2013). Stages of brecciation can be shown to relate to multiple cross-cutting relationships (Silberman & Berger, 1985). This is suggested by the cross-cutting of dykes exposed within Cluster A. In this section of dykes, PBL-2 and 3 run

parallel to one another, cross-cutting PBL-1, which establishes it as the oldest of the group (Chapter 3: Fig.20). Although ultimately limited by the extent of the fracture spaces they infill, their widths may also allow inferences of the strength of the pebble dyke forming system. PBL-2 is the widest, occurring after PBL-1, and PBL-3 is the narrowest of the three. Although between PBL-2 and 3 the relative timing is not apparent, they may have occurred consecutively due to their similar orientations, so conceivably express an increasing intensity of the fluid flow volumes from the initial PBL-1 event. A minor < 2 cm dyke noted cutting across PBL-2 may then reflect a waning of the pebble dyke forming processes. However, due to the limited extent of the exposed system, these relationships may not reflect the full expanse of the system.

7.6 Pebble Dyke Association with Mineralisation

The pebble dykes within the site have been recognised as co-hydrothermal features, having formed during hydrothermal activity. As the Hauraki Goldfield hydrothermal activity has been linked to the development of Au-Ag deposits, the structural influence the presence of the pebble dykes may have had on mineralisation is of possible significance. Direct interaction of ore-bearing fluids with the dykes has not occurred, which would have been the case if gold were recognised within their mineralogy. Despite the pebble dykes within the site having not hosted ore-bearing fluids, this does not eliminate the possibility for successive events or different conditions involving similar pebble dykes influencing ore development.

The timing of pebble dyke formation is a key aspect of possible influence on ore mineralisation. Due to formation prior to ore deposition, they may still be useful for exploration if the ore-bearing solutions utilized the same passages as the altering solutions (Lovering, 1949). Veins striking at 000°-030° and 040°-070° have the highest gold production within the Hauraki Goldfield (Christie et al., 2007). This can also be assumed to be the preferential orientation of fluid flow. As there is a disparity between the pebble dyke orientations which trend ~ NNW,

they are not aligned for preferential fluid movement. Otherwise, if their strikes were more aligned in favour of flow, this may have acted to potentially double permeability, as found in the case of the analogous features of tuffisites (Kolzenburg et al., 2012), therefore promoting ore-bearing fluid access.

The possibility of pebble dykes acting as major fluid channel-ways is most closely linked to them acting as permeable paths. Many indications within the field reflect them as such, with proximal host rock at the local scale having been influenced to a greater degree by alteration. Although this relationship is not apparent at the full scale of the site, the permeability of the host rocks has likely affected their influence. Greywacke, due to its partially metamorphosed character, is known to have an impermeable character (McNamara et al., 2014). Despite this, the greywacke has been intensely altered, radiating away from the southern dyke cluster into an unaltered exposure (Chp 6: Fig.57). This unaltered greywacke otherwise disrupts the zoning expected in such systems, from inner propylitic into phyllic. Due to the presence of discrete illite, this indicates high water-rock influence due to adequate permeability in the altered greywacke, otherwise illite-smectite interstratification would have dominated (Tillick et al., 2001). Therefore, because of the presence of the Cluster B pebble dykes, which are the largest in the field, permeability may have been a notable influenced in the event of impermeable host rock. As pebble dykes form within competent host rock (Bryner, 1961), they may also preferentially develop within country rock with similar impermeable qualities.

7.7 Discussion and Summary

Alteration within the study site has been recognised as relating to the broader Hauraki Goldfields low-sulfidation system. Hydrothermally related propylitic and phyllic zones of alteration host assemblages formed from near neutral fluid interactions at temperatures between 240 – 260°C, with post-hydrothermal supergene argillic overprinting introducing more acidic mineral phases. Within this system, co-hydrothermal pebble dykes also developed, which due to

providing further permeability within the host rock, modified alteration intensity proximal to their clusters. Down the study site, although disrupted due to host rock qualities, the change in alteration intensity and alteration zone indicates an associated trend towards focal hydrothermal mineralisation to the southern boundary (Fig. 59).

The pebble dykes hosted within this system are clearly related to hydrothermal activity within the site. The timing of their formation likely occurring during early phases of the system indicated by the presence of variably altered clast components and matrix textures. Due to the involvement of hydrothermal fluid in their formation in conjunction with features characteristic of turbulent flow, the mechanism of fluidisation is likely to have had a significant role in the formation of the pebble dykes. Although the model of fluidisation is limited by the requirement of significant fluid volumes, the extent of the system and multiple dyke forming events minimises its likelihood. Further investigations into the volumes of fluid circulated into the hydrothermal system and pressure of flow required to form such deposits would allow for a more definitive acknowledgement of this however.

The depth of the extent of the pebble dyke forming processes can be best defined due to the presence of greywacke clasts. Due to the clast morphologies, it is evident considerable vertical ascent has occurred to allow for their sub-rounded character. However, the limited extent of the study site and possibility of the greywacke being sourced from an uplifted bed, basement level depths of initiation are not able to be confirmed. Shallower depths are more likely, as some of the greywacke clasts have been altered independently of the pebble dykes, therefore the source stratigraphy must occur at depths within the epithermal alteration zone. Due to the presence of greywacke exposed on the field site, altered in a similar nature as these clasts, this also upholds the interpretation of non-basement depths. However, despite the shallower depths, mechanisms involved in initial fragmentation and transport must have remained considerable to transport milled clasts 12 cm in size.

Interaction between the pebble dyke and ore-bearing fluids has also been ruled out. However, although the pebble dykes within the study site did not reflect direct influence in channelling ore-bearing fluids, this does not eliminate the possibility of them being used as permeable pathways within an otherwise impermeable host rock. Hydrothermal breccia pipe systems have been identified and linked to productive mining districts worldwide. Ore deposits in such environments are often either hosted by breccia units or have some form of contextual relationship due to the permeability they offer (Weisheit et al., 2013). As the pebble dykes within the field have proven a means of increasing permeability, under the right circumstances; where emplaced during or pre-mineralisation, orientated preferential to fluid flow direction and hosted within otherwise impermeable host rock, they could act as a vector towards potential mineralisation. Therefore, their presence within lucrative environments of ore-bearing hydrothermal systems may represent an aid in explorative geology.

References

Adams, C.J., Graham, I.J., Seward, D., and Skinner, D.N.B. (1994). Geochronological and geochemical evolution of the late Cenozoic volcanism in New Zealand. *NZ Geological Survey Bulletin*. v. 37, p. 359-379.

Allen, R. (1996). Atlas of alteration: A field and petrographic guide to hydrothermal alteration minerals (Vol. 6): Geological Association of Canada.

Ballance, P. (1976). Evolution of the upper Cenozoic magmatic arc and plate boundary in northern New Zealand. *Earth and planetary science letters, 28*(3), 356-370.

Barker, S.L.L., Hood, S., Hughes, R.M., & Richards, S. (2019). The lithogeochemical signatures of hydrothermal alteration in the Waihi epithermal district, New Zealand. *New Zealand Journal of Geology and Geophysics*. DOI: 10.1080/00288306.2019.1651345.

Barnes, H. L. (1997). *Geochemistry of hydrothermal ore deposits*: John Wiley & Sons.

Bailey, S.W. (1988). Chlorites: structure and crystal chemistry. *Mineralogical Society of America Reviews in Mineralogy*, 19, 347–403.

Blatt, H. (1982). *Sedimentary petrology* (M. Tucker Ed.). New York, United States: W. H. Freeman and Company.

Booden, M. (2011). Geochemical Development of the Late Cenozoic Arc Volcanism in Northland and the Coromandel, and Implications for Geochemical Exploration in the Hauraki Goldfield. ResearchSpace@ Auckland, Retrieved from https://researchspace.auckland.ac.nz/handle/2292/8971

Booden, M. A., Smith, I. E., Black, P. M., & Mauk, J. L. (2011). Geochemistry of the Early Miocene volcanic succession of Northland, New Zealand, and implications for the evolution of subduction in the Southwest Pacific. *Journal of Volcanology and Geothermal Research*, 199(1), 25-37.

Booden, M. A., Smith, I. E. M., Mauk, J. L., & Black, P. M. (2012). Geochemical and isotopic development of the Coromandel Volcanic Zone, northern New Zealand, since 18Ma. *Journal of Volcanology and Geothermal Research*, 219-220, 15–32.

Brathwaite, R. L., Cargill, H. J., Christie, A. B., & Swain, A. (2001a). Lithological and spatial controls on the distribution of quartz veins in andesite-and rhyolite-hosted epithermal Au–Ag deposits of the Hauraki Goldfield, New Zealand. *Mineralium Deposita*, 36(1), 1-12.

Brathwaite, R., Simpson, M., Faure, K., & Skinner, D. (2001b). Telescoped porphyry Cu-Mo-Au mineralisation, advanced argillic alteration and quartz-sulphide-gold-anhydrite veins in the Thames District, New Zealand. *Mineralium Deposita*, 36(7), 623-640.

Brathwaite, R. L., & Faure, K. (2002). The Waihi epithermal gold-silver-base metal sulfide-quartz vein system, New Zealand: Temperature and salinity controls on electrum and sulfide deposition. *Economic Geology*, 97(2), 269-290.

Browne, P. R. L., & Ellis, A. J. (1970). The Ohaki-Broadlands hydrothermal area, New Zealand; mineralogy and related geochemistry. *American Journal of Science*, 269(2), 97-131.

Browne, P. (1978). Hydrothermal alteration in active geothermal fields. *Annual Review of Earth and Planetary Sciences*, 6(1), 229-248.

Bryant, D. G. (1968). Intrusive Breccias Associated with Ore, Warren (Bisbee) Mining District, Arizona. *Economic Geology*, 63, 1-12.

Bryner, L. J. (1961). Breccia and pebble columns associated with epigenetic ore deposits. *Economic Geology*, 56(3), 488-508.

Buchanan, L. J., (1981), Precious metal deposits associated with volcanic environments in the southwest, in Dickson, W.R. and Payne, W.D., eds., Relations of Tectonics to Ore Deposits in the Southern Cordillera: Arizona. *Geological Society Digest*, v. 14, p. 237-262.

Byrne, K., & Tosdal, R. M. (2014). Genesis of the Late Triassic Southwest Zone Breccia-Hosted Alkalic Porphyry Cu-Au Deposit, Galore Creek, British Columbia, Canada. *Economic Geology*, 109(4), 915-938.

Christie, A.B., Simpson, M.P., Brathwaite, R.L., Mauk., J.L., and Simmons, S.F., (2007). Epithermal Au-Ag and related deposits of the Hauraki goldfield, Coromandel Volcanic Zone, New Zealand. *Economic Geology*, v. 102, p. 785–816.

Cloos, H. (1942). Bau und Tätigkeit von Tuffschloten. *Geologische Rundschau*, 32(6), 709-800.

Corbett, G. (2002). Epithermal gold for explorationists. *AIG News, 67*, 1-8.

Corbett, G. J., and Leach, T.M., (1998). Southwest Pacific Rim gold-copper systems: structure, alteration, and mineralization. *Society of Economic Geologists*, Special Publication.

Cornelius, K. D. (1967). Hydrothermal pebble dikes at Mount Morgan, Queensland. *Economic Geology*, 62(6), 853-860.

Eberl, D., & Velde, B. (1989). Beyond the Kübler index. Clay minerals, 24(4), 571-577.

Edbrooke, S. (2001). *Geology of the Auckland Area: Scale 1: 250 000*: Institute of Geological & Nuclear Sciences.

Farmin, R. (1934). " Pebble dikes" and associated mineralization at Tintic, Utah. *Economic Geology, 29*(4), 356-370.

Francis E.H. (1989) *Tuffisite*. In: Petrology. Encyclopedia of Earth Science. Springer, Boston, MA

Fraser, C., & Adams, J. H. (1907). *The geology of the Coromandel subdivision, Hauraki, Auckland*: Department of Mines, New Zealand Geological Survey.

Gadsby, M., & Spörli, K. (1989). Structural background to Hauraki goldfield mineralisation: A review. Paper presented at the Proceedings of the 11th New Zealand Geothermal Workshop.

Gifkins, C.C., Allen, R.L., and McPhie, J., (2005). Apparent welding textures in altered pumice-rich rocks. *Journal of Volcanology and Geothermal Research*, v. 142, p. 29-47

Gustafson, L. B., & Hunt, J. P. (1975). The porphyry copper deposit at El Salvador, Chile. Economic Geology, 70(5), 857-912.

Hedenquist, J. W., & Houghton, B. F. (1987). Epithermal gold mineralisation and its volcanic enviroments. *The earth resources Foundation the University of Sydney Taupo Vol. Zone, NZ*, 15-21.

Hedenquist, J. W., Arribas, A., & Gonzalez-Urien, E. (2000). Exploration for epithermal gold deposits. *Reviews in Economic Geology, 13*(2), 45-77.

Hemley, J.J., Montoya, J.W., Marinenko, J.W., and Luce, R.W., (1980). Equilibria in the systems Al2O3-SiO2-H2O and some general implications for alteration/mineralization processes: *Economic Geology*, v. 75, p. 210-228.

Homer, L., & Moore, P. (1992). *Vanishing Volcanoes: A guide to the landforms and rock formations of Coromandel Peninsula*: Landscape Publications.

Hughes R, Barker S.L.L. (2017). Using portable XRF to infer adularia halos within the Waihi Au–Ag system, New Zealand. Geochemistry: Exploration, Environment, Analysis 18:97–108.

Irwin, M. R. (2004). *The structure of epithermal deposits of the Coromandel Peninsula: dynamic processes and three-dimensional strain.* ResearchSpace@ Auckland, Retrieved from https://researchspace.auckland.ac.nz/handle/2292/6049

Jébrak, M. (1997). Hydrothermal breccias in vein-type ore deposits: a review of mechanisms, morphology and size distribution. *Ore geology reviews, 12*(3), 111-134.

Ji, J., & Browne, P. R. (2000). Relationship between illite crystallinity and temperature in active geothermal systems of New Zealand. *Clays and clay minerals*, 48(1), 139-144.

Jochum, K. P., Weis, U., Stoll, B., Kuzmin, D., Yang, Q., Raczek, I., Jacob, D. E., Stracke, A., Birbaum, K., Frick, D. A., Gunther, D., Enzweiler, J. (2011). Determination of reference values for NIST SRM 610–617 glasses following ISO guidelines. *Geostandards and Geoanalytical Research*, *35*(4), 397-429.

John, D. A. (2011). Epithermal Gold-Silver Deposits of the Hauraki Goldfield, New Zealand: An Introduction. *Economic Geology, 106*(6), 915-919.

Kirk, C. T. (1912). Conditions of mineralization in the copper veins at Butte, Montana, *Economic Geology*, vol. 7, p. 35-82.

Kolzenburg, S., Heap, M., Lavallée, Y., Russell, J., Meredith, P., & Dingwell, D. B. (2012). Strength and permeability recovery of tuffisite-bearing andesite. *Solid Earth*, 3, 191-198.

Lagat, J. K. E. (2007). Hydrothermal alteration mineralogy in geothermal fields with case examples from Olkaria domes geothermal field, Kenya. 001045504.

Leach, T.M., and Muchemi, G.G., (1987), Geology and hydrothermal alteration of the north and west exploration wells in the Olkaria geothermal field, Kenya, in 9th New Zealand geothermal workshop, 1987, Auckland, New Zealand, proceedings: Auckland, University of Auckland Geothermal Institute, p. 187-192.

Leitch, C.H.B., and Lentz, D.R. (1994), The Gresens approach to mass balance constraints of alteration systems. *Geological Association of Canada*, Short Course Notes 11, p. 161–192.

Leva, M. (1959). *Fluidization*: McGraw-Hill.

Lindgren, W. (1913). *Mineral deposits*: McGraw-Hill Book Company, Incorporated.

Lindgren, W. (1933). *Mineral deposits*, 4th ed.: New York, McGraw-Hill, 930 p.

Lovering, T. S. (1949). Rock alteration as a guide to ore: East Tintic district, Utah (Vol. 1): *Economic Geology Pub. Co*.

Mathieu, L. (2018). Quantifying Hydrothermal Alteration: A Review of Methods. *Geosciences*, 8(7), 245.

Mauk, J. L., Hall, C. M., Chesley, J. T., & Barra, F. (2011). Punctuated evolution of a large epithermal province: The Hauraki goldfield, New Zealand. *Economic Geology*, 106(6), 921-943.

McCallum, M. E. (1985). Experimental Evidence for Fluidization Processes in Breccia Pipe Formation. *Economic Geology*, 80, 1523-1543.

McNamara, D.D., Faulkner, D., McCarney, E. (2014, February 24-26). Rock Properties of Greywacke Basement Hosting Geothermal Reservoirs, New Zealand: Preliminary Results. Paper presented at the Thirty-Ninth Workshop on Geothermal Reservoir Engineering, Stanford, CaliforniaMeng, L. (1999). Silicification and mineralization in hydrothermal deposits. *Chinese science bulletin*, 44(1), 90-93.

McQueen, K. (2006). Identifying geochemical anomalies. Australian National University.

Merchant, R. (1978). *Metallogenesis in the Thames-Tapu area Coromandel peninsula, New Zealand* (Unpublished doctoral dissertation). University of Auckland, Auckland.

Meyer, C., and Hemley, J.J., (1967). Wall Rock Alteration. Pp. 166-235 in: Geochemistry of Hydrothermal Ore Deposits (H. L. Barnes, editor). Holt Rinehart and Winston, New York.

Moore, D. M., & Reynolds, R. C. (1989). *X-ray Diffraction and the Identification and Analysis of Clay Minerals* (Vol. 322, p. 321). Oxford: Oxford university press.

Morris, H. T., & Lovering, T. S. (1979). *General geology and mines of the East Tintic mining district, Utah and Juab counties, Utah* (Vol. 1024): US Govt. Printing Office.

Muffler, L.P.J. and White, D.E., (1969). Active metamorphism of Upper Cenozoic sediments in the Salton Sea Geothermal Field and the Salton Trough, southeastern California. *Geological Society American Bulletin*, 80:157-182.

Nobarzad, A. K. E. (2014). Phase Identification by X-ray Diffraction.

Oliver, N., Rubenach, M., Fu, B., Baker, T., Blenkinsop, T. G., Cleverley, J., Marshall, L. J., Ridd, P. J. (2006). Granite-related overpressure and volatile release in the mid crust: fluidized breccias from the Cloncurry District, Australia. *Geofluids*, 6(4), 346-358.

Paton, C., Hellstrom, J., Paul, B.,Woodhead, J. and Hergt, J. (2011). "Iolite: Freeware for the visualisation and processing of mass spectrometric data." *Journal of Analytical Atomic Spectrometry*. DOI:10.1039/c1ja10172b.

Pirajno, F., (2009). *Hydrothermal Processes and Mineral Systems. Geological Survey of Western Australia*. Springer. p. 121-123, 422,448.

Pollastro, R. M. (1993). Considerations and applications of the illite/smectite geothermometer in hydrocarbon-bearing rocks of Miocene to Mississippian age. *Clays and Clay minerals*, 41(2), 119-133.

Reber, L. E. (1916) The mineralization at Clifton-Morenci, Economic Geology, vol. 11, p. 528-573.

Reyes, A.G., (1990). Petrology of Philippine geothermal systems and the application of alteration mineralogy to their assessment. *Journal of Volcanology and Geothermal Research*, 43, 279-309.

Reynolds, D. L. (1954). Fluidization as a geological process, and its bearing on the problem of intrusive granites. *American Journal of Science*, 252(10), 577-613.

Richard, K. (1969). Process of formation of mineralized breccia pipes. *Economic Geology*, Vol. 64, No. 7, p. 832.

Rose, A.W., and Bart, D.M. (1979). *Hydrothermal alteration*, in Barnes, H.L., ed., Geochemistry of hydrothermal ore deposits, 2nd edition, New York, John Wiley & Sons, p. 173-227.

Thomas, J. A., & Galey, J. T. (1982). Exploration and geology of the Mt. Emmons molybdenite deposits, Gunnison County, Colorado. *Economic Geology*, 77(5), 1085-1104.

Tillick, D. A., Peacor, D. R., & Mauk, J. L. (2001). Genesis of dioctahedral phyllosilicates during hydrothermal alteration of volcanic rocks: I. The Golden Cross epithermal ore deposit, New Zealand. *Clays and Clay Minerals*, *49*(2), 126-140.

Schardt, C., Cooke, D.R., Gemmell, J.B. & Large, R.R. (2001). Geochemical modeling of the zoned footwall alteration pipe, Hellyer volcanic-hosted massive sulfide deposits, western Tasmania, Australia. *Economic Geology*. 96, 1037–1054.

Schwartz, G. M. (1959). Hydrothermal alteration. *Economic Geology*, 54(2), 161-183.

Sheppard, D., Christie, A., Goff, J., & Carver, R. (2009). Stream sediment geochemical survey in an area of volcanic-hosted epithermal Au–Ag–Zn–Pb–Cu deposits and porphyry Cu prospects, Thames, Coromandel Peninsula, New Zealand. *Geochemistry: Exploration, Environment, Analysis, 9*(3), 279-296.

Silberman, M. L., & Berger, B. R. (1985). Relationship of trace-element patterns to alteration and morphology in epithermal precious-metal deposits. *Reviews in Economic Geology*, 2, 203-232.

Sillitoe, R. H. (1985). Ore-related breccias in volcanoplutonic arcs. *Economic Geology*, 80(6), 1467-1514.

Sillitoe, R. H., & Bonham, H. F. (1984). Volcanic landforms and ore deposits. *Economic Geology, 79*(6), 1286-1298.

Simmons, S. F., White, N. C., & John, D. A. (2005). Geological characteristics of epithermal precious and base metal deposits. *Economic Geology*, 100, 485-522.

Simmons, S. F., Brown, K. L., & Tutolo, B. M. (2016). Hydrothermal transport of Ag, Au, Cu, Pb, Te, Zn, and other metals and metalloids in New Zealand geothermal systems: Spatial patterns, fluid-mineral equilibria, and implications for epithermal mineralization. *Economic Geology*, 111(3), 589-618.

Simpson, M.P., Mauk, J.L., and Simmons, S.F. (2001). Hydrothermal alteration and hydrologic evolution of the Golden Cross epithermal Au-Ag deposit, New Zealand. *Economic Geology*, v. 96, p. 773–796.

Simpson, M. P., & Mauk, J. L. (2011). Hydrothermal alteration and veins at the epithermal Au-Ag deposits and prospects of the Waitekauri area, Hauraki goldfield, New Zealand. *Economic Geology*, 106(6), 945-973.

Skinner, D. N. (1967). *Geology of the Coromandel region with emphasis on some economic aspects* (Doctoral dissertation). ResearchSpace@ Auckland.

Skinner, D. N. B. (1986). Neogene volcanism of the Hauraki volcanic region. *Royal society of New Zealand bulletin, 23*, 21-47.

Skinner, B. J., & Barton Jr, P. B. (1973). Genesis of mineral deposits. *Annual Review of Earth and Planetary Sciences, 1*(1), 183-211.

Spörli, K.B., (1987). Development of the New Zealand microcontinent, in Monger, J.W.H., and Francheteau, J., eds., Orogenic belts and evolution of the Pacific Ocean basin. *American Geophysical Union, Geodynamics Series*, v. 19, p. 115–132.

Spörli, K. B., Begbie, M. J., Irwin, M. R., & Rowland, J. V. (2007). Structural Processes and Tectonic Control on the Epithermal AU-A Deposits of the Hauraki. *Geology and Exploration of New Zealand Mineral Deposits*. New Zealand: GNS Science.

Srodon, J. (1980). Precise identification of illite/smectite interstratifications by X-ray powder diffraction. *Clays and Clay Minerals*, *28*(6), 401-411.

Środoń, J. (2006). Identification and Quantitative Analysis of Clay Minerals. *Developments in Clay Science*, 1, 765-787.

Steven, T.A. and Ratte, J.C., 1960, Geology and ore deposits of the Summitville district, San Juan Mountains, Colorado: *United States Geological Survey*, Professional Paper 343, 70 p.

Suggate, R. P., Stevens, G. R., Te Pungam, M. T. (1978). *The Geology of New Zealand* (Vol. One). Wellington: Government Printer.

Tuffen, H., Pinkerton, H., Dingwell, D., & Davison, B. (2002). *Multiple generations of tuffisite veins record repetitive ductile-brittle deformation of rhyolitic magma rising within an effusive vent: a source of flow banding in silicic lavas and repetitive seismic signals?* Paper presented at the AGU Fall Meeting Abstracts.

Vaughan, D.J., and Craig, J.R., (1997), *Sulfide ore mineral stability, morphologies, and intergowth textures*, in Barnes, H.L., ed., Geochemistry of hydrothermal ore deposits, 3rd edition: John Wiley and Sons, Inc, p. 367–434.

Velde, B. (1992). *Introduction to clay minerals: chemistry, origins, uses and environmental significance*: Chapman and Hall Ltd.

Velde, B. (Ed.). (2013). *Origin and mineralogy of clays: clays and the environment*. Springer Science & Business Media.

Vikre, P.G., (1985), Precious metal vein systems in the National district, Humbolt County, Nevada: *Economic Geology*, v. 80, p. 360-393.

Warren, I., Simmons, S. F., & Mauk, J. L. (2007). Whole-rock geochemical techniques for evaluating hydrothermal alteration, mass changes, and compositional gradients associated with epithermal Au-Ag mineralization. *Economic Geology*, 102(5), 923-948.

White, N.C., Hedenquist, J.W., (1990). Epithermal environments and styles of mineralization: variations and their causes, and guidelines for exploration. *Journal of Geochemical Exploration*, 36: 445-474.

White, N. C., & Hedenquist, J. W. (1995). Epithermal gold deposits: styles, characteristics and exploration. *SEG newsletter, 23*(1), 9-13.

Weisheit, A., Bons, P. D., & Elburg, M. A. (2013). Long-lived crustal-scale fluid flow: the hydrothermal mega-breccia of Hidden Valley, Mt. Painter Inlier, South Australia. *International Journal of Earth Sciences*, 102(5), 1219-1236.

Appendix 1: Samples and Analysis

Sample	Rock Type	Thin Section	SEM	XRD	XRF	ICP-MS
UN-AND	Altered andesite	●	●	●	●	●
OR-AND		●		●	●	●
GR-AND		●	●	●	●	●
HST-AND		●		●	●	●
HST-TRAN		●		●	●	●
RP1		●	●	●	●	●
RP2		●		●	●	●
BRC-1	Altered Andesitic Breccia	●	●	●	●	●
BRC-2		●		●	●	●
G1	Greywacke	●	●	●	●	●
G2	Altered Greywacke	●		●	●	●
G3		●		●	●	●
6-HST-G		●		●	●	●
PBL-1	Pebble Dyke	●		●	●	●
PBL-2				●	●	●
PBL-3		●				
PBL-4		●				
PBL-5		●				
PBL-6		●	●			
PBL-7		●				

Appendix 2: SEM EDS Data

Point count chemical analysis performed by SEM for EDS analysis during host rock and pebble dyke petrology (Chapter 4). Each numbered point corresponds to an element distribution graph.

Fig. 30 – Northern Andesite (sample UN-AND) matrix

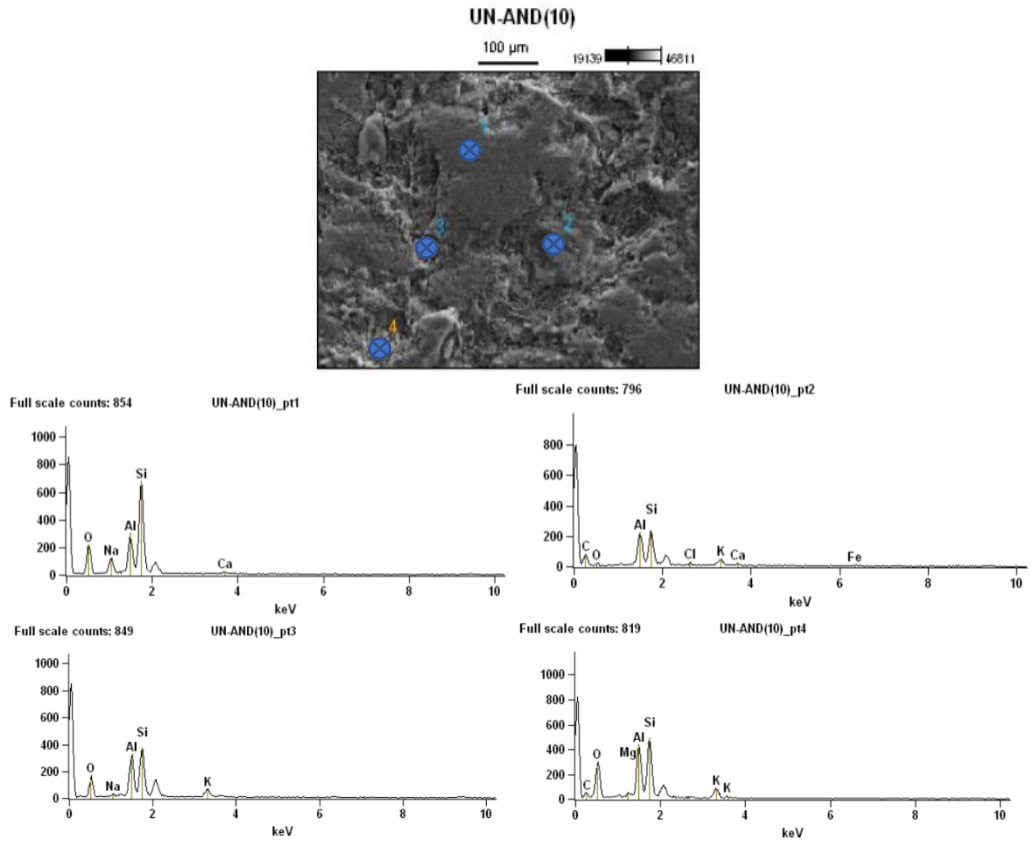

Fig. 32 - Northern Andesite (sample UN-AND) Chlorite Variations

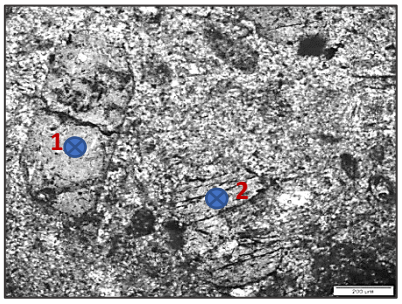

Wt. % Values

	C-K	O-K	Mg-K	Al-K	Si-K	Fe-K	As-K	Co-K
Point 1		19.35	6.39	9.42	18.84	33.33	11.95	
Point 2	2.72	21.24	8.37	10.70	20.83	34.58		1.33

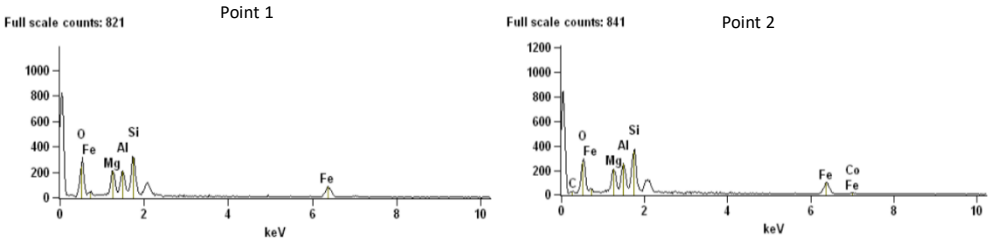

Fig. 45a – Northern altered andesite (sample GR-AND) pyrite

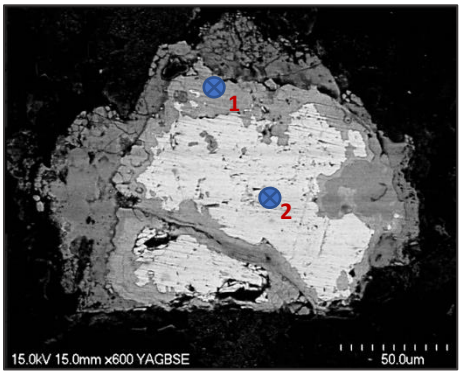

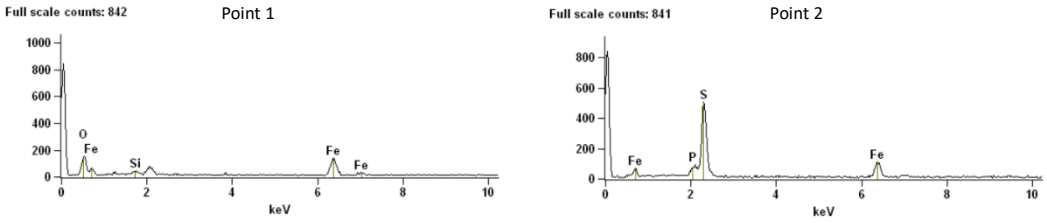

Appendix 3: X-Ray Diffraction Profiles

Bulk rock: Order of profiles is in relation to their position from north to south down the study site.

Sample: GR-AND - Altered andesite

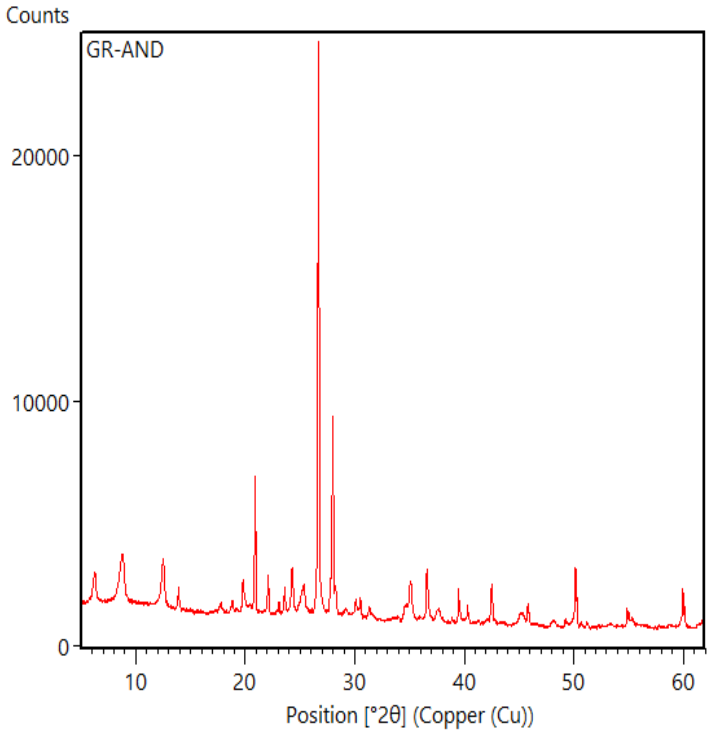

Sample: OR-AND - Altered andesite

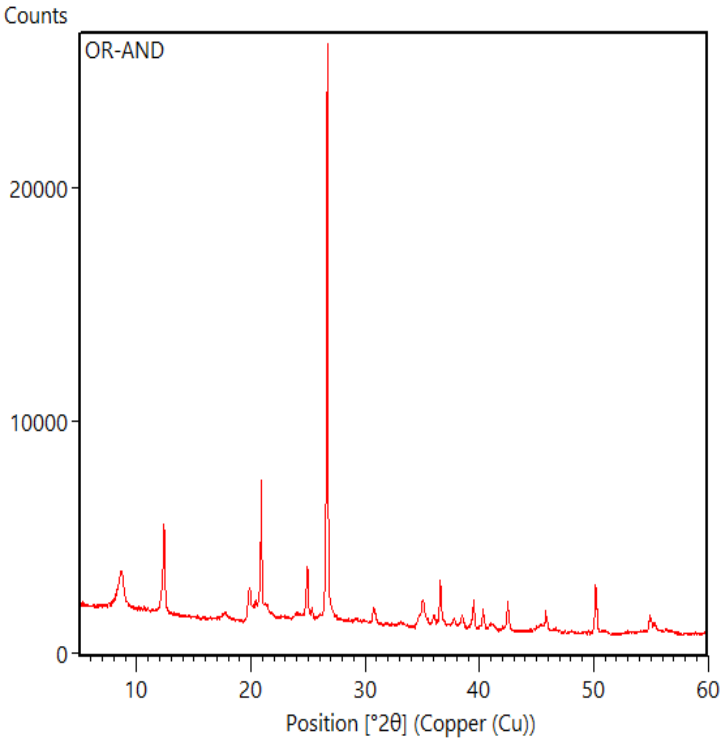

Sample: UN-AND - Altered andesite

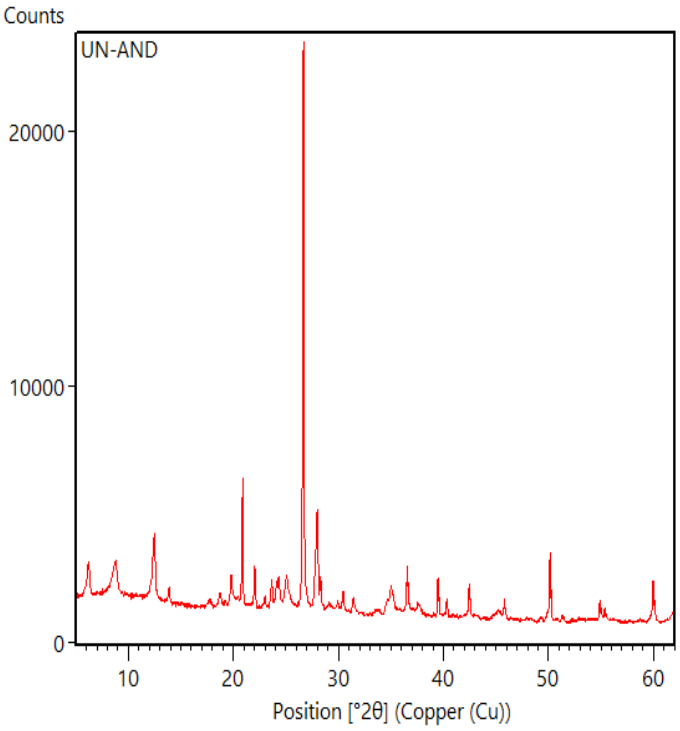

Sample: BRC-2 - Altered andesitic breccia

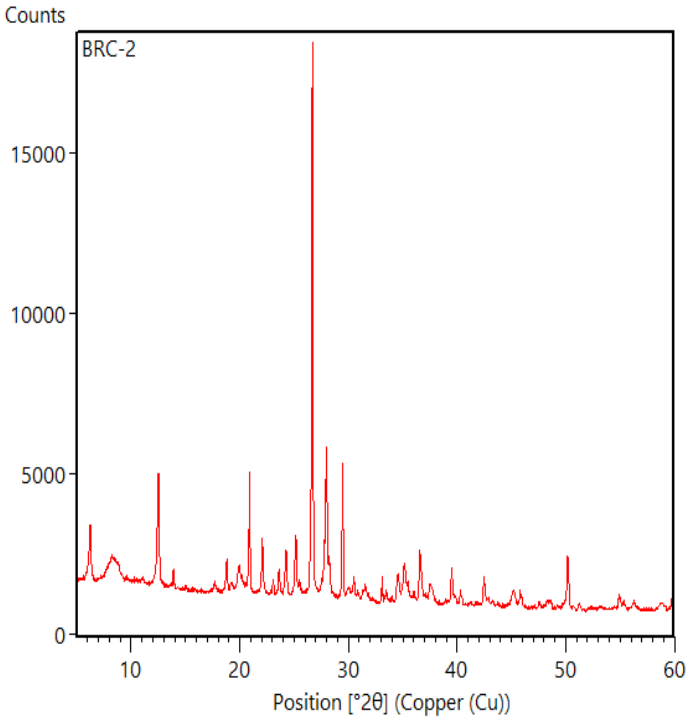

Sample: HST-AND - Altered andesite

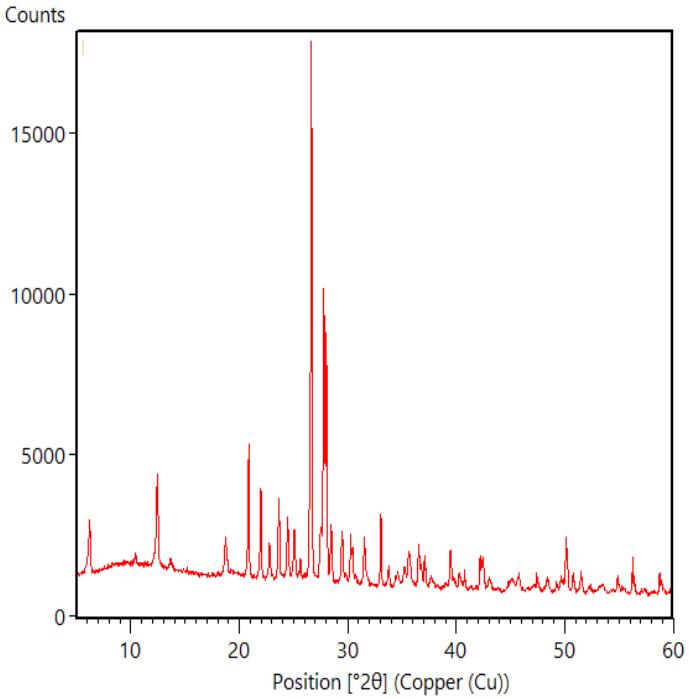

Sample: HST-TRAN - Altered andesite proximal to pebble dyke

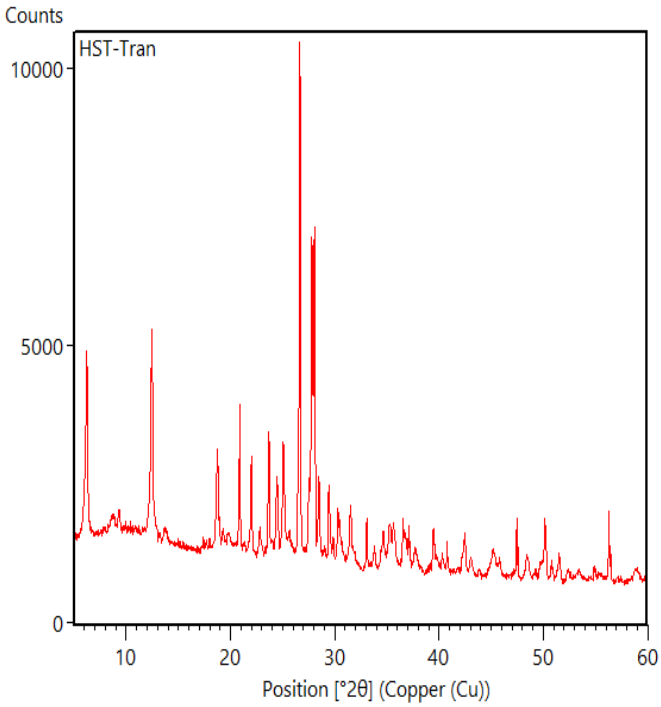

Sample: BRC-1 - Altered andesitic breccia

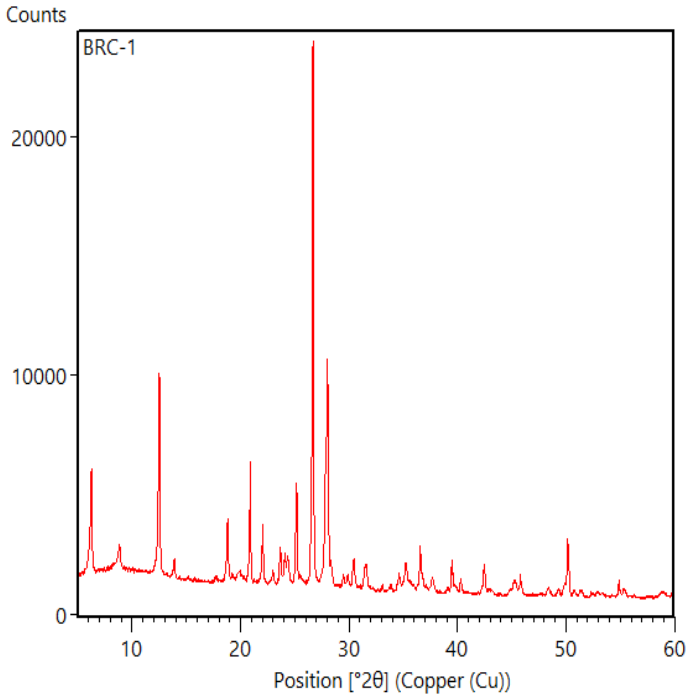

Sample: G1 - Greywacke

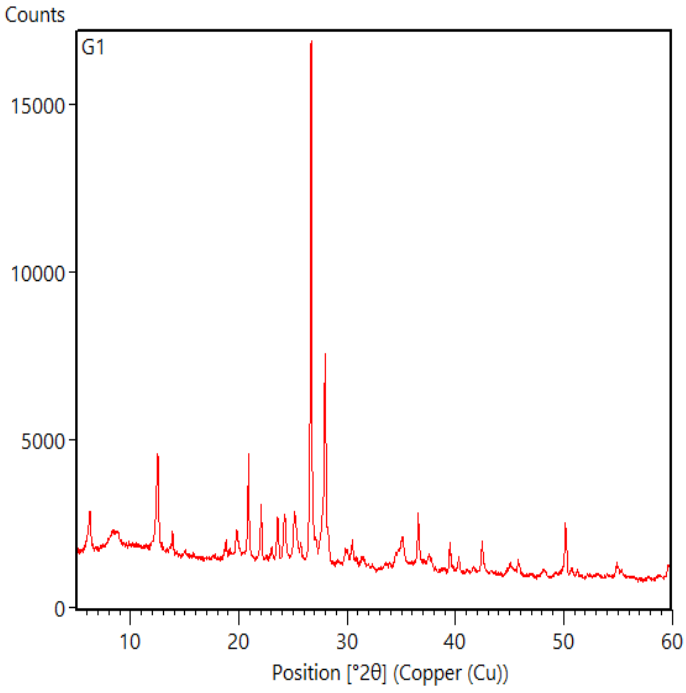

Sample: G2 - Altered greywacke

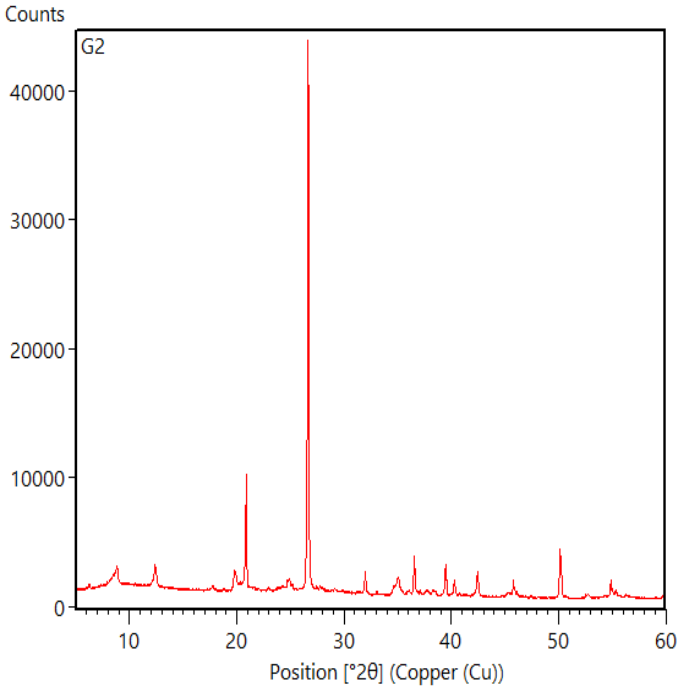

Sample: G3 - Altered greywacke

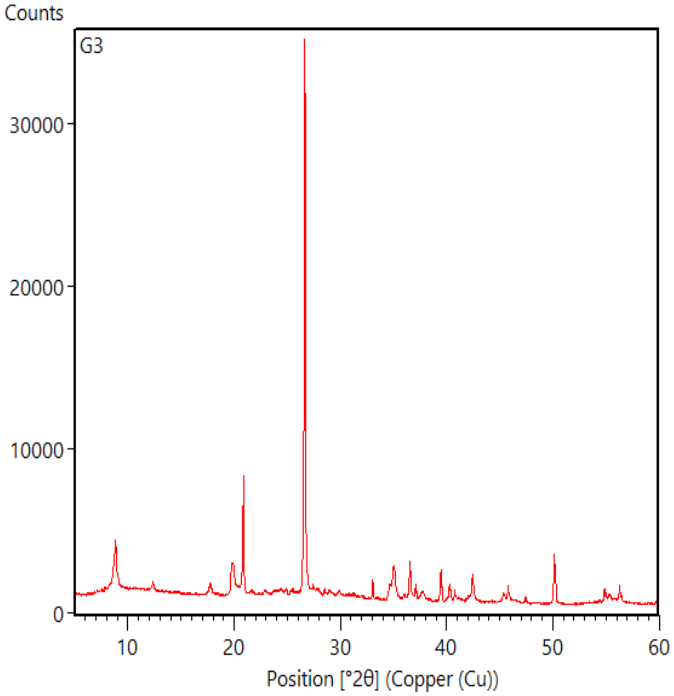

Sample: 6-HST-G - Altered andesite proximal to pebble dyke

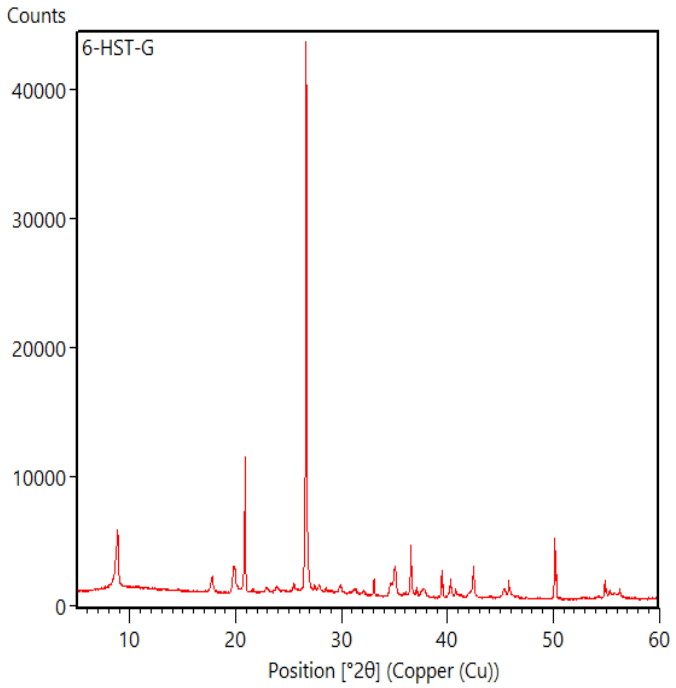

Sample: RP1 - Altered andesite

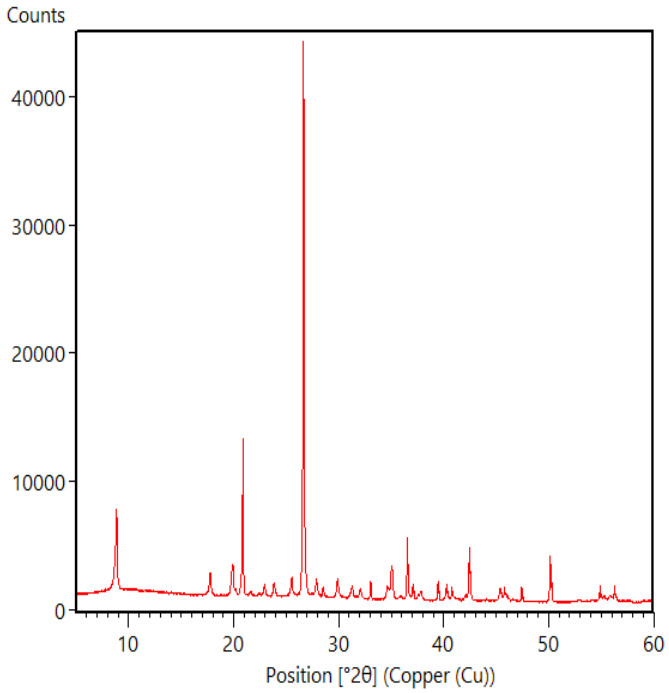

Sample: RP2 - Altered andesite

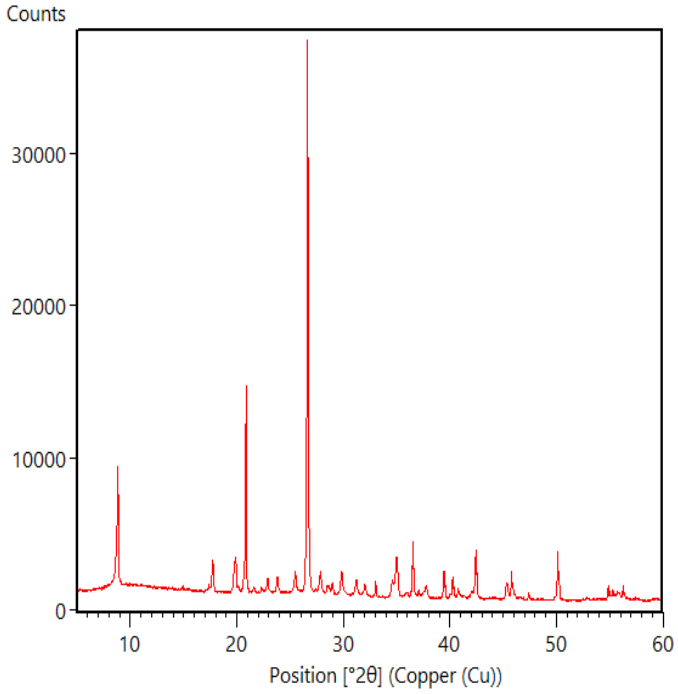

Clay Separates

Untreated profiles are in red and treated with ethylene glycol is in blue.

Sample: GR-AND – Altered andesite

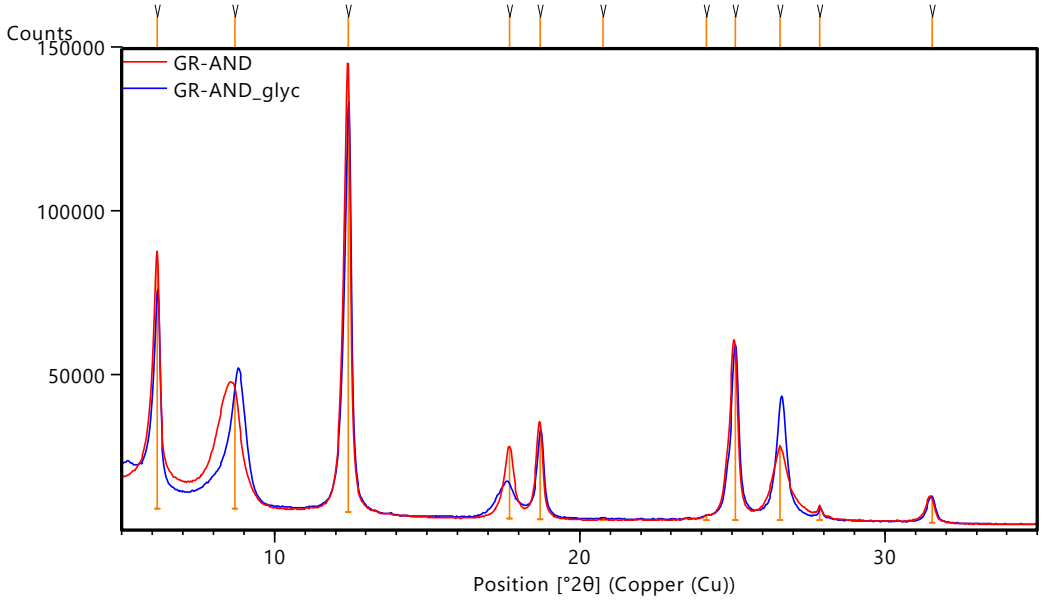

Sample: Or-AND – Altered andesite

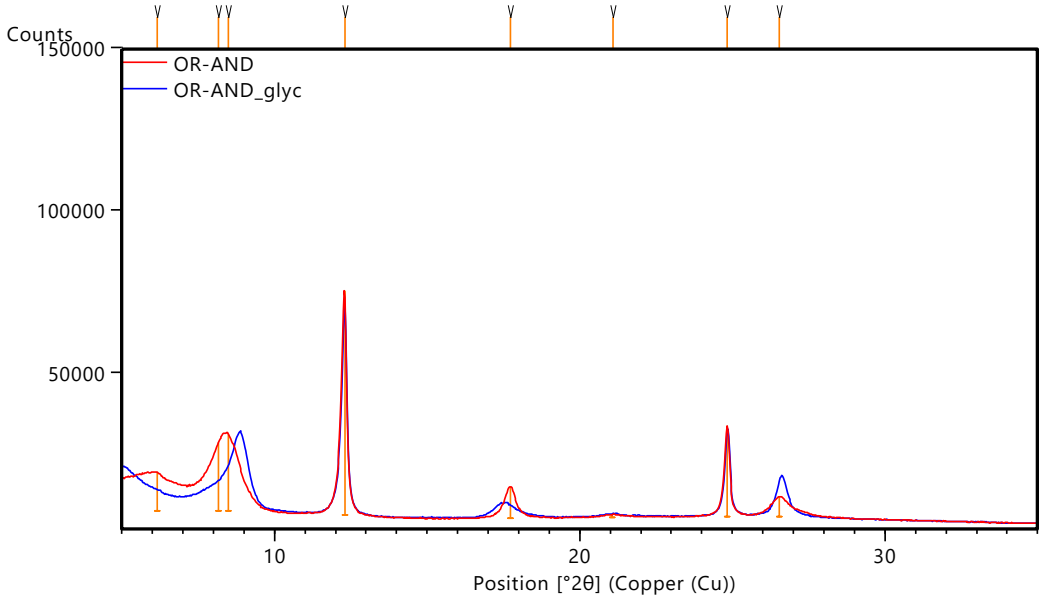

Sample: UN-AND - Altered andesite

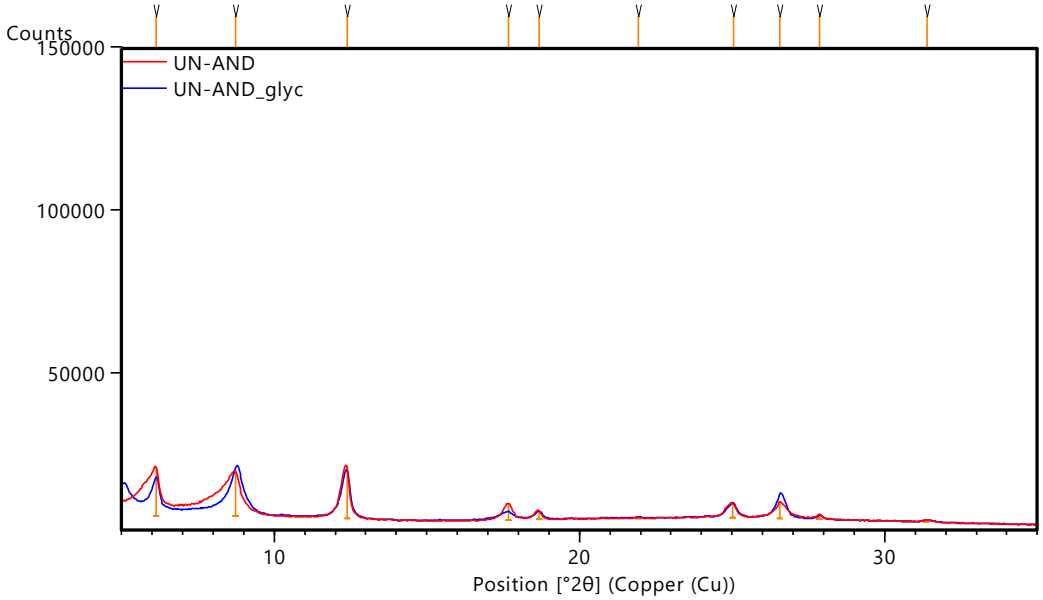

Sample: HST-TRAN – Altered andesite

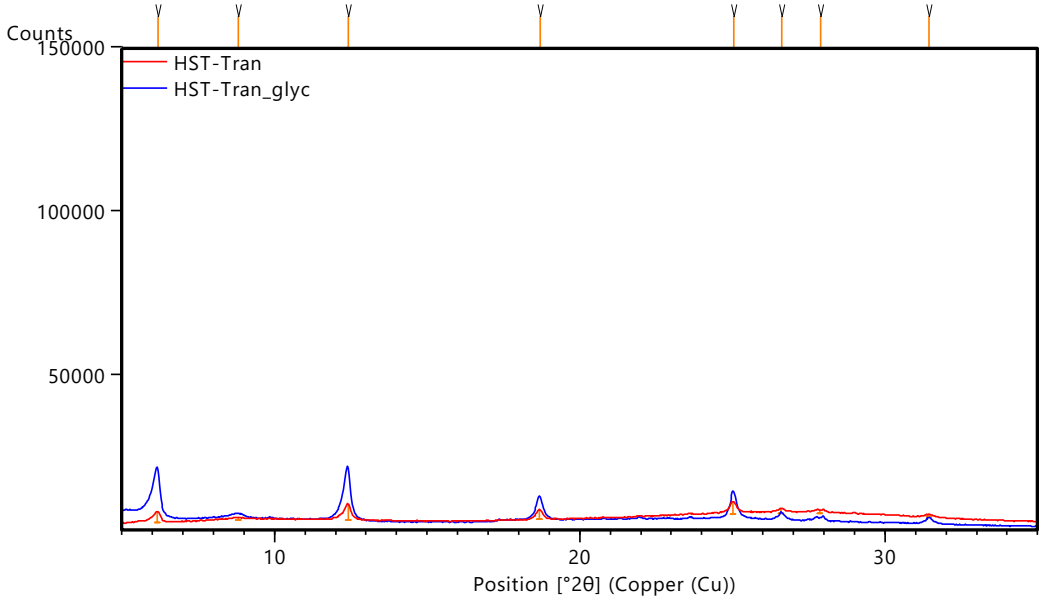

Sample: BRC-1 – Altered andesitic breccia

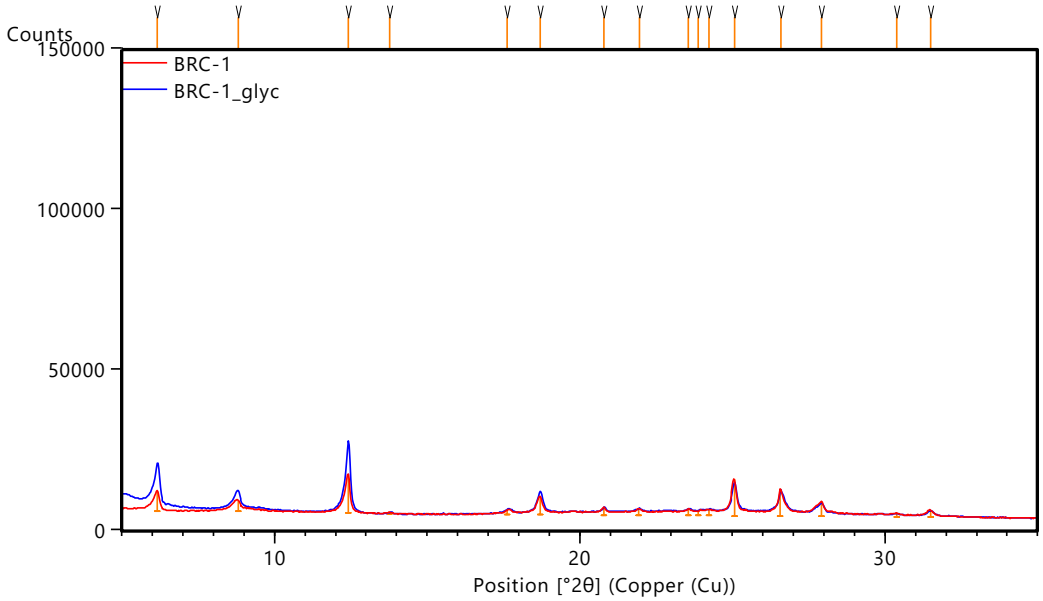

Sample: PBL-1 – Pebble dyke (matrix)

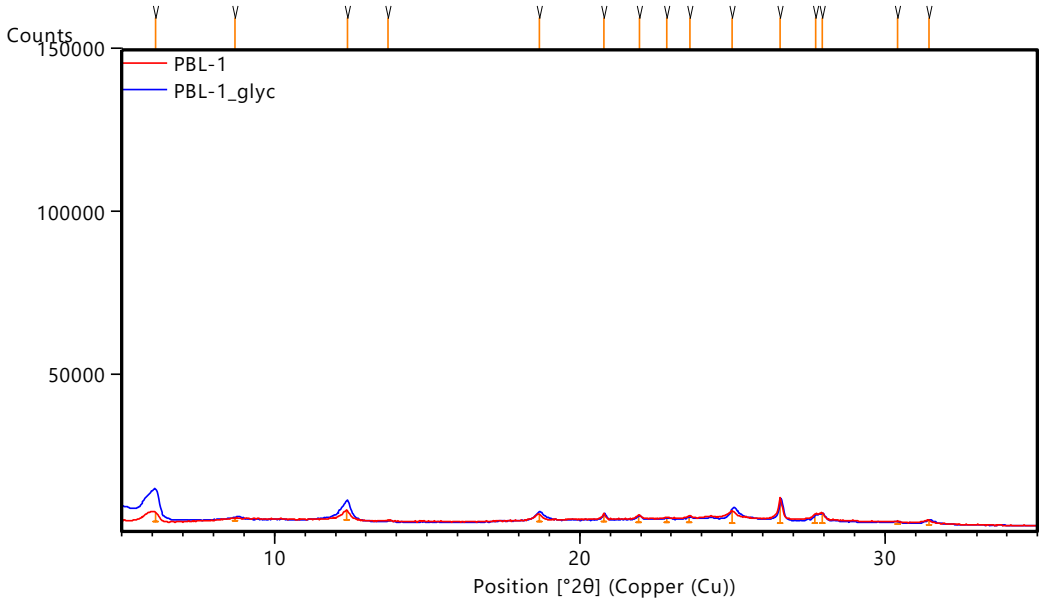

Sample: PBL-2 – Pebble dyke (Matrix)

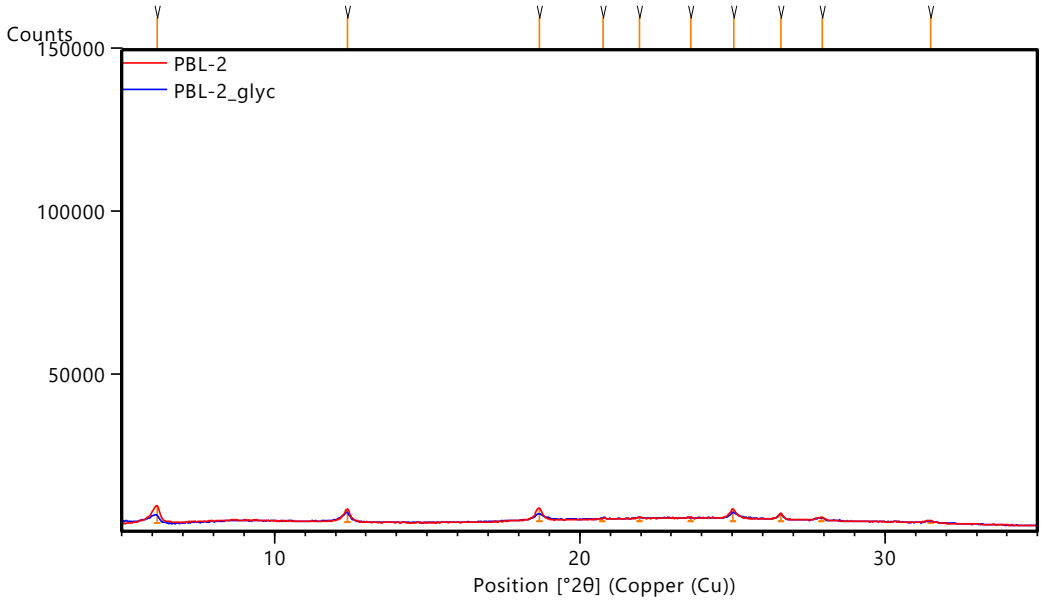

Sample: G1 – Greywacke

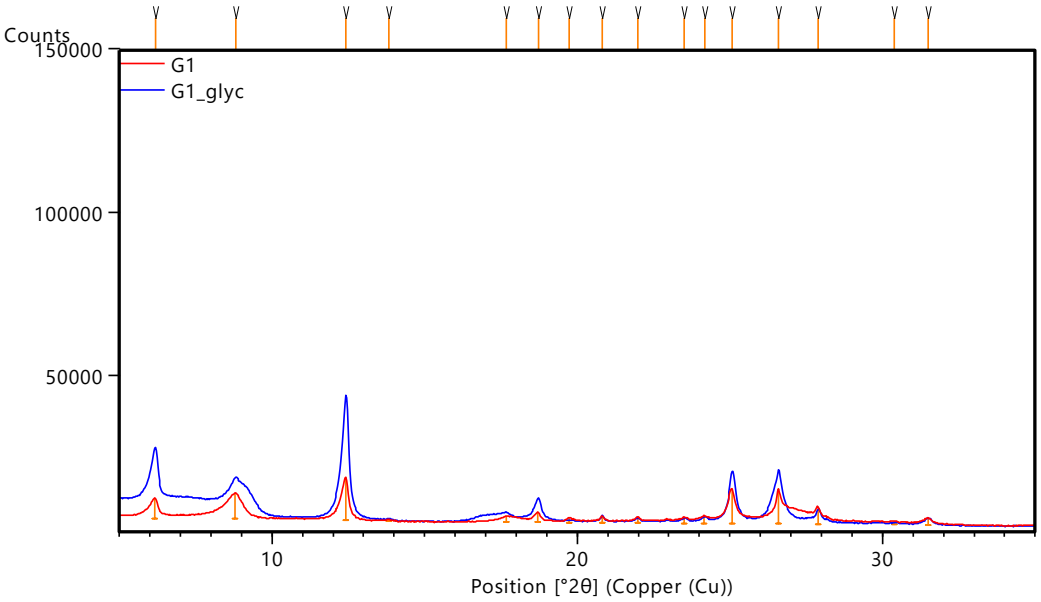

Sample: G2 – Altered greywacke

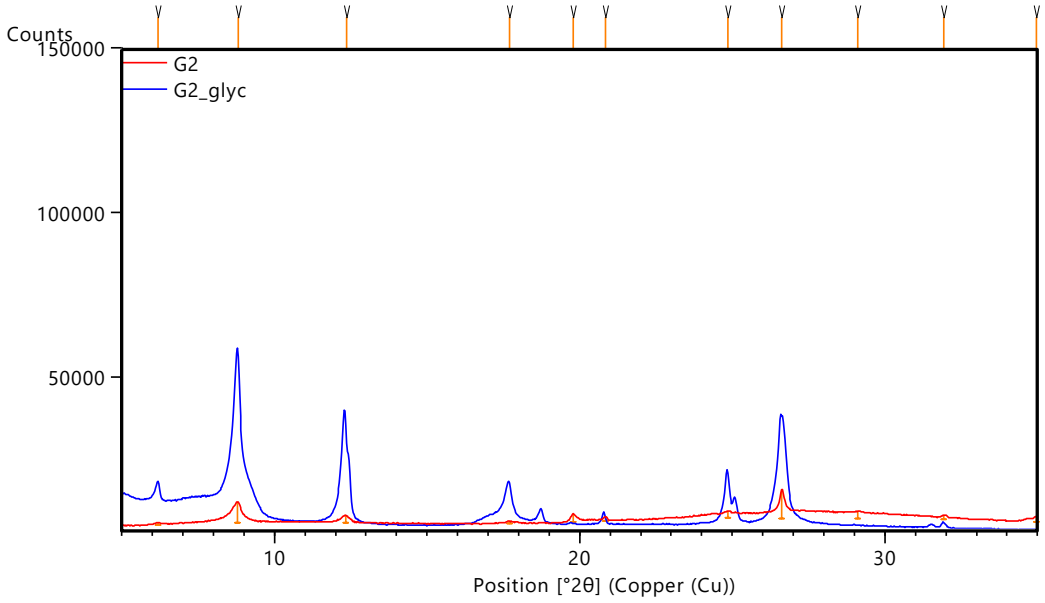

Sample: G3 – Altered greywacke

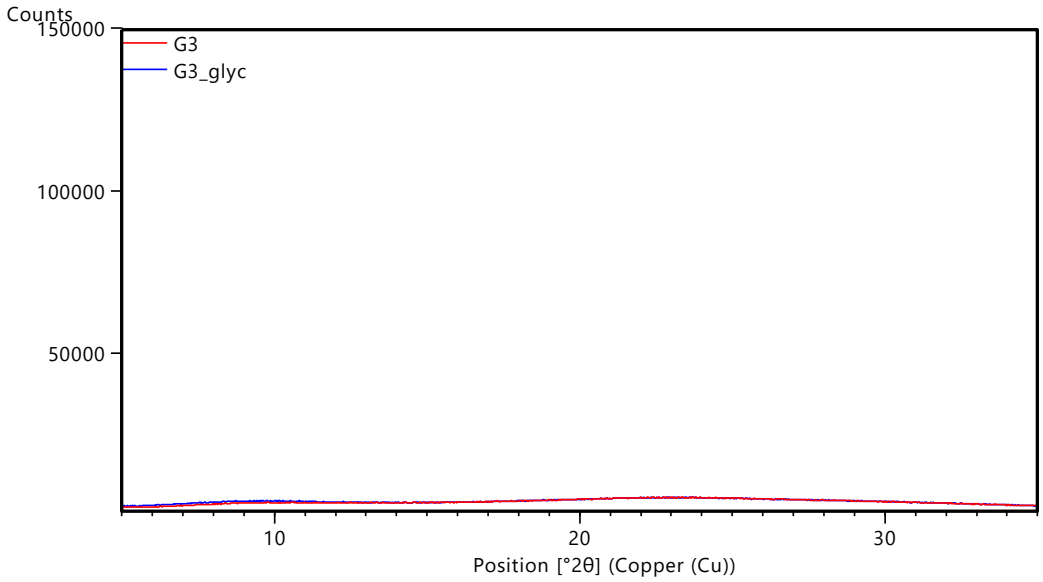

Sample: RP1 – Altered andesite

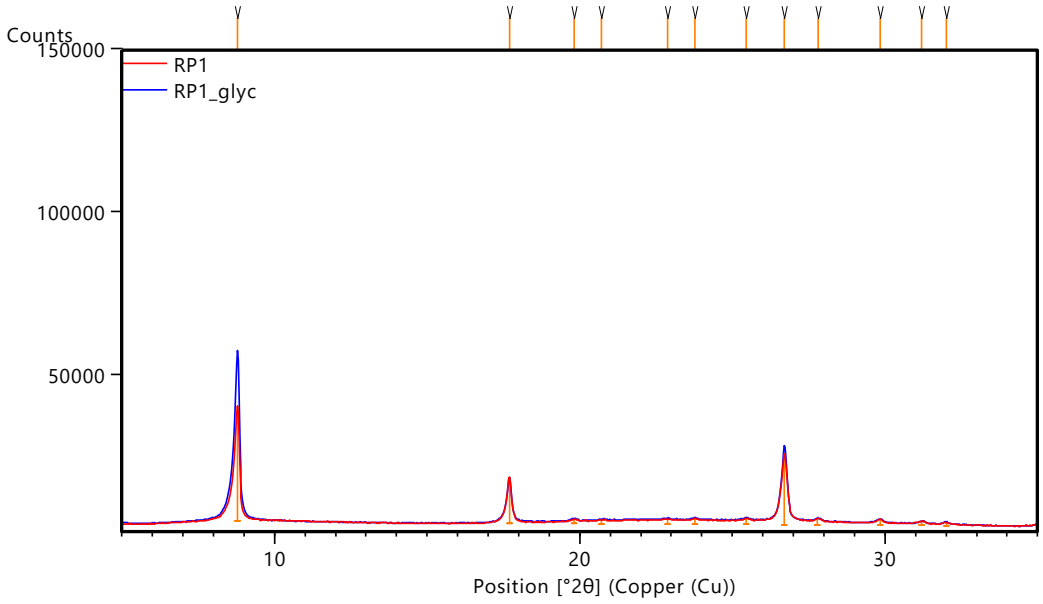

Sample: RP2 – Altered andesite

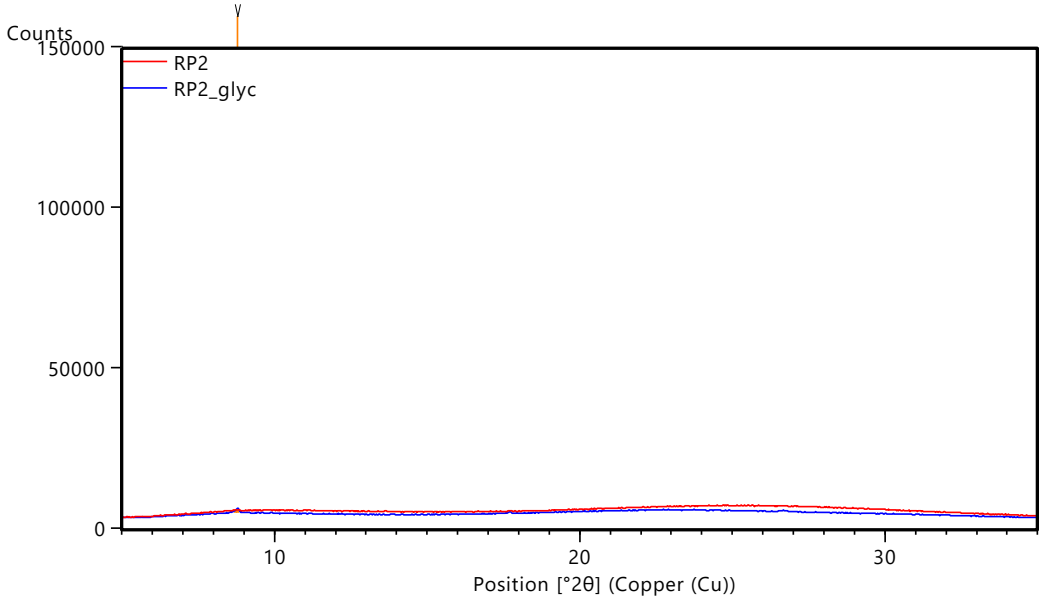

Appendix 4: LA-ICP-MS Instrument Settings and Data

INSTRUMENT SETTINGS FOR LA-ICPMS

ICP-MS		
Model		Elan 6100 DRCII ICP-MS (Perkin Elmer Sciex)
Gas flows	Plasma (Ar)	15 L.min
	Auxiliary (Ar)	1.2 L.min
	Carrier (He)	1.0 L.min
	Nebuliser	0.6 to 0.7 optimised range
Shield torch		Used for most analyses
Vacuum pressure		1 x 10^{-5} Torr
Software		Elan 3.4
LASER		
Model		RESOlution SE series excimer laser
Wavelength		193 nm
Repetition rate		10 Hz
Pre-ablation laser warm-up		Laser fired continuously
Spot size		100 µm
Incident pulse energy		c. 0.04 mJ
Energy density on sample (fluence)		c. 5 J.cm^2
Software		Geostar v8.50
DATA ACQUISITION PARAMETERS		
Data acquisition protocol		Time resolved analyses
Scanning mode		Peak hopping, 1 point per peak
Detector mode		Pulse counting, dead time correction applied
Quadrapole settling time		c. 2 ms
Data acquisition		35 s background, 45 s ablation
Software		Elan 3.4

Rock Type	Altered Andesite			Volcanic Breccia	Altered Andesite		Volcanic Breccia	Unaltered Greywacke	Altered Andesite			Altered Andesite		Pebble Dyke (Cluster A)	
Element Analysed (ppm)	GR-AND	OR-AND	UN-AND	BRC-2	HST-AND	HST-TRAN	BRC-1	G1	G2	6-HST-G	G3	RP1	RP2	PBL-1	PBL-2
Mg	10590	4356	13760	18040	15620	22690	19810	13170	5370	3483	2768	2224	3217	13660	20840
Al	99960	96420	96500	93060	97310	105300	94600	91260	82000	94050	103800	86530	92610	74690	83460
K	22120	18890	19440	6693	1048	4038	5273	24070	20140	36830	33150	33210	38750	2709	2318
Ca	2920	9240	6540	26990	56900	45670	19170	5130	2940	3750	2380	2610	2750	21820	26830
Sc	16.98	20.77	16.75	22.7	28.52	32.62	21.67	18.29	10.85	17.47	14.8	22.05	18.08	14.03	16.66
Ti	4140	4370	4100	4210	5100	5520	4070	5740	3920	5030	4780	3726	3691	4240	3970
V	146.3	161.3	143.1	157.3	230.2	237.3	173	137.1	84.5	126.6	116.8	162.2	148.3	116.7	158.2
Cr	30.52	42.17	34.14	79.6	58.31	65.1	66.6	37.71	34.83	44.5	37.57	36.33	37.68	33.74	47.55
Mn	450	1072	496	1638	1277	855	1464	583	1391	96.4	69.6	53	75.8	650	825
Fe	28420	36500	35400	39400	43100	37300	25280	40700	27890	36550	32200	52800	37860	25060	24800
Co	15.54	17.72	19.43	19.57	18.74	17.99	16.56	15.64	17.92	16.41	11.7	44.62	23.84	22.88	16.6
Ni	14.19	28.82	26.06	35.69	24.36	27.44	35.5	19.99	25.75	21.79	21.01	32.45	23.41	21.91	20.84
Cu	24.24	33.13	19.22	29.98	127.1	5.67	17.21	34.1	121.1	57	12.49	9.49	13.22	8.34	12.28
Ga	16.24	16.29	16.9	14.97	16.2	19.1	16.06	18.19	14.75	20.04	21.19	11.09	14.98	12.34	14.39
Ge	1.31	2.31	1.46	1.95	1.46	1.6	1.59	0.94	1.64		1.69	1.94	2.35	1.66	1.41
Rb	96.1	74.7	87	22.18	2.174	8.41	22.53	87	86.4	137.2	114.8	94.5	124.4	6.2	7.55
Sr	98.8	30.24	167.7	172.7	275.4	285.3	370	154	27.87	41.4	256.1	28.58	35.7	382	334
Y	20.8	15.37	11.88	13.98	16.45	17.57	14.95	16.29	12.58	19.88	21.12	14.44	10.13	15.1	12.91
Zr	109.3	105.5	104.7	84.8	83.2	86.7	84.9	168.5	168.1	190.9	199	86	92.6	129.9	89.4
Nb	4.84	4.55	4.72	2.909	2.774	3.08	2.72	6.77	5.46	8	7.13	2.593	2.74	4.47	2.96
Te				0.163	0.203	0.137			0.22		0.59	0.265	0.089	0.07	0.237

Cont.

Rock Type	Altered Andesite			Volcanic Breccia	Altered Andesite		Volcanic Breccia	Unaltered Greywacke	Altered Andesite			Altered Andesite		Pebble Dyke (Cluster A)	
Element Analysed (ppm)	GR-AND	OR-AND	UN-AND	BRC-2	HST-AND	HST-TRAN	BRC-1	G1	G2	6-HST-G	G3	RP1	RP2	PBL-1	PBL-2
Cs	4.38	3.34	3.73	1.506	0.96	2.604	3.8	2.87	3.58	3.31	2.96	1.52	1.831	0.615	2.508
Ba	493	340.3	415.8	330.8	125.1	423	164.7	839	267.4	717	652	549	467.5	193	182.4
La	14.53	12.24	9.13	7.33	8.12	12.75	7.91	15.77	16.16	22.31	20.11	2.211	3.88	7.42	7.95
Ce	27.73	25.11	17.85	15.62	17.39	27.28	17.75	36.63	35.75	50.4	44.1	5.08	8.68	16.7	16.27
Pr	3.26	2.91	2.3	1.921	2.197	3.4	2.255	4.5	4.1	6.12	5.08	0.683	1.076	2.09	1.968
Nd	13.07	11.87	8.86	8.46	9.52	14.46	10.14	18.94	15.72	24.83	20.82	3.19	4.63	8.67	8.31
Sm	2.61	2.63	1.88	1.9	2.58	3.37	2.57	4.11	3.12	5.63	4.38	1.124	1.195	2.14	1.92
Eu	0.776	0.734	0.51	0.669	0.884	1.014	0.805	0.843	0.621	0.953	1.012	0.294	0.234	0.64	0.525
Gd	3.07	2.71	1.98	2.26	2.83	3.31	2.7	3.55	2.56	4.81	3.87	1.72	1.44	2.45	2.08
Tb	0.464	0.402	0.307	0.365	0.457	0.543	0.395	0.502	0.403	0.729	0.619	0.331	0.231	0.383	0.321
Dy	3.13	2.74	1.933	2.39	3.11	3.38	2.8	3.03	2.56	4.47	3.99	2.31	1.597	2.54	2.27
Ho	0.653	0.588	0.423	0.523	0.619	0.671	0.557	0.623	0.487	0.864	0.802	0.483	0.363	0.553	0.463
Er	2.13	1.721	1.354	1.567	1.86	1.95	1.665	1.9	1.503	2.47	2.31	1.537	1.091	1.676	1.391
Tm	0.306	0.248	0.206	0.235	0.26	0.273	0.238	0.303	0.218	0.327	0.366	0.229	0.17	0.241	0.232
Yb	2.07	1.758	1.477	1.609	1.744	1.751	1.64	2.11	1.54	2.22	2.38	1.52	1.2	1.63	1.52
Lu	0.314	0.26	0.229	0.232	0.246	0.261	0.233	0.33	0.229	0.325	0.355	0.217	0.201	0.247	0.253
Ta	0.589	0.534	0.597	0.42	0.412	0.405	0.415	0.695	0.623	0.804	0.704	0.412	0.433	0.524	0.444
Tl	0.243	0.193	0.266	0.097	0.064	0.126	0.078	0.464	0.373	0.228	0.388	0.335	0.323		0.068
Pb	5.88	5.24	6.1	5.19	13.01	8.33	14.02	6.35	3.14	10.76	6.78	4.11	11.9	13.33	13.05
Pb	5.36	5.05	5.94	4.84	11.86	7.93	12.59	5.83	2.84	9.72	6	3.77	11.29	12.23	11.99
Pb	5.61	4.93	5.93	4.88	12.22	7.92	12.96	5.84	2.92	9.83	6.25	3.97	11.33	12.37	12.43
Th	6.52	5.91	6.3	2.674	2.976	3.16	2.577	8.24	7.29	10.63	9.88	2.338	2.619	5.79	3.2
U	1.514	1.536	1.313	0.605	0.653	0.675	0.631	2.004	1.657	1.963	2.43	0.735	0.626	1.227	0.795